Tropical cyclone hazards in the Caribbean

Analysing historical and synthetic events by modelling wind, surge, and rainfall

Lisette de Valk

TU Delft

Tropical cyclone hazards in the Caribbean

Analysing historical and synthetic events by modelling wind, surge, and rainfall

by

Lisette de Valk

Student number:	4967496	
University:	Delft University of Technology	
Faculty:	Civil Engineering and Geosciences	
Master programme:	Environmental Engineering	
Master programme track:	Water Resources Engineering	
Thesis committee:	Dr. Stef Lhermitte,	TU Delft, supervisor (chair)
	Prof. dr. ir. Pieter van Gelder,	TU Delft, supervisor
	Dr. ir. Arjan Droste,	TU Delft, supervisor
	Prof. dr. Marc van den Homberg,	Netherlands Red Cross 510
Project duration:	April 2025 - November 2025	

TU Delft Delft University of Technology

510 AN INITIATIVE OF THE NETHERLANDS RED CROSS

Preface

This report presents my master's thesis on the various hazards associated with hurricanes in the Caribbean. The topic was quite new to me, which was a bit of a challenge at the start, but it always sparked my interest. As this thesis marks the end of my years at TU Delft, I am looking forward to putting all that I have learned into practice.

During the project, I had the opportunity to join the Data & Digital Team 510 of the Netherlands Red Cross and work at their office in The Hague. This gave me valuable insight into the field of humanitarian response and the practice of anticipatory action. I am grateful to everyone for their openness and the welcoming atmosphere. In particular, I would like to thank Aklilu Teklesadik (Aki) for sharing his expertise and Sahara Sedhain for helping to shape the research. My sincere thanks go to Marc van den Homberg, as my main supervisor, for his weekly meetings and close involvement.

I would also like to thank my supervisors at TU Delft: Stef Lhermitte, Pieter van Gelder, and, during the second half of the project, Arjan Droste. Thank you for your guidance and feedback, understanding, and for thinking along about research directions.

Finally, a big thank you to my parents and Yfke and Brent for many phone calls and, of course, for reading interim reports. A special thank you to Thomas, who has read my thesis multiple times (very patiently) and contributed many ideas throughout the process (very helpful). For all the fun I had during my time in Delft and Rotterdam, I would like to thank all my friends.
Above all, I am thinking of my brother Merijn, without whom I probably never would have studied in Delft and who has stood beside me, always.

Lisette de Valk,
21 November 2025

Summary

The Caribbean region is highly exposed to natural hazards, particularly tropical cyclones (TCs). Their impacts vary between islands, depending on hazard intensity and duration, as well as local exposure and vulnerability. While national early action protocols (EAPs) have been developed for several countries, a regional approach has not yet been implemented within collaborations of Red Cross and Red Crescent National Societies and the IFRC.
This study focuses on a regional approach for the Leeward Islands (from Martinique up to Puerto Rico), investigating the spatial variability of three TC-related hazards: high wind speeds, storm surge, and extreme precipitation. Maximum wind speeds and their return periods are quantified using the numerical Holland (2008) wind field model. Storm surge is estimated with a simplified approximation based on the SLOSH model, which is translated into flooded areas and corresponding return periods. Total precipitation during a storm is modelled using the parametric Tropical Cyclone Rainfall (TCR) model.

As input data, historical TC tracks from the IBTrACS database (1940–2024) are used, as well as synthetic tracks. The synthetic data was generated by the STORM algorithm and contains 10,000 years of TC tracks. Additionally, for the precipitation modelling, climate data from the reanalysis dataset ERA5 of the ECMWF is used. All hazard modelling is carried out in CLIMADA, an open-source Python framework for climate risk assessment developed by ETH Zurich. Results are compared between islands and against regional averages, supporting the PARATUS project's feasibility study on a regional EAP for TCs in Antigua and Barbuda, Dominica, and Saint Kitts and Nevis.

The findings indicate a high degree of spatial coherence in wind speeds across neighbouring islands, and it is concluded that approximately 52% of the storms affect over five countries in the same event. Based on the synthetic dataset, we find that for a five-year return period (a common threshold for EAPs), experienced one-minute sustained wind speeds of approximately 28 m/s are expected. A total deviation of 8 to 10% is found between the mean values per country and the regional mean, up to return periods of 1,000 years. This is considered a rather equal distribution of the hazard.
Storm surge shows a significantly less equal distribution based on synthetic data, with the countries Saint Barthélemy and Saba and Sint Eustatius as extreme outliers showing almost no surge on land. When excluding these two small and mountainous countries, the relative deviation as opposed to the regional mean is about 20 to 30%, for return periods up to 1,000 years. This is considered quite a large range, which is mainly attributed to steep elevation on land, close to the coast. However, it is concluded that the output variable of surge inundation is less suited to express the spatial variation of surge between the countries, and that the employed elevation map of 0.5-km resolution was too coarse to adequately estimate experienced surge inundation.
The largest spatial variation is found for experienced precipitation, showing relative deviation of the maximums of the accumulated precipitation amounts per country, as opposed to the regional mean, of 150 to 240%, for return periods up to 40 years. Precipitation is only modelled for historical tracks. For a return period of five years, accumulated precipitation of 100 to 900 mm is shown over the islands. It is suspected that peak precipitation amounts are overestimated by the model in steep mountainous areas, and therefore also that the deviation based on the maximum values per country is overestimated. The clearest driver for high precipitation is the presence of high elevation differences in a country.
Ranking historical events on a multi-hazard tropical cyclone severity scale shows a higher score for many events, mainly driven by the occurrence of extreme precipitation. However, due to the limitations in both the surge modelling and the precipitation modelling, no further conclusions are drawn from this ranking.
To conclude, this study demonstrates that integrating parametric hazard models with synthetic track data can provide valuable regional-scale insights even in data-scarce environments. The findings support future integration of multi-hazard trigger models and cross-island early action coordination in the Caribbean context.

Table of contents

Nomenclature

Abbreviations

A list of abbreviations has been included for reference while reading the report. All abbreviations are spelled out when first used in the text. The list starts with general terms, and subsequently includes organisations. The abbreviations are listed alphabetically.

Abbreviation	**Definition**
AA	Anticipatory Action
DEM	Digital Elevation Model
EAP	Early Action Protocol
FbF	Financing-based Forecasting
IBF	Impact-based Forecasting
IBTrACS	International Best Track Archive for Client Stewardship
SCSSM	Simple Coastline Storm Surge Model
SIDS	Small Island Developing States
SLOSH	Sea Lake and Overland Surges from Hurricanes
STORM	Synthetic Tropical cyclOne geneRation Model
SSHWS	Saffir-Simpson Hurricane Wind Scale
TC	Tropical Cyclone
TCSS	Tropical Cyclone Severity Scale
CDEMA	Caribbean Disaster Emergency Management Agency
ECMWF	European Centre for Medium-Range Weather Forecasts
GADM	Database of Global Administrative Areas
IFRC	International Federation of Red Cross and Red Crescent societies
KNMI	Koninklijk Nederlands Meteorologisch Instituut
NLRC	NetherLands Red Cross
NOAA	National Oceanic and Atmospheric Administration
UNDRR	United Nations Office for Disaster Risk Reduction

1 Introduction

Tropical cyclones are considered the second-most dangerous natural hazards, after earthquakes. The World Meteorological Organisation states that in the 50-year period since 1970, daily 43 deaths and 78 million US dollars in damages have been caused by tropical cyclones and related hazards, worldwide. Climate change is linked to an increased likelihood of major hurricanes, and also to an increase in destructive power (World Meteorological Organization 2025b).

In another report of the World Meteorological Organisation, it is stated that in comparison to other hydrometeorological natural hazards, storms have caused the second-highest number of fatalities, including two devastating tropical cyclones in Bangladesh. Tropical cyclones have caused the greatest economic losses over the past five decades, followed by floods (World Meteorological Organization 2025a).

Early warnings and early action, also known as anticipatory action or forecast-based action, are believed to significantly reduce the impact of natural hazards such as tropical cyclones (abbreviated to TCs in this report). It stands as one of the best-proven and cost-effective methods for reducing disaster deaths and losses (UNDRR 2025a). In 2022, the UN Secretary-General launched the Early Warnings for All (EW4All) initiative, stating that:

> *"All people on Earth must be protected by early warning systems within five years."*

Together with the UN and other partners, the International Federation of Red Cross and Red Crescent Societies (IFRC) is working on this goal (IFRC 2025). Part of their work is the development of Early Action Protocols (EAPs). Currently, the IFRC has functioning EAPs in approximately 40 countries, on natural hazards such as riverine floods, coastal floods, droughts, and tropical storms. Each EAP requires a trigger model, which determines the activation of the anticipatory action included in the protocol. Trigger models can be based on hydrological models, real-time measurements, GloFAS, or other models.

The subject of this study is the characterisation of the spatial distribution of various hazards of tropical cyclones and what that means for the development of an Early Action Protocol and its trigger model on a regional level for tropical cyclones in the Caribbean. This chapter entails an introduction to this study. A general background outlines the relevance of extreme weather forecasting and disaster management in relation to natural hazards, already briefly introduced above. Subsequently, the position of this research as opposed to other studies and current developments and projects is described. The chapter concludes by stating the main research goal and the research questions.

1.1 Research context

This study contributes to a feasibility study on the development of a regional Early Action Protocol for tropical cyclones for three states in the Eastern Caribbean. This development complies with recent shifts in humanitarian aid, from solely post-disaster to the inclusion of pre-disaster measures. The relevance of anticipatory action and the different possibilities in designing such forecast-based protocols is outlined in this section. The vulnerability of these, and other, states, is highlighted thereafter.

1.1.1 Early warnings and anticipatory action

The availability of forecasts for large-scale weather systems has enabled early warning and anticipatory action for natural hazards (World Meteorological Organization 2025a). Since 1970, the number of disaster-related deaths has declined nearly threefold. An impressive reduction, especially when accounting for global population growth, thanks to improved early warning systems and disaster risk reduction strategies. A visualisation of the effect of anticipatory action is shown in Figure 1.1.

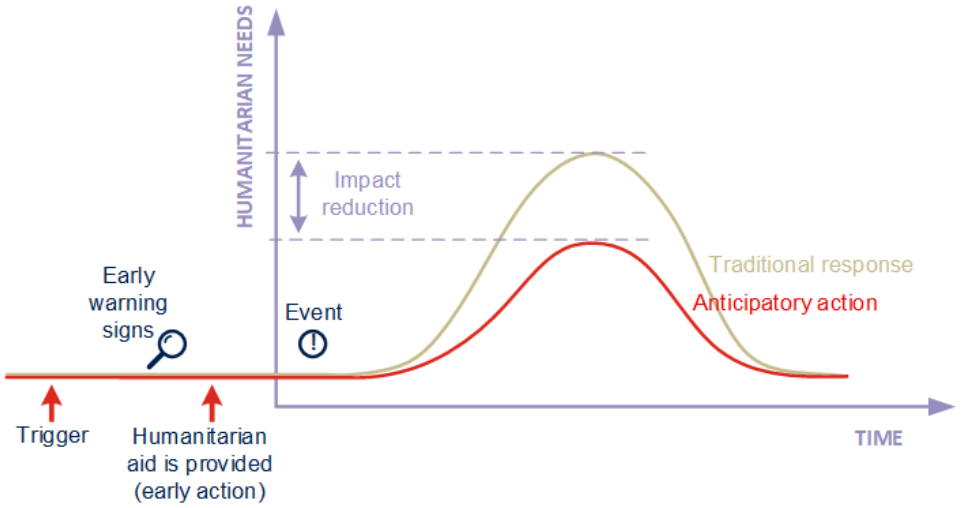

Figure 1.1. Visualisation of the potential reduction of humanitarian needs when applying anticipatory action as opposed to traditional emergency response, adapted from the Netherlands Red Cross.

Anticipatory action (AA) aims to prevent or mitigate disaster impacts through timely, constructive, and cost-effective measures (UN OCHA 2025). It typically relies on three core elements:

- pre-agreed triggers;
- pre-agreed activities;
- pre-arranged financing.

In other words, AA can be defined as pre-planned, forecast-based interventions that are formalised in protocols and backed by pre-arranged funding (Anticipation Hub 2023). A prerequisite is sufficient lead time and forecast skill. Some examples of anticipatory actions are the distribution of cash or relief goods, the evacuation of people, the sharing of climate information and advice, the upscaling of water-harvesting activities, and more. The starting point of an AA protocol is always the impact one wants to reduce by acting early.

1.1.2 Hazard-based or impact-based forecasting

The aim of early action is to reduce the impact of a disaster. Effective action, therefore, requires more than hazard data alone, as the impact of similar events can vary significantly depending on exposure and vulnerability. When early action protocols are based on predicted impacts rather than just hazard forecasts, this is known as Impact-Based Forecasting (IBF). IBF provides a more objective basis for targeted action, helping to reduce hazard impacts (Moraes 2024). In short, focusing on **what the weather will do**, its risks to people, livelihoods, and property, rather than solely on **what the weather will be**.

While traditional forecasts are hazard-based and focus solely on physical characteristics (rainfall, wind, etc.), impact-based forecasts translate these events into potential impacts (e.g., number of people affected, services disrupted) , (Bazo et al. 2021). Impact-based forecasts can help practitioners decide when, where, and how to act early and provide trigger actions. The trigger threshold can be defined by either

- predicted impact,

- or predicted weather and hazard, with the hazard-impact relationship established separately.

The trigger threshold should be defined carefully in order to prevent acting in vain or failing to act. The way impact-based trigger development relates to standard components of early warning systems is illustrated in Figure 1.2.

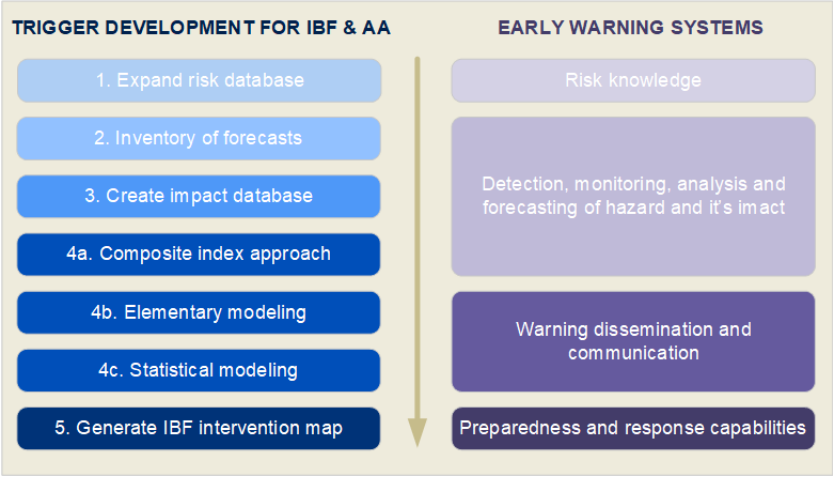

Figure 1.2. The five steps of trigger development for impact-based forecasting and anticipatory action, next to the four components of early warning systems. Step 4 describes three possible ways of impact-based forecasting. Adapted from (Homberg et al. 2025).

IBF is still a relatively new approach, and only a few fully operational impact-based forecasting and warning systems exist. A recent study of Harrison et al. (2025) evaluated the effectiveness of IBF and explored ways to refine impact-based threshold definitions. Their study concluded that effective systems require a combination of hazard information, exposure data, and vulnerability data to accurately assess risks and potential impacts on different communities. Implementing IBF systems also demands improved methods for collecting and storing comprehensive data on impacts, vulnerability, and societal capacity. One potential pitfall that is highlighted in this article is the urban-rural bias: focusing solely on exposure can result in rural areas receiving fewer warnings, even if the hazard poses a significant risk to the people present (Harrison et al. 2025).

1.1.3 Vulnerability of Small Island Developing States

The research context, geographically, is the Caribbean region. The region counts many small islands, of which many are considered Small Island Developing States (SIDS). This term, created by the United Nations, covers a total of 57 islands worldwide, of which 29 are situated in the Caribbean. The population of all SIDS together is 65 million, which is slightly less than 1% of the global population. Yet, this group faces disproportionate social, economic and environmental challenges. SIDS are very susceptible to extreme weather events, which are considered to increase due to climate change; an aspect highlighted in the feasibility report of the IFRC on regional forecast-based financing for hurricanes in the Eastern Caribbean. Shultz et al. (2019) state that the Caribbean SIDS are highly exposed to tropical storms, excessive rainfall, droughts, dry spells and heatwaves, as well as floods and landslides, while storm surge is enhanced by rising sea levels.

A good example of how big the impact of extreme weather events on a small island can be is shown by the impact of Hurricane Maria in 2017 on Dominica. The disaster caused losses of 1.3 billion US dollars, which is equivalent to 224% of the yearly Dominican Gross Domestic Product (World Bank Group 2025). Recovering after such an event is nearly impossible for SIDS without help, making them relatively more vulnerable. The United Nations Office of Disaster Risk Reduction (UNDRR) states that on average, SIDS experience 2.1% of GDP loss due to disasters, whereas other countries face an average of 0.3% of GDP. Also, about 18% of the total population is affected after each disaster in SIDS on average, compared to 6% in non-SIDS countries. The Sendai Framework for Disaster Risk Reduction 2015-2030, created by the UNDRR, highlights the need for disaster risk reduction as a key

priority for SIDS. Still, only 39% of SIDS have reported having a multi-hazard early warning system (UNDRR 2025b).

1.2 Position of this research

This section outlines the position of this research in regard to other studies and projects. Current practices of early action protocols, where the Red Cross plays a role, are outlined for tropical cyclones in the Philippines, Bangladesh, and Mozambique. These examples are given as exemplary applications of anticipatory action and hazard- or impact-based forecasting. Subsequently, the project currently focusing on the development of regional early action protocols in the Caribbean is introduced, which was the main motivation for this study.

1.2.1 Early action for tropical cyclones worldwide

Currently, three Early Action Protocols by the IFRC for tropical cyclones are active worldwide. In this section, they are introduced. All three EAPs are focused on only one country. Regional approaches, such as those proposed for the Caribbean, do not exist yet within the IFRC. A similarity between the protocols is the focus on impact reduction. The existing protocols differ in their trigger mechanisms (impact-based, hazard-linked-to-impact-based, or purely hazard-based). Additionally, none of the current EAPs focus on an island nation; a critical distinction, as TCs impact small islands differently than large mainland areas, since TCs barely experience overland decay of intensity. Another difference is given by the hazards that are included in the trigger. A focus on wind speeds reflects typical early action practices for tropical cyclones worldwide, where, only occasionally, other hazards than wind speed are included in the forecasts and triggers. Even though it is known that hazards such as storm surge and precipitation have a high impact, and that these hazards do not overlap perfectly with wind fields.

Early action in the Philippines

The Philippines is very prone to tropical cyclones. The impact of these natural hazards can be huge, especially when multiple events follow each other within a season. With the support of the German Red Cross, the 510 team has developed a typhoon impact forecasting model (IFRC 2019b). This model functions as the triggering mechanism for the EAP of the Philippines Red Cross Forecast-based Financing (FbF) project.
The IBF model uses machine learning to find patterns in historic events to predict the impact of an incoming typhoon. The model uses hazard, exposure, and vulnerability indicators (Forooshani et al. 2024).

- Hazard indicators include wind speed, typhoon track, rainfall and the susceptibility to storm surges and landslides. The wind speed and typhoon tracks are used to create parametric wind fields, resulting in the maximum wind speed on the municipality level.
- Vulnerability indicators include geo-spatial information such as slope, ruggedness, elevation and the length of the coast. Also, demographic properties are included, such as poverty percentage and building properties.
- Exposure indicators include the number of households per municipality and population density.

Early action in Bangladesh

Bangladesh lies north of the Bay of Bengal, which is known for its frequent and catastrophic tropical cyclones. The country experiences two cyclone seasons on a yearly basis: the pre-monsoon period of April and May, and the post-monsoon months of October and November, when the impact of these events is large. In the Early Action Protocol of the IFRC in 2021, it is stated that, during the 10 years prior, over a million people were affected by cyclones making landfall in the country.
The Early Action Protocol was revised, and the actions aim to reduce impact by providing people with an incentive to evacuate to the cyclone shelters. The Bangladesh Red Crescent Society (BDRCS) is the main actor to implement the protocol, but many more organisations are involved.

1. The trigger model is set on the primary hazard of cyclones, namely wind speed. The trigger is activated upon a forecast of a cyclone making landfall in Bangladesh's coastal districts with wind speeds of $125\ km/h$ or greater. This corresponds to a return period of approximately 1 in 5 years (IFRC 2021).

2. A wind speed reduction factor is applied to estimate the expected wind speeds after landfall.
3. The impact is predicted with the help op damage curves and a simulation done on buildings for identifying damage at different wind speeds. A damage curve is a relation between damage and hazard (in this case, wind speed) based on historical events. The early actions are prioritised based on a vulnerability index, calculated by a weighted overlay method (Sedhain et al. 2025).

To conclude, in this EAP the trigger is set on the hazard, and an impact forecast is made afterwards for further advice in the protocol. As opposed to the EAP in the Philippines, where the trigger itself is set on the impact forecast. These two options of impact-based forecasting are mentioned in Section 1.1.2.

Early action in Mozambique

The long coastline of Mozambique is highly exposed to extreme weather events. The southwest Indian Ocean is one of the most active cyclonic zones in the world. The TC season lasts from October to March. In their summary of the local current Early Action Protocol of the IFRC, it is stated that Mozambique was hit by at least thirteen cyclones with wind speeds above 120 km/h in the period 1984 to 2017.
The trigger is managed by the Mozambican management system INAM, which sends out different levels of alerts. The threshold for activation of the protocol is set on expected wind speeds of 120 km/h or above at landfall. Activation is based on forecast information at least 72 hours before landfall, at which the margin of error is approximately 240 km (IFRC 2019a). Therefore, this can be called a hazard-based trigger model. However, historical events and their respective impact are used to set the thresholds.
The focus within the impact reduction of the protocol is set on the destruction of houses, the destruction of classrooms, and an increase in endemic diseases (IFRC 2019a).

1.2.2 PARATUS project

This study aims to contribute to the role of the Netherlands Red Cross Data and Digital team 510 (in this report referred to as 510) in the PARATUS project. The PARATUS project, funded by EU Horizon, is a consortium of 20 partners, led by ITC, the Faculty of Geo-Information Science and Earth Observation of the University of Twente.

> The 510 team is the Netherlands Red Cross's data and digital team. The team was established in 2016 and currently consists of more than 100 team members, of whom approximately half are professional volunteers or academic students (The Netherlands Red Cross 510 2025). The goal of the team is to *"improve speed, quality and cost-effectiveness of humanitarian aid by creating products and services using data and digital"*. The team focuses on five key thematic areas: anticipatory action, cash & voucher assistance, community engagement & accountability, emergency support, and water & landscape. This project is related to the Anticipatory Action team, which aims to *"enable National Societies of the Red Cross worldwide and local humanitarian partners to leverage data and technology to make data-driven, life-saving decisions and act before disasters strike" (The Netherlands Red Cross 510 2025)*.

The PARATUS project focuses on assessing complex hazard interactions and their resulting impacts, including how future scenarios could change impacts. The aim is to co-design multi-hazard impact scenarios with stakeholders (PARATUS-EU 2025). Specifically, four case study areas are chosen: the Caribbean, Romania, Istanbul, and the Alpine areas, all prone to multiple and interacting hazards. The Caribbean is seen as one of the most disaster-prone regions in the world. The hazards selected in this project include volcanic eruptions, COVID-19 pandemic, tropical cyclones and floods. It is stated that for effective anticipatory action, especially during the hurricane season, the development of a regional standard operating procedure, such as an Early Action Protocol (EAP), is required (NRC 510 and FRC PIRAC 2025).

Currently, work is being done on a regional EAP by a collaboration between NLRC's Data and Digital team and the French Red Cross's reference centre in the Caribbean, Plateforme d'Intervention Régionale d'Amériques-Caraïbes (PIRAC), as well as the Red Cross National Societies of Saint Kitts & Nevis, Antigua & Barbuda and Dominica. These three island states represent the focus area of an EAP development within PARATUS.

Stakeholder consultations revealed that the key contribution of the PARATUS project is the definition of triggers at a **regional** rather than a **national** level. Consequently, this study concentrates on investigating the feasibility of this regional trigger approach.

1.3 Research goal

The main research question is defined as:

How can the spatial distribution of wind speeds, storm surge, and precipitation from tropical cyclones be quantified for the Leeward Islands in the Caribbean?

This main research question is addressed through a set of sub-research questions.

1. What are the spatial distributions and return periods of maximum wind speeds, from historical and synthetic tropical cyclone tracks?
2. What are the spatial distributions and return periods of storm surge heights, from historical and synthetic tropical cyclone tracks?
3. What are the spatial distributions and return periods of extreme precipitation, from historical tropical cyclone tracks?
4. How do historical tropical cyclone rankings vary between the multi-hazard tropical cyclone scale TCSS and the wind speed-oriented scale SSHWS, for the Leeward Islands?

2 Theoretical background

This chapter provides the theoretical framework for the study. It first outlines the formation and characteristics of TCs, followed by a geographical introduction to the Caribbean region, its vulnerability, and relevant disaster management stakeholders. Finally, the rationale for the regional scope, focusing on the feasibility of regional trigger models for the Caribbean, is discussed.

2.1 Tropical cyclones

This study focuses on the impact of tropical cyclones on the Caribbean. Tropical cyclones are severe whirlwinds that can cause devastating wind speeds, significant storm surges, strong and high waves, extreme precipitation and landslides (KNMI Kennis- & Datacentrum 2025).
Tropical cyclones develop above tropical oceans; around the equator, between the tropic of Cancer and the tropic of Capricorn, see Figure 2.1. In order to form, a large body of water is required with a minimum surface temperature of 26.5 degrees Celsius. Then, the rate of increase of saturation due to absorption of latent heat becomes high enough (Wallace and Hobbs 2006). A tropical cyclone derives its potential energy from these fluxes of latent and sensible heat at the sea-air interface.

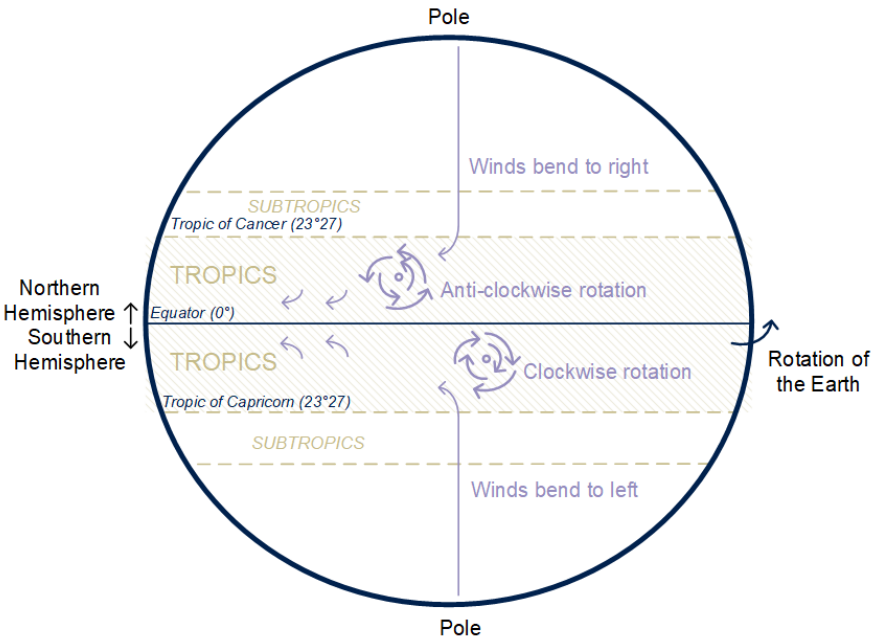

Figure 2.1. Tropical cyclone formation: position and rotation on Earth.

Tropical cyclones are named differently worldwide.

- On the Indian Ocean, the Bay of Bengal, the Arabian Sea, and the western South Pacific Ocean, they are called (severe) tropical cyclones;

- in Australia, they are called Willy Willies;
- in America, coming from the North Atlantic Ocean, the eastern and central North Pacific Ocean, the Gulf of Mexico and the Caribbean Sea, they are called hurricanes;
- and lastly, in East Asia, coming from the western North Pacific Ocean, typhoons.

In total, approximately 85 tropical storms develop annually worldwide, of which more than half intensify into tropical cyclones, as is stated by (World Meteorological Organization 2025b). 72% of these tropical cyclones form in the Northern Hemisphere, occurring between July and October (summer period, with most sunshine). In the Southern Hemisphere, the season is from December to March.
Due to the Coriolis effect, caused by the rotation of the Earth, the large storm systems become whirlwinds, going anti-clockwise in the Northern hemisphere and clockwise below the equator, see Figure 2.1. Typically, a TC travels about a week westward and then turns poleward (Wallace and Hobbs 2006). On average, a TC travels at a speed of about 5 to 10 meters per second.

2.1.1 Tropical cyclone formation

In the tropics, due to the high temperatures, low-pressure areas form, which attract wind from higher-pressure areas. In the eye of a tropical cyclone, exceptionally low pressures can be reached, with Typhoon Tip (1979) holding the record of 870 hPa (Wallace and Hobbs 2006), as opposed to normal sea-level pressure, which is around 1013 hPa. The rotating system of clouds and wind is centred around the eye of the storm, where conditions are calm and cool air descends. The eye has a diameter of 30 to 50 kilometres (Claassen 2021). Around the eye, there is the eye wall, along which warm air rises. The eye is known for its warm and moist air below, and dry air above (Wallace and Hobbs 2006). The eye wall gives the most extreme weather conditions, including the maximum wind speeds. In the outer bands, air rises. A cross-section of a TC is illustrated in Figure 2.2.

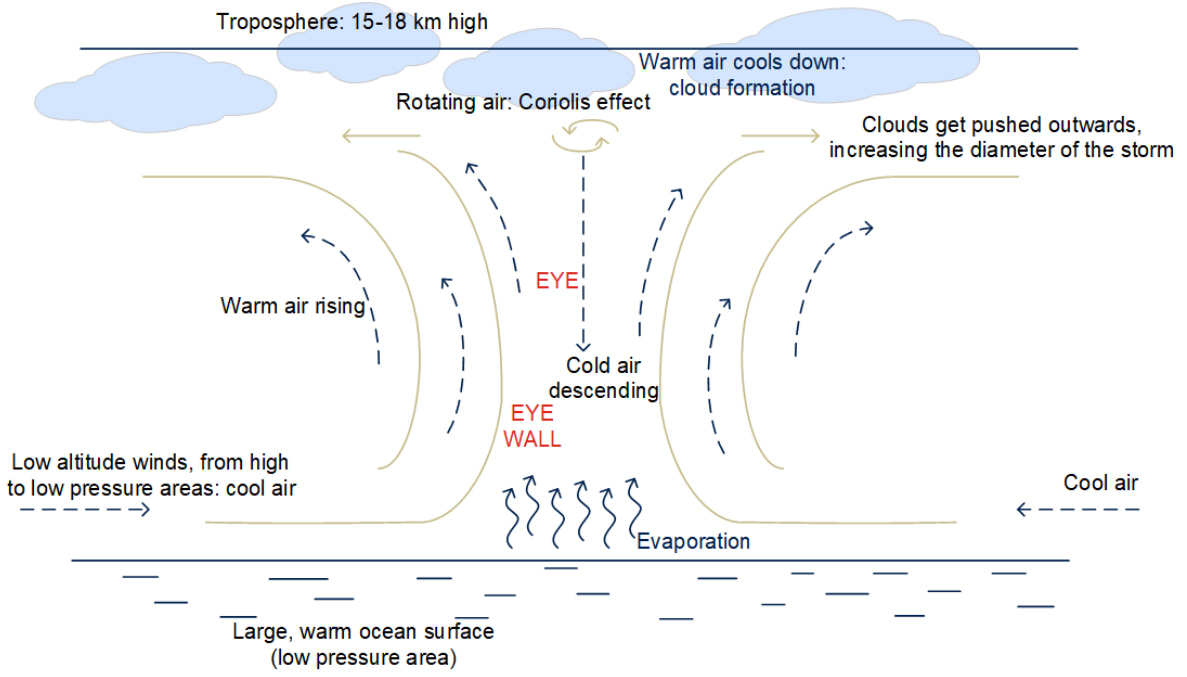

Figure 2.2. Tropical cyclone system: a cross-section.

When reaching the top of the cyclone, the warm and humid air cools down and forms clouds, which are pushed outwards due to the rotation of the system. The radius of the storm increases when the storm grows and can typically span 200 to 500 km, up to a diameter of 1000 km (Claassen 2021). Powered by the low-altitude winds and the heat from the water body, they can last from 24 hours to as long as a month or even weeks. A tropical cyclone comes to its end when either:

- The system has travelled polewards where the ocean surface temperatures become too low to supply sufficient latent and sensible heat;
- or the storm has encountered land, where it can transform within hours due to a lack of moisture and therefore latent heat supply from the air-sea interface. The centre cannot sustain its low pressure, and the depression fills up. The circulation will slow down due to friction (Wallace and Hobbs 2006).

However, the moist core remains intact after reaching land, causing a risk of flooding for storms with low speed, when large precipitation amounts fall within one watershed. Some tropical cyclones turn into, or attach to, extratropical cyclones (Wallace and Hobbs 2006).

2.1.2 Effects of climate change

Climate change has contributed to the increased frequency of extreme weather and climate events, such as temperature extremes, heavy precipitation, pluvial and river floods, droughts, storms and compound events. The latest IPCC report states that for tropical cyclones, it is likely that the global proportion of category 3-5 TCs has increased over the past four decades. Additionally, it is stated that average and maximum rain rates associated with TCs increase with global warming, as well as average TC peak wind speeds and the most intense TC peak wind speeds (IPCC 2021).
A new study in 2025 has provided new insights into the occurrence of clustered tropical cyclones. By this, the presence of multiple tropical cyclones within one ocean basin is meant, which dynamically interact (thus not being completely independent). The study states that, based on probabilistic modelling, a tenfold increase in the likelihood of tropical cyclone cluster frequency has occurred in the North Atlantic (the TC ocean basin bordering the Caribbean), from 1.4 ± 0.4% to 14.3 ± 1.2% over the past 46 years (Fu et al. 2025). Clustered TCs can lead to compound hazards at one place, for which the impact will increase drastically.

2.1.3 Related hazards

As mentioned above, tropical cyclones are associated with many hazards.

1. A tropical cyclone is characterised by its very high wind speed and the size of the storm. This is considered the primary hazard, and can lead to damage to buildings, infrastructure and nature (KNMI Kennis- & Datacentrum 2025). The winds in a TC are the superposition of the cyclonic circulation and the movement of the storm itself (Wallace and Hobbs 2006).
2. The shoreward wind, wind-driven onshore current (can go up to meters), combined with low air pressure being compensated by a rise of sea level (approximately 1 m per 100 hPa), will lead to storm surge, a temporary rise in sea level beneath a storm (Wallace and Hobbs 2006). The tide can both exacerbate and reduce the severity of storm surge. A storm surge coinciding with high tide is called a storm tide. Additionally, river runoffs from rain-swollen rivers lead to coastal sea level rise (Wallace and Hobbs 2006). Storm surge can become dangerous when the storm reaches land, where it can lead to flooding, land erosion, damage to buildings and saltwater intrusion. The risk associated with storm surge depends on the length of the coast, and also the track of the TC relative to the coastline (Science Education 2025).
3. Another characteristic of a tropical cyclone is the high amount of precipitation it contains. Rainfall is found in the outer bands, and so-called rain bands, far away from the storm centre (Wallace and Hobbs 2006). Extreme rainfall can lead to high river discharges, flash floods, flood inundation, and it can trigger landslides and mudslides. The occurrence of these hazards has to do with geographical characteristics of a region, like steepness, soil type, elevation, and soil moisture content (World Meteorological Organization 2025b).

A study on the spatial-temporal variability of TC-related rainfall in the Caribbean Lesser Antilles confirms that precipitation fields don't overlap with wind fields, and therefore should be incorporated in risk forecasts. Similar winds can lead to different precipitation amounts as well as flood depths depending on the slice of the storm that hits a region. Determining risk scenarios only on wind, while not including precipitation, can both lead to under- and overestimating impact (Nabukulu, Jetten, and Ettema 2024).

2.1.4 Scaling of tropical cyclones

Tropical cyclones are categorised in severity using the Saffir-Simpson hurricane wind scale (SSHWS), which is based on the measured maximum wind speed. It can be categorised from 1 to 5, where 5 indicates very severe. A category 0 is given to tropical storms (a severe storm, but less severe than tropical cyclones), for wind speeds of 18 to 33 m/s. Below those wind speeds, a system can be called a tropical depression. From category 1 onwards, the wind speeds exceed the Beaufort scale, which scales all tropical cyclones with a wind force of 12.

Table 2.1. Saffir-Simpson hurricane wind scale, adapted from KNMI Kennis- & Datacentrum (), with damage as is described by the National Hurricane Center.

Category	Wind speed (m/s)	Description	Damage
1	33-42	Weak	Mostly light damage
2	43-49	Moderate	Roof and window damage, significant damage to trees and crops
3	50-58	Strong	Major damage with extensive destruction to buildings
4	59-69	Very strong	Very severe: roofs blown off, significant water damage on ground floors of coastal buildings
5	more than 70	Devastating	Catastrophic: nearly all roofs blown off, small lighter structures destroyed

In 2021, Nadia Bloemendaal et al. published an alternative scale to reflect the severity of tropical cyclones, called the new Tropical Cyclone Severity Scale (TCSS). Where the Saffir-Simpson Hurricane Wind Scale only includes the wind hazard of a TC, the new proposed scale aims to represent the TC's total severity, as tropical cyclones can also cause severe conditions through their high storm surges and extreme rainfall. By stating examples like Hurricane Harvey (2017), which ranked as a Tropical Storm (Category 0) on the SSHWS, but caused precipitation up to totals exceeding 1.5 meters, and caused high impact in the Houston area, Bloemendaal shows how risk communication can be challenging using the SSHWS (Bloemendaal, Moel, Mol, et al. 2021).
The new TCSS includes three major TC hazards, being wind, storm surge, and precipitation, in its classification and uses the same categories as the SSHWS for recognition and familiarity. Category 1 represents moderate damage, and Category 5 represents catastrophic damage. The thresholds for the categories are based on recorded impacts of historical events. The thresholds and categories are included in Table 2.2.

Table 2.2. The thresholds and categories for the three hazards included in the Tropical Cyclone Severity Scale (Bloemendaal, Moel, Mol, et al. 2021).

Category	Wind speed (m/s)	Storm surge (m)	Accumulated rainfall (mm)
0	less than 33	less than 0.75	less than 100
1	33-42	0.75-1.54	100-262
2	43-49	1.55-2.34	263-425
3	50-58	2.35-3.14	426-588
4	59-69	3.15-3.99	589-749
5	more than 70	more than 4.00	more than 750

The methodology on how to define a total score is explained by Bloemendaal, Moel, Mol, et al. (2021). The categorisations for the separate hazards are combined to communicate risk levels to the general public. The scores are rescaled such that the total categories maintain a list of constraints. Events scoring high in all three of the hazard classifications score a final Category 6. As can be seen in Table 2.1 and 2.2, are the thresholds for the hazard of high wind speeds equal. The other two hazards are classified such that for historical events in the North Atlantic basin, the impact as given in the description and damage per category in Table 2.1, are similar. The highest and lowest thresholds are determined for known high-impact and low-impact events for that specific hazard. The categories in between are

equally distributed.

Table 2.3. The thresholds and categories for the sum of rescaled values for the categories per hazard in the Tropical Cyclone Severity Scale (Bloemendaal, Moel, Mol, et al. 2021).

Category	Sum of rescaling values
0	less than 0.5
1	0.5-2.4
2	2.5-8
3	9-17
4	18-39
5	40-80
6	more than 80

A set of constraints was designed to which the total categories should comply. In short, these are:

- The final category can not be lower than the highest of the categories per hazard;
- the categories per hazard should increment to higher final categories, for example, a 3-3-1 score should result in a 4 score;
- an additional category 6 is used to represent high categories in multiple hazards, where two 5 scores should result in a 6 score, or two 4 scores and one 5 score should result in a 6 score.

These constraints resulted in the following rescaling factors: A category 0 is rescaled to a score of 0; a category 1 is rescaled to 0.5; a category 2 is rescaled to 2.5; a category 3 is rescaled to 9; a category 4 is rescaled to 20; and a category 5 is rescaled to 40. These rescaled scores are summed and then translated to discrete categories, see Table 2.3.
For the top-20 costliest U.S. hurricanes, the TCSS scores are higher than the SSHWS scores, hence better reflecting the relationship between TC severity and potential impact. The hazard data is collected for wind speeds by combining satellite data, aircraft flights (the 'Hurricane Hunters'), ship reports, radars, automated weather stations, and ocean buoys. For surge levels, tide gauge stations (of the NOAA) and high-water mark surveys are used. Accumulated rainfall is retrieved from rainfall measurement stations. The TCSS is set up to assign scores to tropical cyclones pre-landfall by only including parameters that are also given in forecasts.

Limitations of this new scale are mentioned by (Bloemendaal, Moel, Mol, et al. 2021) and include, among others, that further improvement on the thresholds is possible, as well as confirming thresholds scaled to other basins. More events with known impact per hazard could be used for this. Additionally, more research could be done towards the advantages and disadvantages of communicating only one category per storm, representing the total expected severity, or communicating categories per hazard. Finally, it is stated that compound effects of multiple hazards are not included in the classification.

2.2 Regional context

The Caribbean region includes the Caribbean Sea, a portion of the North Atlantic Ocean, and the many islands within this area. Several mainland countries, such as Belize, Suriname, Guyana, and French Guiana, are also considered part of the Caribbean, culturally and historically. Similarly, certain coastal areas of other countries bordering the Caribbean Sea share this regional identity.

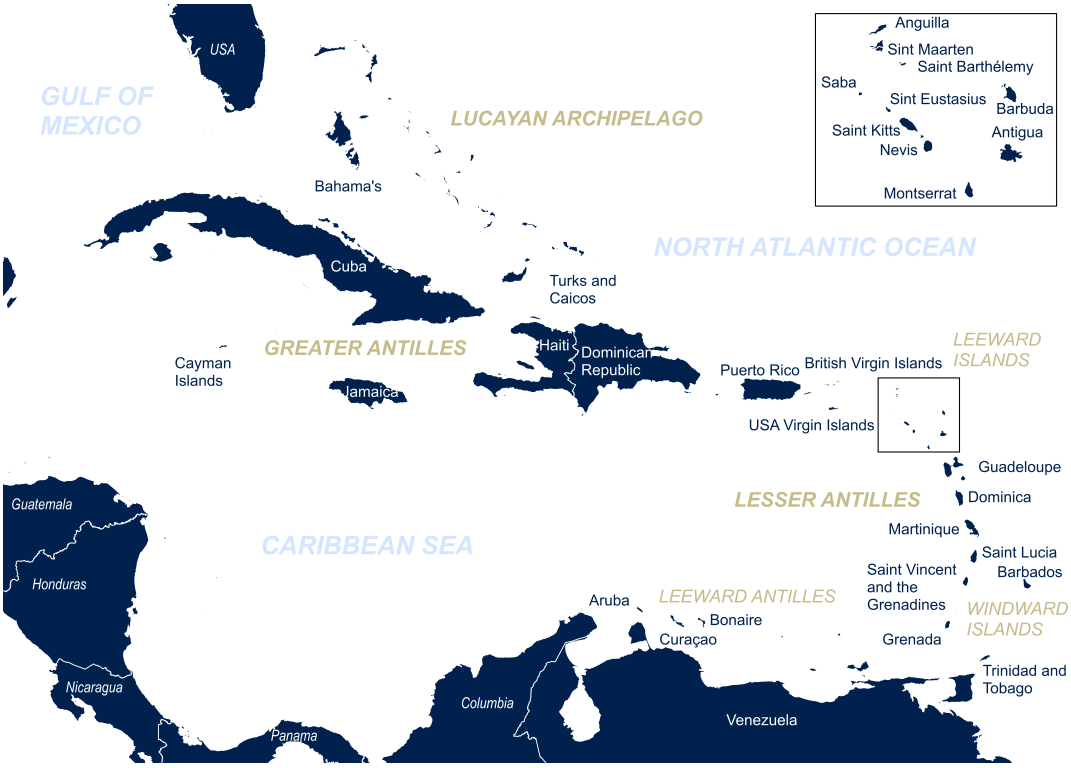

Figure 2.3. Map of the Caribbean and its geographical groups (names in brown), adapted from (geoBoundaries n.d.). The inset gives a zoomed-in view of a part of the Leeward Islands, included for readability.

When talking about the islands only, the name West Indies is used as well (Worldatlas 2025). When excluding the Lucayan Archipelago (the Bahamas and the Turks and Caicos Islands), the islands are also known as the Antilles. The Antilles can be separated into two main groups: (a) the Greater Antilles, which include the larger islands of Cuba, Jamaica, Hispaniola (Haiti and the Dominican Republic), and Puerto Rico, and (b) the Lesser Antilles, which include the smaller islands to the east and south of the Greater Antilles. Additionally, within the Lesser Antilles, some island groups are geographically distinguished, namely the Leeward Islands, the Windward Islands, and the Leeward Antilles. The first two together form the Eastern Caribbean states, where the Leeward Islands are the northern half, from the Virgin Islands down to Dominica, and the Windward Islands are the southern half, from Martinique down to Grenada, and sometimes also including Barbados and Trinidad and Tobago. Along the Venezuelan coast, the island chain is distinguished as the Leeward Antilles, including the Dutch ABC Islands and the Venezuelan islands. Figure 2.3 shows a map of the Caribbean region.

In the region, including many small states, various intergovernmental organisations are active. These organisations, and the roles they play concerning weather forecasts and disaster risk reduction, are introduced in Appendix A.

2.2.1 Local forecasting providers and stakeholders

On tropical cyclones, mainly two types of forecasts can be identified. For both forecasting types, it is common for national meteorological stations to combine information from (multiple) external organisations, and internal measurements and calculations (IFRC Climate Centre 2022). In this paragraph, the types of forecast information and the exact given parameters are discussed, and some of the providers are mentioned.

Seasonal forecasts

The Atlantic hurricane season runs from June until November. On an ocean basin-wide level (like the North Atlantic), a forecast is made on the Accumulated Cyclone Energy (ACE) of the season. The ACE index is a metric used to express the energy of a specific storm during its lifetime, or of a group of storms (Bell and Chelliah 2005). It is calculated by summing the squares of the maximum sustained

wind speed (in knots) every six hours for storms at or above tropical storm strength (34 knots).

$$ACE = 10^{-4} \sum v_{max}^2, (v_{max} \geq 34kn) \tag{2.1}$$

The ACE index is often used to express the total activity of tropical cyclones per basin, or per region. When considering the North Atlantic Ocean as a basin, the seasonal ACE index is the sum of all ACE values of all storms in the basin for the entire season. ACE reflects both the intensity and duration of tropical cyclones, making it a widely used metric for comparing seasonal or regional cyclone activity. Usually, the total number is divided by 10,000 for a more manageable scale. When forecasting the ACE index for a season and a certain basin, this is usually done probabilistically. For example, NOAA's outlook for the 2025 Atlantic Hurricane Season stated a 50% chance of an above-normal season, a 35% chance for a near-normal season and a 15% chance for a below-normal season (Climate Prediction Centre 2025).
According to the feasibility study on EAP development for TCs in the Eastern Caribbean, there are three main providers for the seasonal forecast: NOAA's Climate Prediction Center, the Department of Atmospheric Science of Colorado State University, and the Tropical Storm Risks developed at University College, London. All of them issue a forecast multiple times per season. The feasibility study, however, indicates that the seasonal ACE index is not an appropriate parameter for anticipatory action (IFRC Climate Centre 2022). The islands should prepare on a seasonal basis every year, and the seasonal forecast might lead to an underestimation of the season, since a single significant event is enough to cause a catastrophic impact on a small island.

Active storms

After a storm has been recognised and named, a storm-specific forecast is given. In general, this forecast includes the estimated track, maximum sustained wind speed, and minimum pressure. Some providers also provide storm surge estimates, probabilities of certain wind speeds, and probabilities of the timing of landfall. Some providers include an estimated uncertainty of the forecast, and sometimes the overall forecast is accompanied by an uncertainty range of past forecasts. The storm forecast is given for the next five days. The NOAA is one of the main providers of short-term storm forecasts for the Caribbean (IFRC Climate Centre 2022). The Caribbean Institute for Meteorology and Hydrology (CIMH) also provides a regional weather forecast, partly based on the global numerical weather predictions (IFRC Climate Centre 2022). This model runs twice daily and provides a lead time of 48 hours. The Caribbean Dewetra Platform combines two regional forecasts and the catastrophe risk modelling of the CCRIF to provide real-time risk monitoring and impact-based forecasting at local levels, in order to support disaster risk management.

3 Data

All data that is employed is outlined in this chapter, including any pre-processing steps. The main data consists of tropical cyclone tracks that are either historically observed or synthetically generated. Additionally, some bathymetry and elevation data of the study are is employed, as well as some historical climate data.

3.1 Historical and synthetic tropical cyclone track-related data

Both historical and artificially generated storms are utilised in this study. While synthetic data offers a statistically valuable longer dataset, historical data allow for validation against observed data and for combination based on location and time.

3.1.1 Historical tropical cyclone tracks

The dataset IBTrACS has been selected as historical TC tracks. IBTrACS provides a best-track database, which combines tracks from multiple sources and averages them to obtain the best track. The provided parameters, as well as the interval, vary over the TC basins worldwide and depend on the reporting agencies. A storm ID, year, basin, latitude and longitude, and some sort of wind speed parameter are always included (National Oceanic and Atmospheric Administration 2025b).

> The International Best Track Archive for Climate Stewardship (IBTrACS) merges historical tropical cyclone data from multiple agencies to create a publicly available global, best track tropical storm database. The database is developed collaboratively between various stakeholders (National Oceanic and Atmospheric Administration 2025b). Observed track and wind speed of a tropical storm can vary between agencies, as different metrics are used for calculations. IBTrACS averages these differences and gives the mean position, original intensities from the agencies, and provides summary statistics, instead of preferentially selecting one track and intensity (Knapp et al. 2010).
> Another possible source is HURDAT2; the hurricane database of the NOAA. The National Oceanic and Atmospheric Administration (NOAA) is a governmental agency of the United States, which governs the forecasting of weather, atmospheric and oceanic conditions, and manages and protects sea life (National Oceanic and Atmospheric Administration 2025a). It contains Atlantic hurricanes from 1851 to 2024. The dataset is in text format, and includes six-hourly data on the location, maximum winds, central pressure, and (since 2004) the size of all known tropical and subtropical cyclones (NOAA Hurricane Research Division 2025). The HURDAT2 dataset isn't included in the analysis, since over 99% of the IBTrACS data points for the Caribbean come from HURDAT2.

The time period 1940 - 2024 is used; a total of 85 years. In total, approximately 1,000 tracks are included in IBTrACS over that period, in the North Atlantic basin, ranked as at least a Tropical Storm (category 0). For data handling purposes, a pre-selection is made such that only tracks passing the region of interest are included:

- For the wind speed modelling and storm surge modelling: all tracks passing the region around the Leeward Islands. This region is defined as anywhere between 58 and 69 degrees North, and 12 and 21 degrees East. Resulting in 209 included tracks.
- For the precipitation modelling, the region is expanded to ensure all storms affecting the study area are included: all tracks passing anywhere between 55 and 85 degrees North and 10 and 25 degrees East. Resulting in 443 included tracks.

3.1.2 Synthetic tropical cyclone tracks

This study explores the possible applications of large synthetic datasets, in this case, the dataset STORM. The KNMI developed STORM in 2020 and has extended the dataset over the past years with extreme value analyses and additional datasets for future climate scenarios (Bloemendaal, Muis, et al. 2018). The study group is currently focusing on additional hazards of tropical cyclones. Synthetic tracks are commonly used in hazard mapping, since a variation of scenarios can be considered. Another common use of synthetic data is to dive into the consequences of climate change. Synthetic data can be generated based on climate scenarios. However, the effects of climate change are not included in this study.

STORM is available as a set of ten txt files, each containing 1,000 years of TC tracks, generated by the STORM algorithm. There is a set for each of the basins worldwide; in this study, only the North Atlantic basin is considered.

Each track is provided at 3-hourly time steps. The parameters are: year (starting at 0 in each txt file), month, a TC number, basin ID, latitude, longitude, minimum pressure, maximum wind speed, radius to maximum winds, category, landfall (yes or no), and the distance to land (Bloemendaal, Haigh, et al. 2020).

Nadia Bloemendaal of the KNMI has generated a dataset of 10,000 years of hurricane tracks under present climate conditions, using the Synthetic Tropical cyclOne geneRation Model (STORM) algorithm, introduced in (Bloemendaal, Haigh, et al. 2020). The input was 38 years of historical meteorological data from the International Best Track Archive for Climate Stewardship (IB-TrACS), which is the most comprehensive global dataset containing six hurricane basins. This synthetic data enables the use of stochastic models. STORM contains for each hurricane: The position of the eye, the maximum wind speed, the radius to maximum wind, the minimum pressure at a three-hour time step, and the month and year.

3.2 Elevation and bathymetry data required for storm surge and precipitation modelling

The modelling of both storm surge and precipitation requires bathymetry and/or elevation data of the study area. This study employed the SRTM15Plus dataset, which provides high-resolution bathymetry and topography of approximately 500 by 500 meters.

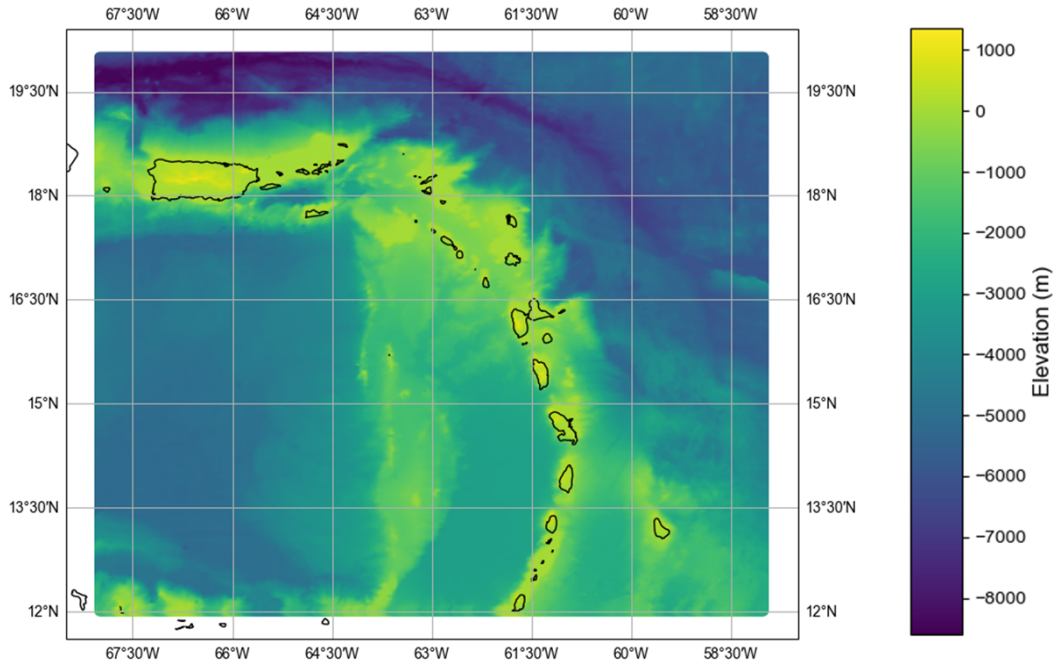

Figure 3.1. Digital elevation model of the countries and bathymetry of the surroundings of the geographical scope. Data extracted from SRTM15+ and plot created using CLIMADA.

Figure 3.1 shows the elevation and bathymetry of the Leeward Islands and surroundings, used as input for the storm surge modelling. In total, the elevation ranges from approximately -8600 meters below sea level in the waters north of Puerto Rico, to approximately +1360 meters above sea level in Guadeloupe. Digital Elevation Models often include holes, or so-called sinks, in their data. Within the QGIS software, the application Fill Sinks (Wang & Liu) is applied to smooth the model. The SRTM15+ data is used at its maximum resolution of 0.0042 degrees (approximately 500 by 500 meters) when modelling storm surge, but at a lower resolution of 0.045 degrees when modelling precipitation.

Modelling of TC-related precipitation requires drag coefficients as well. These drag coefficients for wind are based on surface roughness, depending on land use and geophysical aspects. CLIMADA provides default data sets (ETH Zürich 2025) from ERA5, which were further assessed by Feldmann et al. (2019). This default data is used, hence no additional data sources are considered for the drag coefficients.

3.3 Climate parameters required for precipitation modelling

The modelling steps for TC-related precipitation require additional climate parameters (ETH Zürich 2025), namely the along-track temperature in the storm centre and the along-track wind speeds over an annulus around the storm centre. Due to the need for additional climate parameters in the TCR model, it is not possible to model precipitation for synthetic TC tracks, as for these tracks, no additional climate parameters are available. The two climate parameters are taken from the climate reanalysis dataset ERA5 of the ECMWF.

> ERA5 is an atmospheric reanalysis of the climate from ECMWF, the European Centre for Medium-range Weather Forecast (European Centre for Medium-Range Weather Forecasts 2025). The ERA5 provides estimated hourly values for a large number of atmospheric parameters, at a 0.25 by 0.25 degrees resolution (around 25 km, near the equator). ERA5 is openly available and contains climate data from 1940 to the present (Copernicus 2025).

Along-track 600 hPa temperature at the storm centre

For each tropical cyclone track, climate reanalysis data from ERA5 are retrieved for the full duration of the storm across the study area. The temperature corresponding to a pressure level of 600 hPa is extracted at the storm centre for all points and time steps along the track. This temperature data is then added as an additional parameter to the track dataset.

Along-track 850 hPa wind speeds averaged over an annulus of 200-500 km around the storm centre

For each tropical cyclone track, the same ERA5 selection is used to extract the u- and v-components of wind speed at a height of 850 hPa, as an average value over an annulus of 200 to 500 kilometres around the storm centre, for each point and time step of the track. In order to calculate the distance to the eye of the storm, the Haversine method is applied. The u-component is called the zonal wind speed and describes wind speed in an east-west direction. The v-component is known as meridional wind speed and describes the north-south wind speed. Both parameters are added as parameters of the track dataset. A modelled wind field using the Holland model is available as well; however, this represents wind speeds at 10 meters from the ground, and in the precipitation modelling, wind speed at a height of 850 hPa is required as well.

4 Methodology

Tropical cyclones lead to three main hazards, defined as high wind speeds, storm surge, and extreme precipitation. These three hazards were modelled for both historical and synthetic tracks, all following a similar structure, which is summarised in Figure 4.1.

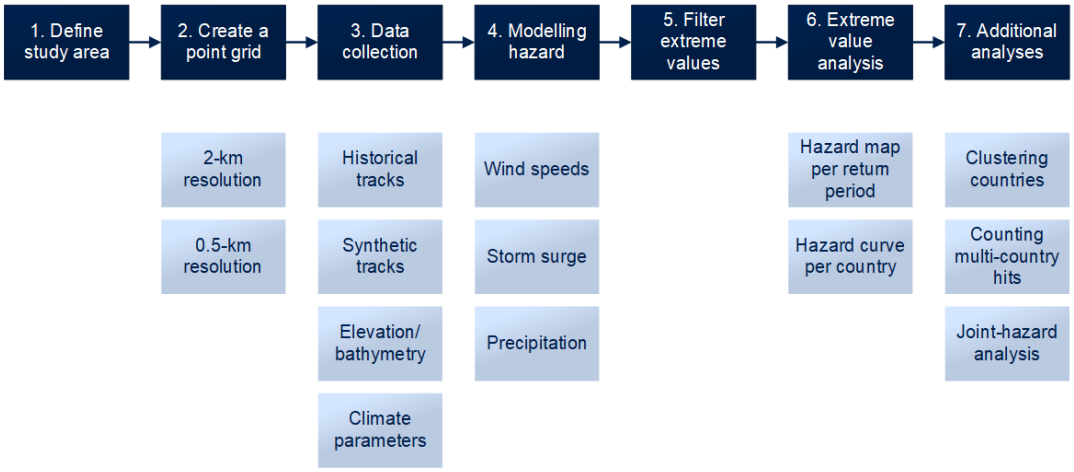

Figure 4.1. Step-by-step overview of the methodology of this study. Per step, different options are included.

In this chapter, the methodology of these steps is outlined. Additional information is added in separate boxes for clarification. Furthermore, the ratio of the number of countries that are affected by a single storm is outlined, based on the hazard of high wind speeds. For historical tracks, a ranking is given for two different tropical cyclone scales, of which one only includes wind speeds, and one includes all three hazards.

Data collection

Table 4.1 provides an overview of the input used per modelling step.

Table 4.1. Overview of the used input for the three hazards that are modelled, per hazard.

		Wind speeds	Storm surge	Precipitation
Grid resolution	2 kilometres	x		x
	0.5 kilometres		x	
Data input	Historical TC tracks	x	x	x
	Synthetic TC tracks	x	x	
	Elevation/bathymetry maps		x	x
	Climate parameters			x

Either a grid of 2-km resolution or 0.5-km resolution is used to model the hazard for the countries. The hazards are modelled for both historical and synthetic tracks; however, the use of synthetic tracks for the precipitation modelling is not possible. Both the precipitation modelling and the storm surge modelling require some additional data inputs, also given in Table 4.1.

4.1 Geographical scope

The geographical scope of this study is set on the island states Puerto Rico, U.S. Virgin Islands, British Virgin Islands, Anguilla, Sint Maarten, Saint Martin, Saint Barthélemy, Saba and Sint Eustatius, Antigua and Barbuda, Saint Kitts and Nevis, Montserrat, Guadeloupe, Dominica, and Martinique. These fourteen countries are together referred to as the Leeward Islands in this report. In reality, the Leeward Islands are commonly defined as Dominica up to the Virgin Islands. The scope is visualised in Figure 4.2.
The study also aims to contribute to the PARATUS project, which focuses on the development of a regional Early Action Protocol for the three states, Saint Kitts and Nevis, Antigua and Barbuda, and Dominica. These three states all lie within the Leeward Islands.

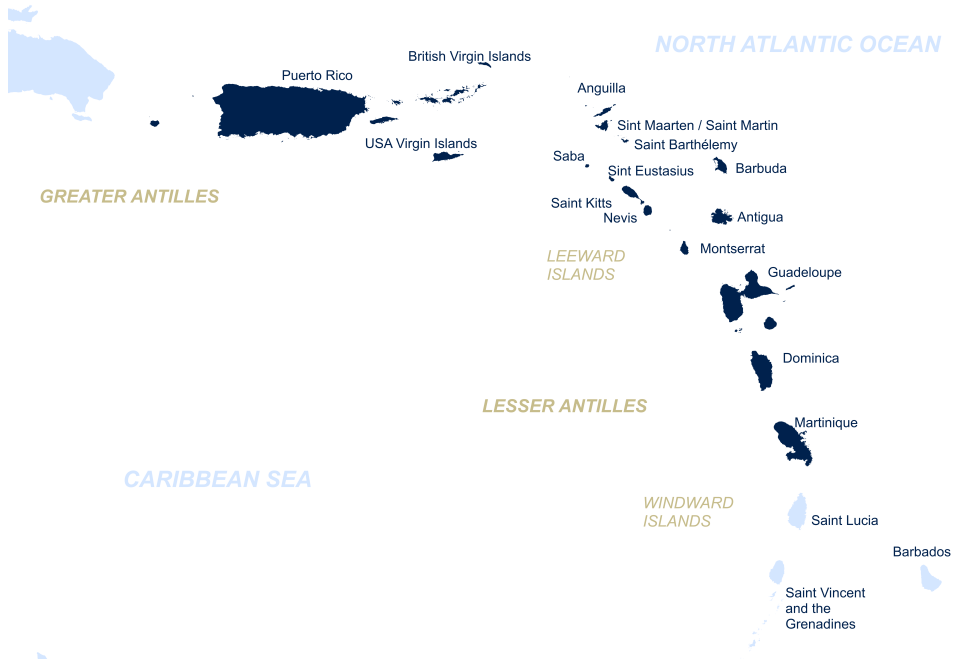

Figure 4.2. Chosen geographical scope, represented by the dark-blue countries. These are approximately the Leeward Islands, ranging from Puerto Rico to Martinique. Country boundaries adapted from geoBoundaries ().

4.1.1 Selecting a study area

A geographical scope for the study is chosen based on *a)* historical data on the impact of hydrological and meteorological disasters in the EM-DAT database, and *b)* on the spatial distribution of TC tracks in the IBTrACS database. A region is defined as a group of island states, as they are clustered geographically. The regions are described in Paragraph 2.2.

Historical frequency and impact of tropical cyclones

Findings on the spatial distribution of historical TC tracks and impact are given in Section B.1 of Appendix B, showing that the Leeward Islands have:

- experienced a relatively high impact due to hydrological and meteorological disasters in terms of the number of affected people and the number of deaths compared to the total population per country, and in terms of total damage compared to the total GDP per country,
- and experienced a high number of hurricane tracks going over the islands (including a buffer of 100 km in all directions).

Clustering of countries

The likelihood of different countries being hit by the same storms is considered, following the reasoning that a regional joint trigger model would be most effective for a region experiencing the same storms. This is done by creating a binary dataset of ranking whether a country was affected by a maximum wind speed of over 25 m/s by a tropical storm originating from 1,000 years of synthetic hurricane tracks. The rates of being affected by the same storm for all Caribbean islands are determined and clustered hierarchically. This concluded that the Leeward Islands form a cluster, including both Puerto Rico and Martinique. The clustering is illustrated in Figure 4.3. Paragraph B.2 of Appendix B expands on the method and results of the clustering steps.

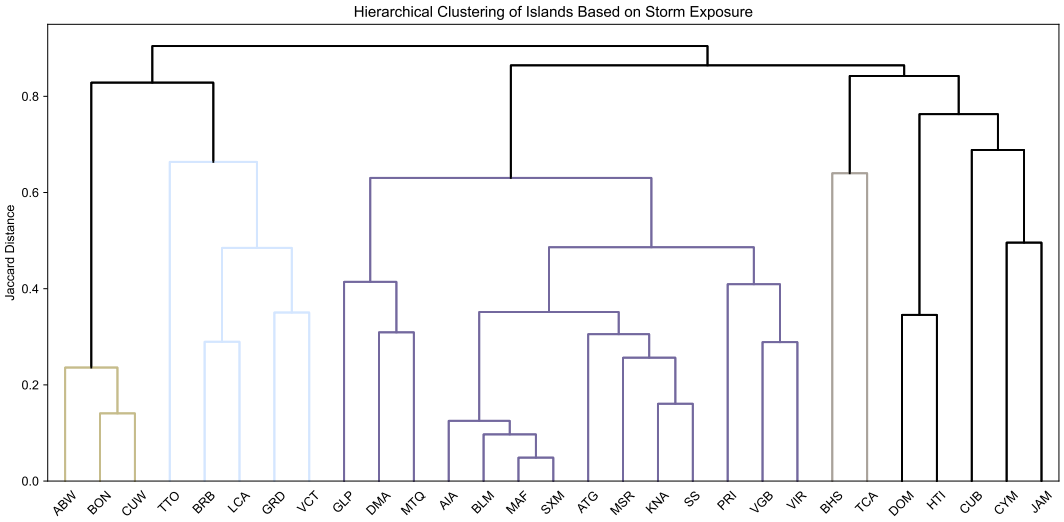

Figure 4.3. Clustering of countries based on estimated experienced wind speeds per synthetic TC track for a total dataset of 1000 years, showing the average Jaccard distance within a cluster per country on the y-axis.

When zooming in, four subgroups could be defined (from north to south):

- British Virgin Islands, U.S. Virgin Islands, Puerto Rico;
- Anguilla, Saint Barthélemy, Saint Martin, Sint Maarten;
- Antigua and Barbuda, Saint Kitts and Nevis, Saba and Sint Eustatius, Montserrat;
- Guadeloupe, Dominica, Martinique.

4.1.2 Creating a point grid

The three hazards that are included in this study are modelled for a point grid over the land surface of the fourteen countries from Puerto Rico to Martinique.
This point grid is made using the GADM boundaries as the shape of a country, in which a point is set either every 2 kilometres or every 0.5 kilometres. In Figure 4.4, the point grid for the Leeward Islands is visualised. The number of points per country highly depends on the country's size and also on its shape.

1. The two-kilometre grid is used when modelling the wind speed. This is considered an appropriate scale since it does give at least four measuring points for each country (even for the very small ones), but is also not too small-scaled since wind speed is not expected to vary highly spatially in the model output. This grid results in a total amount of 3,669 points.
2. When modelling storm surge, however, the outputs are expected to vary more spatially. In these modelling steps, an elevation map with a resolution of approximately 0.5 kilometres is used. Therefore, the point grid is also changed to a 0.5 km resolution. This grid results in a total amount of 58,963 points. A buffer of one kilometre around the coastline is added to secure inclusive modelling of all relevant storm surges.
3. When modelling precipitation, spatial variation is expected as well. However, due to the sensitivity of the model, the elevation input is downscaled to a resolution of approximately 5 km. Therefore, the 2-km point grid is used.

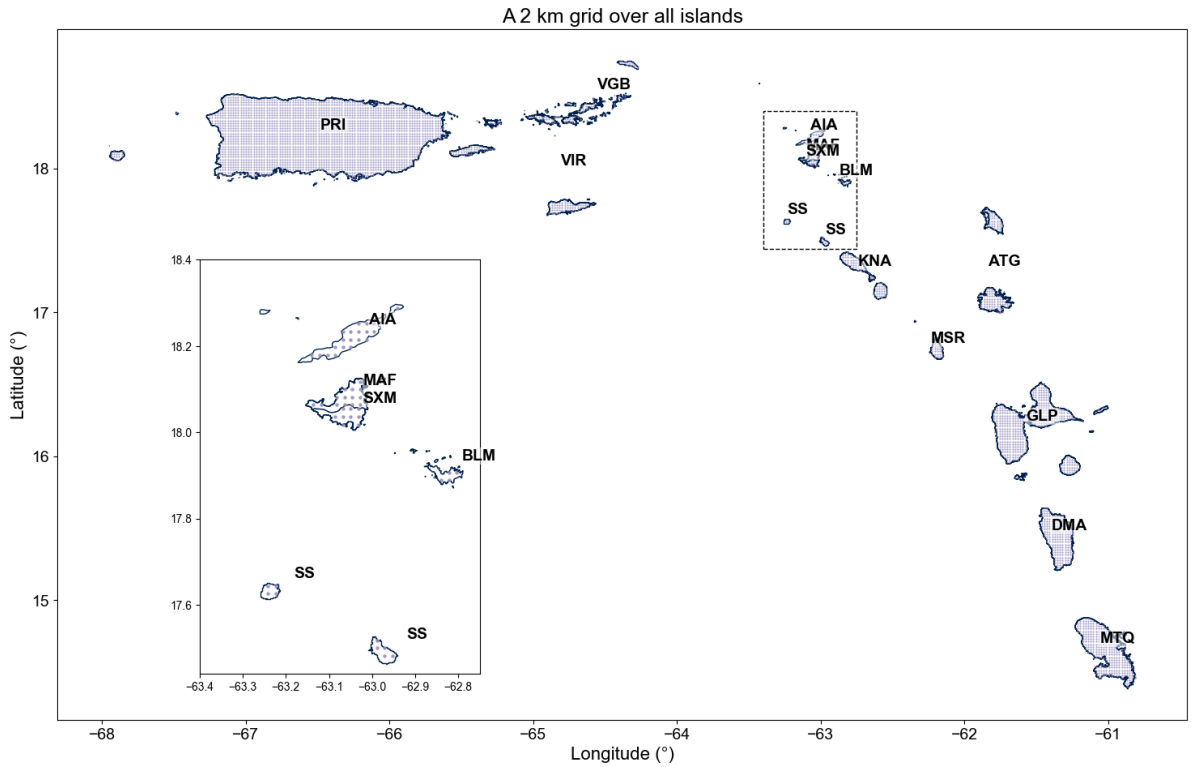

Figure 4.4. The point grid created for the wind field calculations, for the specified region of all Leeward Islands and Puerto Rico and Martinique. In total, there are 3,669 points in this 2-km grid. An additional zoomed map is given for the small islands Anguilla, Sint Maarten/Saint Martin, Saba, Sint Eustatius and Saint Barthélemy for readability of the point grid for these islands.

4.2 CLIMADA

Various steps in the methodology rely on CLIMADA, a Python package for natural hazard modelling created by ETH Zürich. To choose the same package in different steps is done so that this research contributes to the exploration of the possible applications of this package. Currently, CLIMADA is still a work in progress. The 510 team also partners in a new project where CLIMADA will be used for impact assessments of natural hazards.

> CLIMADA (CLIMate ADAptation), an open-source climate risk modelling framework from ETH Zürich, enables the assessment of natural hazard impacts by combining hazard, exposure, and vulnerability data to estimate potential damages. CLIMADA supports probabilistic risk analysis and the evaluation of adaptation strategies, making it particularly suitable for research on disaster risk reduction and climate resilience (ETH Zürich n.d.).

4.3 Modelling tropical cyclone-related wind speeds

Wind and pressure fields can represent a tropical cyclone using just a few physically significant parameters. In this study, we use the widely applied Holland model (Holland 1980). This method is updated and improved with time (Harper and Holland 1999), (Holland 2008). By means of wind and pressure fields, the experienced maximum sustained wind speed caused by a TC can be calculated at a certain point. Specifically, we are interested in the maximum 1-minute sustained wind speed at 10 metres height.

The Holland model is not the only possibility to model wind fields of tropical cyclones, although it is perhaps the most used. In a research progress study of Yan and Zhang (2022), two general approaches are defined. Firstly, atmospheric numerical models, and secondly, parametric models representing wind field characteristics based on TC observations and statistical approaches, by applying simple parameterised formulas (Yan and Zhang 2022). The Holland model is considered relatively easy to apply since it requires the fewest parameters, compared to other parametric models such as Willoughby and

Rahn (2004) and Georgiou (1985). Another possibility is to use reanalysis-based wind fields, for example of ERA5 (reanalysis dataset of the ECMWF), or NCEP/NCAR (reanalysis dataset of the NOAA). These are numerical assimilation products, including environmental conditions and are often available globally. However, winds are often underestimated in intense storms, and the resolution could be too low. Also, it is only available historically.

For the 2-km point grid, the distance from the eye of the storm, and therefore the estimated experienced maximum wind speed at the point, are determined using the wind and pressure fields. This was calculated using CLIMADA, which can extract IBTrACS data and create wind fields for a tropical storm. One of the main assumptions made in the Holland model is that it creates a symmetric wind and pressure field around the eye of the storm. It is known that in reality, the wind field is asymmetric and depends on atmospheric conditions. As well, around landfall, the wind field deviates largely from its symmetric form. Frictional decay over land and the effect of varying surface roughness are not included in the model. This can lead to both under- and overestimating wind speeds.

In this study, we have chosen to use the Holland (2008) method. The azimuthal wind speed v_s at a radial distance r from the cyclone centre is computed as given in Equation 4.1.

$$v_s = \begin{cases} \frac{1}{0.88} \cdot v_{\text{max}}, & \text{if } r \leq r_{vm} \\ \frac{1}{0.88} \cdot \left(\frac{100 B_s \Delta p_s \left(\frac{r_{vm}}{r}\right)^{B_s}}{\rho_s e^{\left(\frac{r_{vm}}{r}\right)^{B_s}}} \right)^{0.5}, & \text{otherwise} \end{cases} \tag{4.1a}$$

$$B_s = -4.4 \times 10^{-5} \Delta p_s^2 + 0.01 \Delta p_s + 0.03 \frac{\partial p_{cs}}{\partial t} - 0.014 \phi + 0.15 v_t^x + 1.0 \tag{4.1b}$$

$$x = 0.6 \left(1 - \frac{\Delta p_s}{215}\right) \tag{4.1c}$$

$$\Delta p_s = p_{ns} - p_{cs} \tag{4.1d}$$

Where:

- B_s is the Holland B parameter at the surface;
- e is Euler's number (approximately 2.718);
- $\frac{\partial p_{cs}}{\partial t}$ is the intensity change at the surface, in hPa per hour;
- ϕ is the absolute value of the latitude of the eye of the hurricane, in degrees;
- p_{cs} is the central pressure at surface, in hPa;
- p_{ns} is the external pressure at surface, in hPa;
- p_s is the surface pressure at radius r, in hPa;
- r is radius, in kilometres;
- r_{vm} is radius of maximum winds, in kilometres;
- ρ_s is the air density at the surface, in kg/m^3;
- v_s is the wind speed at the surface, in metres per second;
- v_t is hurricane translation speed, in metres per second;
- and v_{max} is 10-minute sustained wind speed in the eye of the hurricane, in metres per second.

The Holland (2008) model refines the estimation of the B parameter and r_{vm} based on storm intensity, latitude, and environmental pressure. When r_{vm} is not provided, it is estimated using regression relationships derived from historical best-track data.

The variable r, radius in km, is determined for each centroid using the Haversine method. This method derives from navigation calculations in the 18th and 19th century. The formula was first notated by *James Inman (1835)*. The Haversine method determines the distance between two coordinates, as given by the Equation 4.2.

$$a = \sin^2 \frac{lat_{point} - lat_{storm}}{2} + \cos lat_{storm} * \cos lat_{point} * \sin^2 \frac{lon_{storm} - lon_{point}}{2} \tag{4.2a}$$

$$c = 2 * \sin^{-1} \sqrt{a} \tag{4.2b}$$

$$d = R * c \tag{4.2c}$$

Where:

- lat_{point}, lon_{point} are the location coordinates of the point of interest, in degrees;
- lat_{storm}, lon_{storm} are the location coordinates of the eye of the storm, in degrees;
- R is the Radius of the Earth (6371.0 km);
- d is the distance between the eye of the storm and the point of interest, in kilometres.

CLIMADA performs these computations for each storm time step at each centroid (representing a geographic point of interest), typically within a radius of up to 300 km from the cyclone centre. In the TropCyclone class of CLIMADA, wind speeds below a threshold of 17.5 m/s are automatically filtered out and set to zero to exclude weak storm influences. This threshold is chosen as the filtering method to select extreme values for the wind speed output values.

4.4 Modelling tropical cyclone-related storm surge

In addition to the high wind speeds, a potential hazard of tropical storms and cyclones is flood risk due to storm surge. Storm surge is defined as a temporal sea level rise at the location of the storm region due to low air pressure. Combined with wind surge, blowing surface water forward, the sea level rise and high waves can lead to coastal flooding. Dependent on the movement of the TC, a storm surge lasts on average six hours.
Storm surge depends on wind speed, pressure deficit, TC size, translation speed, and the moving direction of the storm. The actual storm surge at a specific coast also depends on coastal bathymetry, topography, barriers, waterways, and astronomical tide (Harris 1963).

Modelling storm surge is done in various ways. The more detailed the approach, the better the result. However, not always is all the necessary data available. Empirical models are relatively simple to develop and to apply, but have limited capability, as they rely on simplified relationships and historical data, and are no longer widely used. The availability of historical storm surge data varies widely worldwide. Numerical models (including parametric models or simplified dynamic models) offer moderate accuracy. Hydrodynamic models are considered to be typically the most accurate, as they combine physics with complex interactions like tides, winds, pressure gradients and bathymetry. A widely used example of such a hydrodynamic model is the Global Tide and Surge Model (GTSM) developed by Deltares, utilising the Delft3D FM Suite (Deltares 2025). Muis et al. (2016) have assessed the performance of GTSM by creating a global reanalysis of storm surges and extreme sea levels. Validation showed good agreement between modelled and observed sea levels; however, extremes are slightly underestimated, and in particular, tropical cyclone-related extreme sea levels (Muis et al. 2016). This confirms that storm surges related to tropical cyclones are difficult to model, even when using complex hydrodynamic models. High-resolution data input is vital.
Choosing a type of model depends on the required accuracy, the availability of local data, and the computational resources.

In this study, a Simple Coastline Storm Surge Model (SCSSM) developed by Xu et al. (2010) is selected. This approach is based on the SLOSH model, which is a numerical (parametric) model and was designed by the NOAA in 1984, and is still in practice by the NOAA and other institutes. The SLOSH model is only available for the coastline of the U.S. and is meant for real-time surge forecasts as a hurricane threatens (Jelesnianski, J. Chen, Shaffer, and Gilad 1984). Comparison with historical observations showed that the SLOSH outputs agreed within approximately 20%, when the tropical cyclone is accurately described (Jelesnianski, J. Chen, and Shaffer 1992).

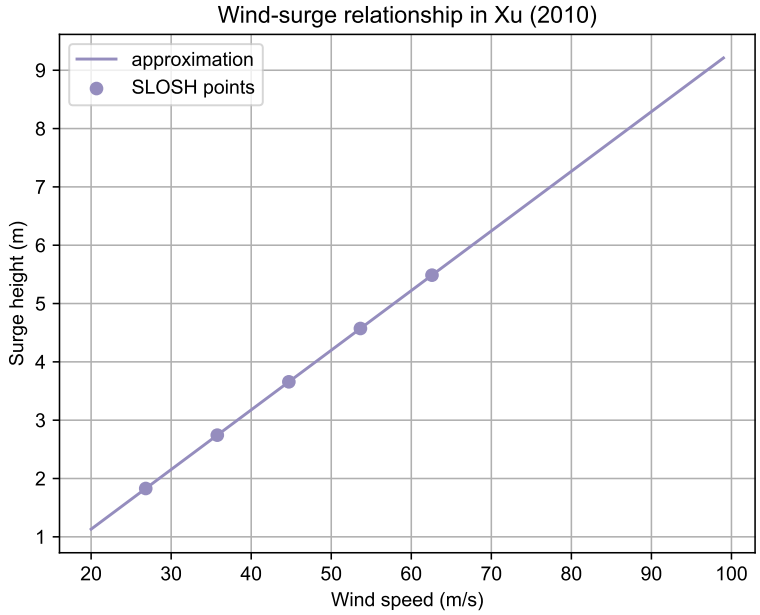

Figure 4.5. Wind-surge relationship as established by Xu based on pre-run SLOSH outputs. Adapted from Xu (2010).

Xu has combined empirical wind models with surge data from SLOSH. Pre-run surge outputs are interpolated to relate wind speed to surge heights, which offers a fast and more accurate alternative to purely empirical models and is built to work for the U.S. coastlines (Xu 2010). In CLIMADA, this wind speed vs surge height relation is taken as an input, and when supplying an elevation map and ocean bathymetry, the surge height for a certain TC event is modelled (CLIMADA contributors, ETH Zurich 2025). The method is called TCSurgeBathtub and is able to estimate the maximum surge at certain locations, but cannot give the surge over time. The model is developed for land-falling hurricanes and for open coastlines. The linear wind-surge relation is drawn in Figure 4.5.

Firstly, the wind speed at a certain location is required. This is done using the Holland model for consistency, although Xu applies a different wind profile model in his paper (Xu 2010). To translate wind speed to surge heights, the wind-surge relation should be interpreted as F in Equation 4.3:

$$G(X) = F_{H,X}(V, X) \tag{4.3}$$

Where:

- $G(X)$ is the surge height at location X;
- $F_{H,X}$ is the general function for hurricane H at location X;
- and (V, X) represents the input wind speed V and location X.

Additionally, a decay of surge height is implemented over flat land (up to 10 m elevation) until 50 km inland with a decay factor of 0.2 metres per kilometre, based on (Pielke and Pielke 1997).

Most parametric models do not include the full hydrodynamic nature of storm surges. It assumes that water levels rise instantaneously and uniformly to a given height, similar to filling a bathtub. It does not account for the momentum of the water mass, bed friction, or complex coastal geomorphology. Wave run-up and tidal-surge interactions are not included, although these can be significant contributors to coastal inundation. Given these limitations, the method is best suited for first-order hazard and risk assessments, but should not be used for detailed, site-specific engineering design.

4.5 Modelling tropical cyclone-related precipitation

The Tropical Cyclone Rainfall model (TCR) is used to model TC-related precipitation. This model assumes that the precipitation rate at a specific point is proportional to the vertical vapour flux, following

the framework of Zhu, Quiring, and Emanuel (2013) and Emanuel (2017). This is described in Equation 4.4.

$$w_q = q_s * w \tag{4.4a}$$

$$w = w_f + w_h + w_t + w_s + w_r \tag{4.4b}$$

Where:

- w_q is the vertical vapour flux, in metres per second;
- q_s is the saturation specific humidity (assumed to be constant over the rain field), in kg/kg;
- w is vertical velocity, in metres per second, consisting of
  - w_f: friction-induced;
  - w_h: topographically induced;
  - w_t: vortex stretching induced;
  - w_s: shear-induced;
  - w_r: radiative cooling-induced.

This vertical velocity is the main focus of the physics-based, parametric model. For a given TC track and associated state variables, the model computes at each time step for every grid centroid the upward velocity w. This is multiplied by the specific humidity to yield the moisture flux at that location. The precipitation rates are estimated by means of a precipitation efficiency factor, as described in Equation 4.5.

$$P_{rate} = \epsilon_p \frac{\rho_{air}}{\rho_{liquid}} w_q \tag{4.5}$$

Where:

- P_{rate} is the precipitation rate, in metres per second;
- ϵ_p is the precipitation efficiency, assumed constant, set to 0.9;
- ρ_{air} and ρ_{liquid} are the densities of water vapour and liquid water (ratio is set to 0.0012);
- w_q is the vertical vapour flux, in metres per second.

CLIMADA follows the implementation of the TCR model as is described in Lu et al. (2018), where all components of the vertical wind speeds are illustrated. Through time integration along the track, the storm's total accumulated rainfall over each centroid is obtained.

Sensitivity to topographically-induced vertical velocity

Even though the topography effect is already reduced outside the storm centre by Lu et al. (2018) compared to Zhu, Quiring, and Emanuel (2013) and Emanuel (2017), the model is still very sensitive to steep slopes, as well as to drag coefficients (drag is the effect of surface friction on near-surface winds). Frictional convergence appears to be the dominant mechanism, contributing over 70% of total rainfall in two case studies of Lu et al. (2018). The precipitation modelling is strongly dependent as well on the wind input, for which the Holland model was found to perform the best by Lu et al. However, taking a moving average on the wind outputs is recommended, which is not applied in this study.
As is expected, precipitation is found to interact with wind fields in a more complex way than storm surge, causing high precipitation to also be associated with weaker winds.

4.6 Clustering countries

A country is considered to be 'hit' when a certain threshold is reached for at least one grid point within the country boundaries, per hazard. For wind speed, the threshold is set at 17.5 m/s. This wind speed does not necessarily lead to an impact on the island, but is chosen since it is the lower limit of what is considered a tropical storm in the Saffir-Simpson scale. For storm surge, the threshold is set at 0.2 meters, which is arbitrarily chosen and is suspected to lead to some impact. For precipitation, the threshold is set at 50 mm, a precipitation amount generally considered as the lower limit of 'extreme' precipitation per hour (an hourly precipitation rate of 51.6 mm has a return period of two years in Puerto Rico according to NOAA's National Weather Service ()).

For all hazards, we created a table showing the storm, the country, and whether it was hit: yes or no. So for every storm-country pair, a binary indicator is assigned, resulting in a binary exposure matrix. Subsequently, the similarity between the hit rates of countries is determined using the Jaccard distance, a measure designed for binary data, see Equation 4.6.

$$d_J(A, B) = 1 - \frac{|A \cap B|}{|A \cup B|} \tag{4.6}$$

Where $|A \cap B|$ is the number of storms that affected both country A and country B, and $|A \cup B|$ is the number of storms that affected either one. The lower the $d_J(A, B)$, the higher the overlap of being hit. The Jaccard distance should always be between 0 and 1.
When the Jaccard distance is known for every possible pair of the islands, a hierarchical clustering is applied. Countries are clustered iteratively based on the average pairwise distance between all countries in that cluster.

4.7 Analysing extreme values

Extreme value analysis is used to determine return periods (RPs) of extreme events, indicating hazard probability distributions. Return periods can also be determined empirically when very large time series are available. Bloemendaal et al. determined TC wind speed return periods based on the STORM dataset, both empirically (using Weibull's plotting formula) and by fitting extreme value distributions. This study showed that return values that are determined empirically are typically lower than return values based on extreme value distributions, especially for high RPs (Bloemendaal, Moel, Muis, et al. 2020). It is stated that the empirically determined results are closer to the observed wind speeds when considering historical return periods. The return period graphs similar to the ones mentioned above were created for empirical return periods based on Weibull's plotting formula, described in Equation 4.7 (Weibull 1939).

$$P_{exceedance}(v) = \frac{i}{n+1} * \frac{n}{m} \tag{4.7a}$$

$$T(v) = \frac{1}{P_{exceedance}(v)} \tag{4.7b}$$

Where:

- $P_{exceedance}(v)$ is the probability of exceedance for a certain hazard level;
- i is the rank of the hazard level at a grid point for a certain storm;
- n is the total number of events;
- m is the total length of the dataset, in years;
- $T(v)$ is the return period, in years, for a certain hazard return level.

In order to interpret the results, a map is created showing the result per point grid for a set of return periods: $T = 5, 10, 20, 50, 100, 200, 500, 1000$ for the synthetic dataset of 10,000 years, or $T = 5, 10, 50, 80$ for the historical dataset of 85 years.
Subsequently, the result is processed as a graph showing the return values per country. To gain these results, the return values per grid point are aggregated to one value per country based on all grid points that fall within the country polygon. For wind speed, the average value per storm of the country is considered. For storm surge and precipitation both, the maximum value per storm is considered, since the hazard output varies more over the country, and the extremes will cause the most impact.

The mean of the entire region is included in the graph as well, to enable comparison between national return values and regional values. The regional mean is determined as the mean of all return levels per country, per return period. Hence, all countries have an equal weight.

Analysing these results addresses the extent to which expected hazards differ among countries within the selected region. Critically, for a hazard-based trigger model, this analysis informs the process of setting a trigger based on a predefined return period and its corresponding expected hazard level.

5 Results

The results of the analysis of tropical cyclone-related hazards are given and discussed in this section.

For the hazards of wind speed and storm surge, results for both historical TC tracks and for synthetic TC tracks are given and interpreted. For the hazard of extreme precipitation, modelling was only possible for historical TC tracks. For some results references to Appendices E, F, and G are made.

For comprehension of all steps and insights in the result, all hazard modelling was also applied to the historical tropical cyclone Hurricane Irma, which occurred in 2017 and caused a lot of damage in some Caribbean Islands as well as in the U.S. These results are included and described in Appendix D.

5.1 Modelling tropical cyclone-related wind speeds

In this section, we show the results of the modelled wind speeds for both historical and synthetic tropical cyclone tracks. For all tracks, the maximum reached 1-minute sustained wind speed at 10 m height is modelled. This is translated to return periods, determining the expected exceedence level corresponding to a certain time period; for example, the wind speed that is expected to be exceeded at least every five years, per grid point.

5.1.1 Wind speeds for historical TC tracks

The historical tracks are taken from IBTrACS. The time period 1940 - 2024 is considered, and a preselection is made on the location of the tracks. In total, 209 tracks are included over this 85-year period.

Of all points and all storms, the maximum estimated wind speed was 70.0 m/s, which occurred in Hurricane Maria (2017), followed by Hurricane Irma (2017) with a maximum estimated wind speed at any point of the Leeward Islands of 68.3 m/s and then by Hurricane David (1979), resulting in 61.8 m/s. Of the 209 tracks that were considered, a total of 57 tracks resulted in a modelled output value of at least 17.5 m/s at any point of the grid (so above land). This number does not increase when enlarging the boundaries used in the pre-selection step, meaning that the boundaries are well estimated. These 57 tracks are used for determining return periods. When only considering the maximum values per storm over all centroids, the mean maximum wind speed is 31.9 m/s with a standard deviation of 13.6 m/s, for these 57 tracks.

By means of the Weibull's plotting formula, the return levels per point for a return period of five years are determined. Figure 5.1 shows the map for the exceedance levels corresponding to a return period of five years, retrieved from the wind speeds of historical TC tracks.

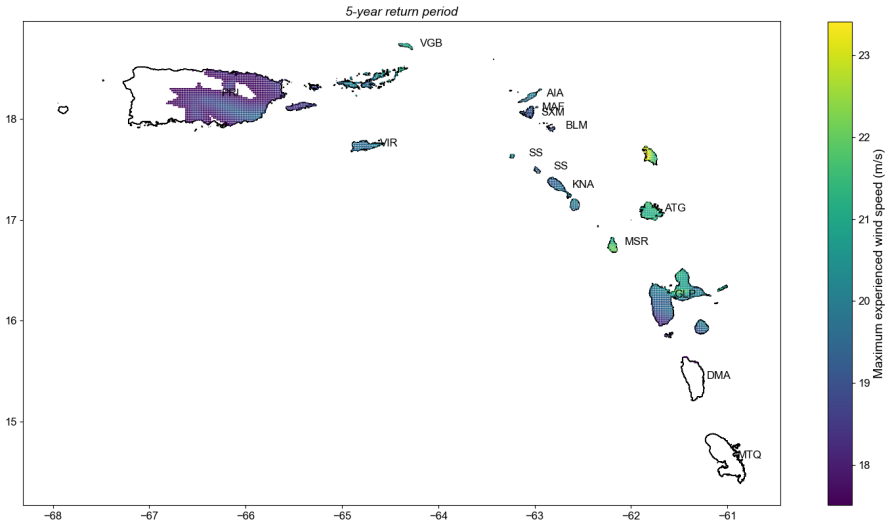

Figure 5.1. The estimated maximum wind speed (m/s) for a return period of five years, for the defined region, based on IBTrACS data. The white areas are to be interpreted as values below the threshold of 17.5 m/s.

The map indicates that Martinique, Dominica, and the western part of Puerto Rico are expected to experience lower maximum wind speeds during tropical cyclones. In total, the map shows wind speeds ranging from 17.5 to 23 m/s. The white areas are to be interpreted as values below the threshold of 17.5 m/s; in other words, a wind speed of 17.5 m/s will not be reached every five years. This large range is not expected for this area, where all countries are expected to experience approximately the same frequency and severity of TC-related wind speed. The range is attributed to the small number of historical storms leading to high wind speeds.

5.1.2 Wind speeds for synthetic TC tracks

For all synthetic TC tracks of the dataset STORM, the wind field is estimated. After pre-selection for the region, STORM gives 11,372 tracks that pass the Leeward Islands, for a period of 10,000 years, that lead to modelled wind speeds of at least 17.5 m/s at at least one of the points in the total grid. The maximum estimated wind speed of all storms was 72.5 m/s.

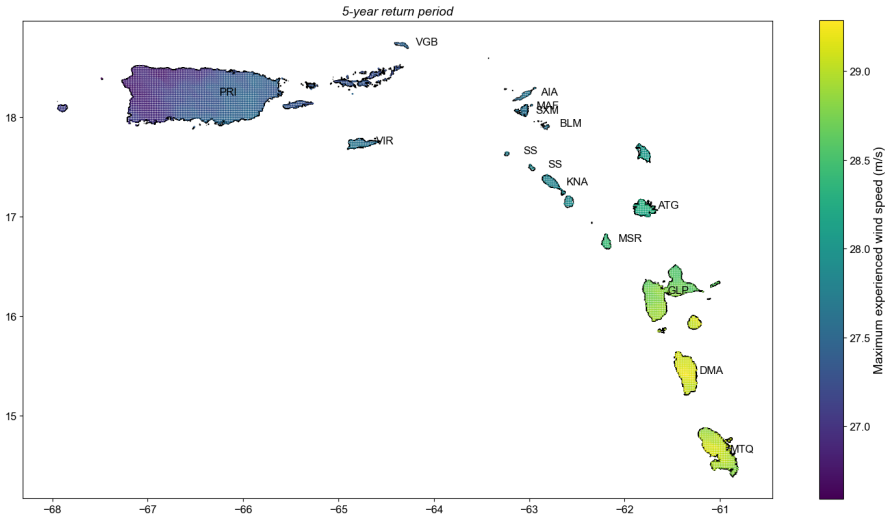

Figure 5.2. The estimated maximum wind speed (m/s) for a return period of five years, for the defined region, based on 10,000 years of TC tracks in the STORM database.

Return periods have been determined empirically for the modelled wind speeds on land. Figure 5.2 shows the estimated maximum wind speed over the total duration of a storm, for a return period of 5

years. This should be interpreted as the expected wind speed that is experienced at least, per point in the grid, every 5 years. The range of the return levels is given by the scale on the right. The map indicates that, in general, higher wind speeds are expected in the south. However, this relation is not as clear for a range of return periods, given in Appendix E. Overall, it is concluded that the range of expected maximum wind speeds is small per return period.

Figures E.3 and E.4 in Appendix E show the results for multiple return periods, namely 5, 10, 20, 50, 100, 200, 500, and 1,000 years. Since the dataset has a total length of 10,000 years, these larger return periods can be determined empirically quite well. For a return period of 5 years, the wind speeds are expected to be at least 25 m/s approximately, going up to expected exceedence levels of 65 m/s for a return period of 1,000 years. Figure E.3 indicates best the deviation of expected return levels over the islands. Southern islands experience a higher probability of high wind speeds than the northern islands. Within one country, the distribution is approximately equal. This last conclusion is a logical result of the distance to the eye being the most important parameter in the model. The difference between the southern and northern islands can be attributed either to a higher frequency of tropical cyclones or higher wind speeds per tropical cyclone in the southern area. These international differences are further considered by quantifying the modelled wind speeds per country.

Spatial distribution per country

Instead of taking all grid points separately, the results are also aggregated per country. Of all points per country for which the maximum reached wind speed is noted, the mean value per storm is determined. This represents the mean estimated wind speed within that country for a particular storm. When operationalising the hazard modelling towards impact modelling and design of thresholds, it would also be important to know the location of the hazard within the country's boundaries. However, here we focus on the mean value per country since we are interested in the general spread of hazards between countries. The distribution between the means for the countries is only included for the results based on the synthetic tracks, since these results have a higher statistical significance.

Table 5.1 shows some statistics for the maximum values of the maximum wind speeds per country over the 11,372 synthetic TC tracks, as well as for the mean values of the maximum wind speeds per country. Of the 11,372 tracks, the number of tracks that reach a wind speed of 17.5 m/s within a certain country is counted, and the mean of their mean values is given as well.

Table 5.1. Summary statistics of modelled maximum 1-minute sustained wind speeds per storm event, in m s^{-1}, per country. The modelled hazard is based on synthetic TC tracks of the STORM dataset. The first two columns consider the mean values per country for the maximum wind speeds per storm. The middle two columns consider the maximum values per country. The last columns consider only the storms reaching over 17.5 m/s of wind speeds within that country.

Country	Max of mean	Mean of mean	Max of max	Mean of max	Number storms (high wind)	Mean of mean (high wind)
Anguilla	65.3	11.3	68.3	12.2	4657	27.5
Antigua and Barbuda	62.0	11.7	69.3	15.1	5548	24.1
Saint Barthélemy	64.2	11.4	64.5	11.6	4533	28.6
Dominica	64.7	12.8	67.5	15.0	5615	25.8
Guadeloupe	63.8	12.3	68.9	16.8	6094	23.0
Saint Kitts and Nevis	66.1	11.6	69.2	13.0	4928	26.7
Saint Martin	64.3	11.3	66.0	12.0	4631	27.8
Montserrat	65.6	11.9	65.9	12.5	4813	28.0
Martinique	70.3	12.7	72.5	15.4	5798	25.0
Puerto Rico	68.3	10.6	71.9	18.1	6268	19.3
Saba & Sint Eustatius	65.1	11.5	66.1	12.3	4746	27.4
Sint Maarten	65.1	11.3	65.3	11.6	4527	28.5
British Virgin Islands	62.0	11.0	68.3	13.4	4975	25.0
U.S. Virgin Islands	62.0	11.1	70.0	14.6	5352	23.6

The maximum values for both the mean wind speeds per country and the maximum wind speeds per country don't differ significantly from each other. The model gives a range of 62.0 to 70.3 m/s and a range of 64.5 to 72.5 m/s, respectively. The highest maximum wind speed is reached in Martinique for both.
The countries Antigua and Barbuda, Dominica, Guadeloupe, Martinique, and Puerto Rico appear to experience high wind speeds more often than the other countries. These are the larger islands of the region. The expected wind speeds per event affecting each country are not necessarily also higher for these countries. Higher mean maximum wind speeds per country are expected for Anguilla, Saint Barthélemy, Saint Kitts and Nevis, Saint Martin, Montserrat, and Saba & Sint Eustatius. These are the smaller islands within the region.

Figure 5.3 shows the wind speeds vs return period as a continuous graph. Per country, the mean of all points is used. The figure shows the result when using the large synthetic dataset.

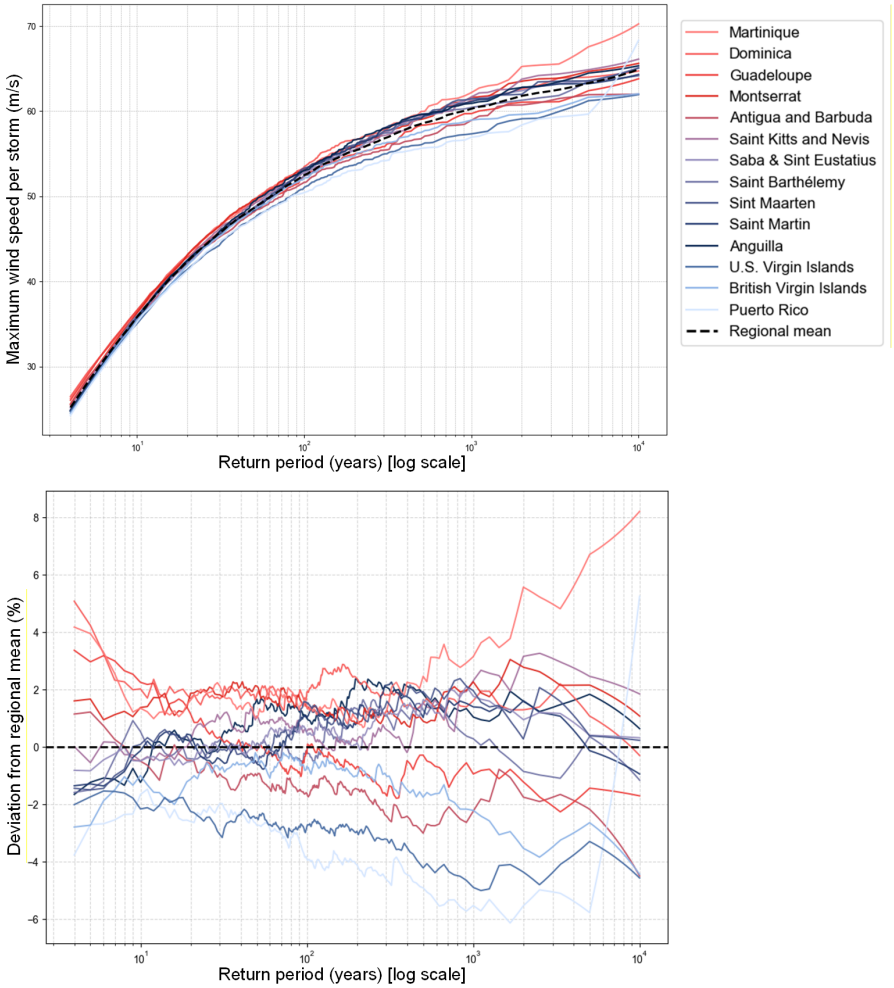

Figure 5.3. Estimated maximum 1-minute sustained wind speeds at 10 m as a mean over all points per country plotted against the corresponding return periods. The colour shades go from light red to red to purple to dark blue to light blue. This order corresponds with the way the islands are ordered, going from Martinique (south-east) to Puerto Rico (north-west). The lower figure shows the deviation from the regional (black striped line) in percentages over the range of return periods.

The purpose of the graph is to show the variation between the different countries in estimated maximum wind speeds per storm. It shows that the countries don't differ very much, and that the variation is greater for higher return periods and thus higher wind speeds. Additionally, the mean of all countries is also plotted. Martinique and Dominica give the highest wind speeds of the region, and Puerto Rico and the British Virgin Islands give the lowest wind speeds per return period. This would mean that if you set the regional trigger at the regional level fitted for a certain return period (for example, 5 years),

this trigger would fit a slightly higher return period for Puerto Rico.

The graphs in Figure 5.3 show that for wind speeds, the spatial distribution is quite equal. The exceedance values for expected maximum wind speeds, taken as a mean over a country, go up for higher return periods, as was already shown in Figure E.4.
Figure 5.3 shows how the slope of the curve decreases for higher return periods, called a logarithmic increase (the inverse of an exponential increase), meaning that the increase slows down over the x-axis (the return period in this case). The red and purple countries result in slightly higher return periods than the blue countries, meaning that the southern countries are expected to be exposed to higher wind speeds at a higher frequency.

The lower graph of Figure 5.3 shows the relative deviation from the regional mean. This gives more easily interpreted results when considering the spread between the countries as opposed to a regional approach. The deviation is divided by the regional mean to get the relative deviation, in percentage.

The relative deviation from the regional mean shows that the total variation is about 10-12% of the value of the regional mean. This is considered a small variation. For the lower return periods, it clearly stands out that the regional mean would underestimate the expected maximum wind speeds for the southern (red) countries, and would overestimate the wind speeds for the northern (blue) countries. For higher return periods, and thus for rarer and more extreme events, this distinction is less clear. In Appendix E, a similar figure showing relative deviation is shown, where the colours are ordered differently. This is done to identify country characteristics that define the spatial distribution of tropical cyclone-related wind speeds. The area of the country does not appear to be a driving feature in wind speed distribution.

5.1.3 Spatial reach of a tropical cyclone

The results above show the expected return values for wind speed either per grid point or per country, based on a large set of tropical cyclones. The spatial reach of a single tropical cyclone is not included yet, but it would provide valuable information on the total impact per event and, therefore, the application within regional early action protocols. In order to quantify the spatial reach of a single TC, the number of countries it affects is counted.

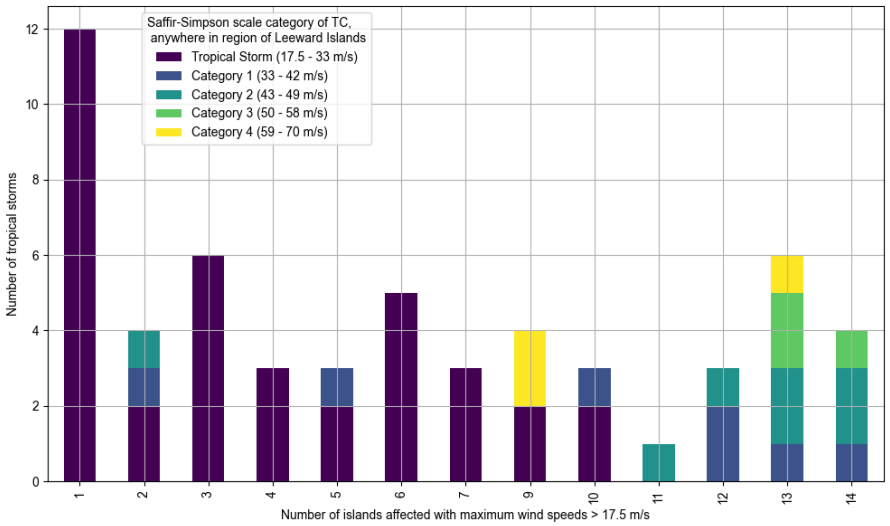

Figure 5.4. Bar chart showing the historical distribution of storms affecting one or multiple countries, for 85 years of historical tropical cyclone tracks.

Firstly, the historical database IBTrACS, between 1940 and 2024, is considered. To gain insight into the number of islands that are affected by one storm, this is counted for the whole dataset. An island is considered affected by the storm when a maximum sustained wind speed of at least 17.5 m/s is modelled, for at least one of the points per country. In total, 57 times a country is considered to be affected by historical storms. Twelve of these storms only affected one country. The remaining storms

have affected multiple countries within the region. The result is shown in Figure 5.4. It can be noticed that hurricanes with a higher category hit more countries. The categories shown in Figure 5.4 are defined as the maximum category of the storm within the boundaries of the region of the Leeward Islands.

The same analysis is done for 10,000 years of the synthetic dataset STORM. The result is included in Figure 5.5. A country is considered affected when the maximum wind speed is estimated to be over 17.5 m/s, for at least one point inside the land boundary per storm. Only the countries within the specified region are considered. Note that here the count is converted to a percentage of the total, on the y-axis.

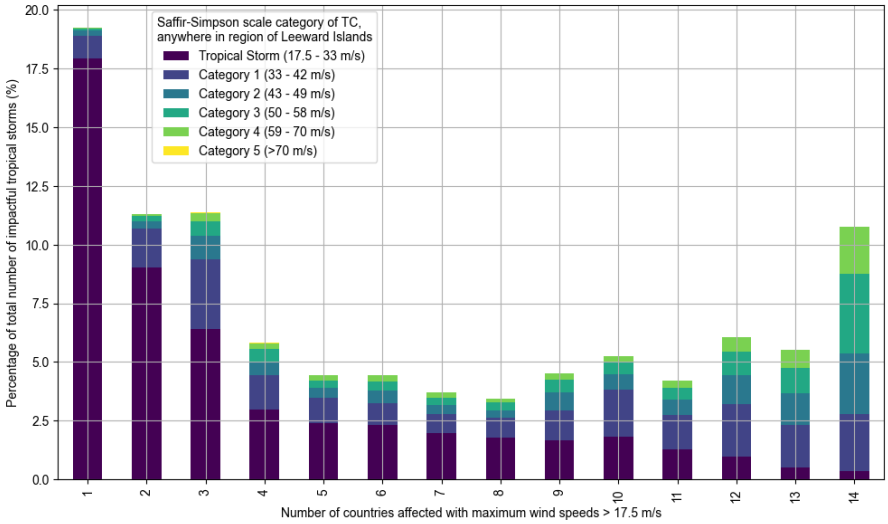

Figure 5.5. Bar chart showing the distribution in percentage of storms affecting one or multiple countries, for 10,000 years of synthetic tropical cyclone tracks.

Per storm, the maximum reached Saffir-Simpson hurricane wind scale that was reached within the area around the Leeward Islands is shown as colours within the bar chart, similar to Figure B.6. It is concluded that storms of a higher scale, hence higher wind speeds, affect more islands than storms of a lower scale. Storms of a higher category reach higher wind speeds and often have a larger span. Approximately 19% of the storms that affect any country within the region affect only one country. About 52% of the storms affect at least five countries. In both figures, we see that the bar chart is a bit of a U-form, meaning that one storm most likely hits only a few of the total countries, or the vast majority of the total, but affecting about half of the countries is less likely. Although the count rates for affecting only a few islands are significantly larger than affecting many countries.

Clustering countries

For the maximum reached wind speed results, a clustering is made based on the similarity between the hit rates of the countries. These hit rates are based on a binary dataset of the results of the synthetic TC tracks, where a country is considered 'hit' when, for at least one point, a maximum wind speed of at least 17.5 m/s is reached.

The clustering is shown in Figure 5.6. When looking at wind speed, based on the modelled output of this study, about three clusters can be defined:

- Dominica and Guadeloupe
- Anguilla, Saint Martin, Saint Barthélemy, Sint Maarten, British Virgin Islands and U.S. Virgin Islands
- Antigua and Barbuda, Montserrat, Saint Kitts and Saba & Sint Eustatius

Figure 5.6 clearly shows how neighbouring countries are affected by the same storms. This is a logical result, since distance from the eye is the main driving parameter in the Holland model. Notably is

however, Puerto Rico is quite 'far away' from the Virgin Islands and seems to be affected by different TC tracks. The same goes for Martinique, which has a large Jaccard distance to its neighbours, Dominica and Guadeloupe.

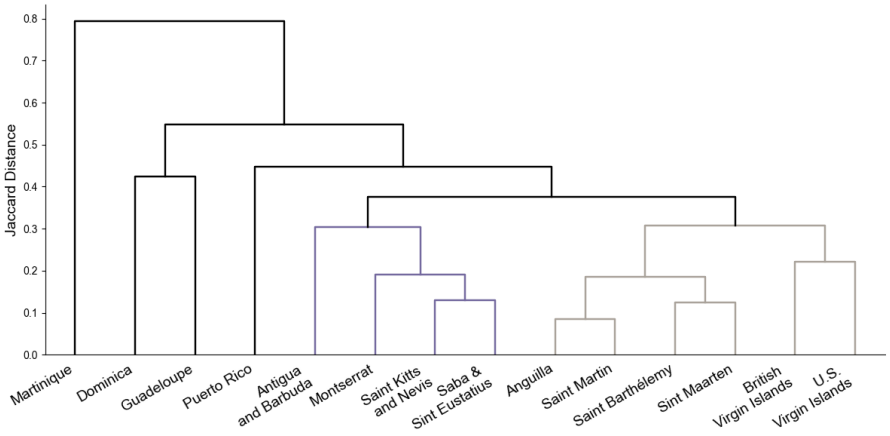

Figure 5.6. Clustered countries based on being affected by the same storms, on their modelled maximum reached wind speeds. Clustering based on modelled hazard from synthetic tropical cyclones (1000 years).

5.2 Modelling tropical cyclone-related storm surge

For both historical and synthetic TC tracks, the surge levels over the point grid covering the islands are modelled. This is translated to return periods, which are visualised in a map for a return level per point, and visualised in graphs for return levels per country.

5.2.1 Storm surge for historical TC tracks

Per storm event, the maximum reached surge level over the whole duration is taken. The output value is the total water level, which is the sum of the mean sea level and the storm surge. The model then compares this water level to the ground elevation at each centroid. If this value is negative, the point is not inundated, and the surge height (e.g. flood depth) is considered zero. For points on the sea, the total water level is compared to the mean sea level.

The 209 tracks that were considered led to modelled surge levels above 0.2 meters for at least one of the points in the total grid for 52 tracks. Of all storms over all points, the maximum estimated surge is 6.09 meters, which occurred in the British Virgin Islands during Hurricane Maria (2017). This is followed by a surge level of 6.00 meters during Hurricane Irma (2017) and by a surge level of 4.57 meters during Hurricane Hugo (1989).
When considering only the maximum surge levels over all centroids, the mean expected value is 2.39 meters, with a standard deviation of 1.17 meters. Only the 52 tracks leading to surge levels of at least 0.2 meters in the point grid are considered for further analysis.

By means of the Weibull plotting formula, an empirical way to determine return periods, the return levels per point for a return period of five years are determined. Figure 5.7 shows the map for the exceedance levels corresponding to a return period of five years, retrieved from the wind speeds of historical TC tracks.

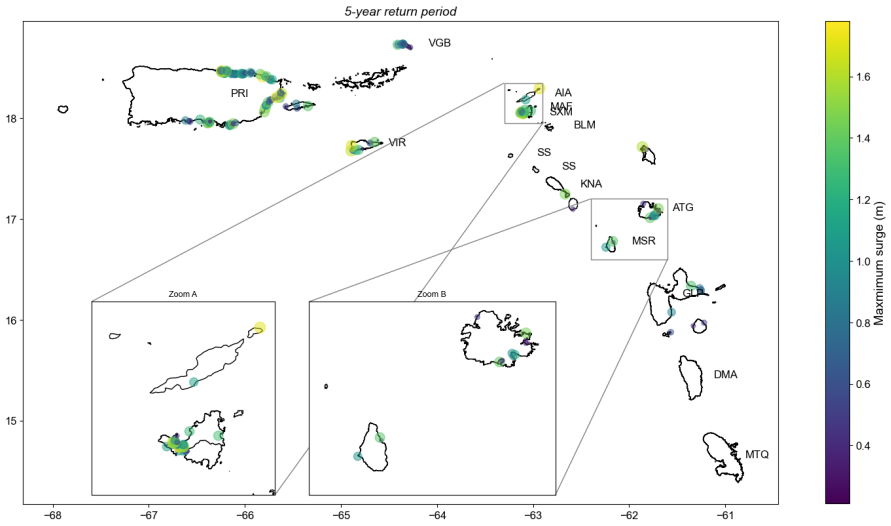

Figure 5.7. The estimated maximum surge (m) for a return period of five years, for the defined region, based on IBTrACS data. Two zoom views are added for readability of the plot.

As is expected, storm surge occurs only at the coasts of the islands and is therefore not clearly visible on the map. For a return period of 5 years, exceedance levels for surge are expected to be up to approximately 1.7 meters, mainly occurring in Puerto Rico, British Virgin Islands, U.S. Virgin Islands, Sint Maarten and Saint Martin, and on Antigua.

The same result is plotted on maps for return periods of 10, 50, and 80 years. These results are included as Figures F.1 and F.2 in Appendix F. Since we determine the surge levels only on land, the output values highly depend on the elevation map on land. The output value is the expected surge level minus the elevation level. The surge levels are determined for the 0.5-km grid, similar to the elevation levels, given by a map with a 0.5-km resolution.

It is important to note that this resolution is not considered to be sufficiently small to accurately estimate surge levels on land. Elevation can vary largely over small areas in a coastal region, which will affect the actual occurring flood heavily. Moreover, no storm barriers are included in the model.

5.2.2 Storm surge for synthetic TC tracks

The same results are created for the synthetic dataset STORM. For a range of 10,000 years of synthetic hurricane tracks, the expected storm surge is modelled using TCSurgeBathtub of CLIMADA. Only the surge levels of at least 0.2 meters are included in the analysis.

Figure 5.8 shows the expected surge levels on land for a return period of five years. The map is similar to the result of the historical tracks (Figure 5.7, but shows additional expected surge inundation on the south and west coast of Puerto Rico, and on Dominica and Martinique. The map shows surge levels on land up to 2.0 meters. Mainly, the coastal areas of Puerto Rico, the Virgin Islands, Anguilla, Sint Maarten, Saint Martin, Antigua and Guadeloupe are prone to experiencing storm surge.

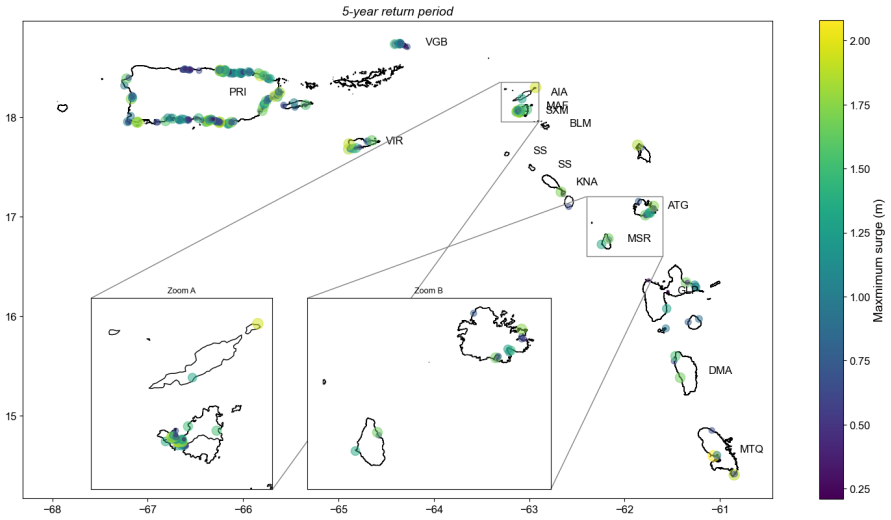

Figure 5.8. The estimated maximum surge (m) for a return period of five years, for the defined region, based on STORM data. Two zoom views are added for readability of the plot.

Spatial distribution per country

The surge height is determined for all centroids, which are formed as a point grid with a resolution of 0.5 km. This is interpreted as a grid cell of $0.5 * 0.5 = 0.25$ km^2, to determine the modelled flooded area. The following outputs are determined for all islands, and summarised in Table 5.2:

- the maximum flood depth (surge level) over all storms, per country;
- the maximum flooded area over all storms, where flooded is defined as a surge height above 0.20 meters, per storm, per country, as a percentage of the total surface of the country (determined based on GADM shapefiles);
- the number of storms leading to surge anywhere in the country, in the total dataset of 1000 years of synthetic hurricane tracks;
- the median value for the percentage of flooded area, when considering only the storms leading to a surge anywhere in the country.

Table 5.2. Summary of storm surge and flooding statistics per country.

Country	Max surge (m)	Max flooded area (%)	Number of storms with surge, per 1000 years	Median flooded area (%) for storms with surge
Anguilla	5.3	4.3	504	0.6
Antigua and Barbuda	5.4	4.9	625	1.0
Saint Barthélemy	1.4	2.4	19	1.2
Dominica	4.7	0.3	630	0.1
Guadeloupe	5.0	1.3	668	0.1
Saint Kitts and Nevis	5.5	0.8	533	0.2
Saint Martin	5.1	23.4	494	9.7
Montserrat	5.2	1.2	540	0.7
Martinique	6.0	0.9	684	0.2
Puerto Rico	5.6	4.3	657	0.7
Saba & Sint Eustatius	0.2	0.0	1	0.0
Sint Maarten	5.1	27.4	484	10.4
British Virgin Islands	4.7	17.3	487	5.1
U.S. Virgin Islands	5.5	3.3	587	0.7

The smaller countries, as Saint Barthélemy and Saba & Sint Eustatius, show significantly lower values. This is attributed to the steep coasts and few low-lying areas, as well as to the low number of measuring points in these small countries. Sint Maarten and Saint Martin share a large low-lying area, which explains the high flood area percentages.

The percentage of flooded area of the total surface is considered a key indicator for the severity of the storm surge. Therefore, the return period graph showing the hazard vs return periods is created for this output value, as well as for the maximum surge anywhere in the country.

Again, it is important to note that the elevation input is too coarse to adequately model surge levels on land.

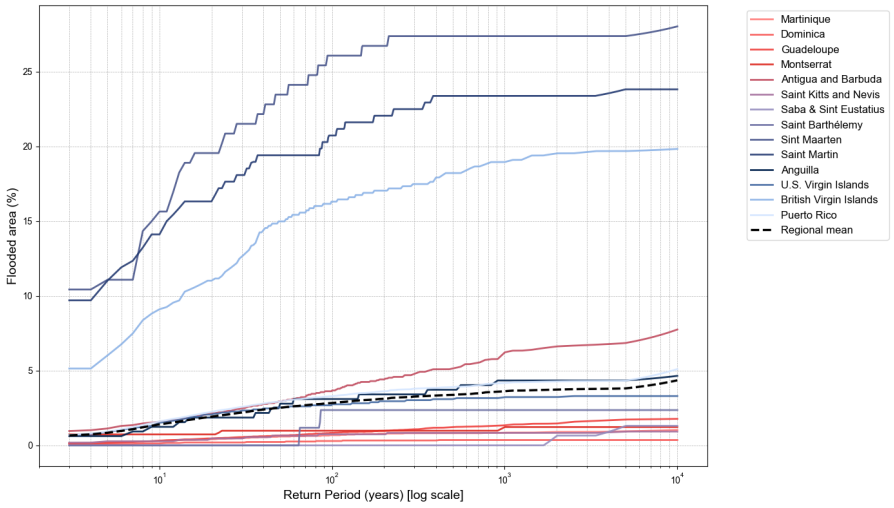

Figure 5.9. Estimated flooded area per country, as a percentage of the total area, plotted against the corresponding return period. The x-axis, showing the return period in years, is on a log scale.

Figure 5.9 shows the flooded area as a percentage of the total area of the country, versus its return period. Additionally, the entire region as a whole is included in the graph.

The different countries show large differences in the surge over land. The return period graphs of the countries Antigua and Barbuda, Saint Martin, and the British Virgin Islands are significantly higher than the others. This is due to the presence of low-lying land within these countries. Many Caribbean Islands are volcanic and consist of mountainous landscapes, resulting in low storm surge over land due to the steep elevation. However, these three countries also consist of large non-volcanic areas. Very flat hazard curves are shown for Saba & Sint Eustatius, Saint Barthélemy and Martinique, indicating that these islands are barely affected by surge relative to their total area.

The maximum surge levels reached at any point per country are also translated to return periods. Figure 5.10 shows the modelled exceedance values of maximum surge over a range of return periods, from 2 to 10,000 years.

All countries seem to follow approximately the same distribution, except for two clear exceptions: Saint Barthélemy and Saba & Sint Eustatius. These outliers were also clear from the results shown in Table 5.2. The countries Puerto Rico, Martinique, and Antigua and Barbuda appear most prone to high maximum surge levels on land in their country. Since Saint Barthélemy and Saba & Sint Eustatius are such clear outliers, they are excluded from the graphs on relative deviation from the regional mean; the lower graph of Figure 5.10. The results show that for smaller return periods, a larger relative deviation between the countries is expected. In total, the maximum surge levels per country show a deviation of approximately 55% to 14% over the range of return periods. This is considered quite a large range, indicating that the modelled output levels for maximum surge levels, to be expected on land, have a large variation in their spatial distribution.

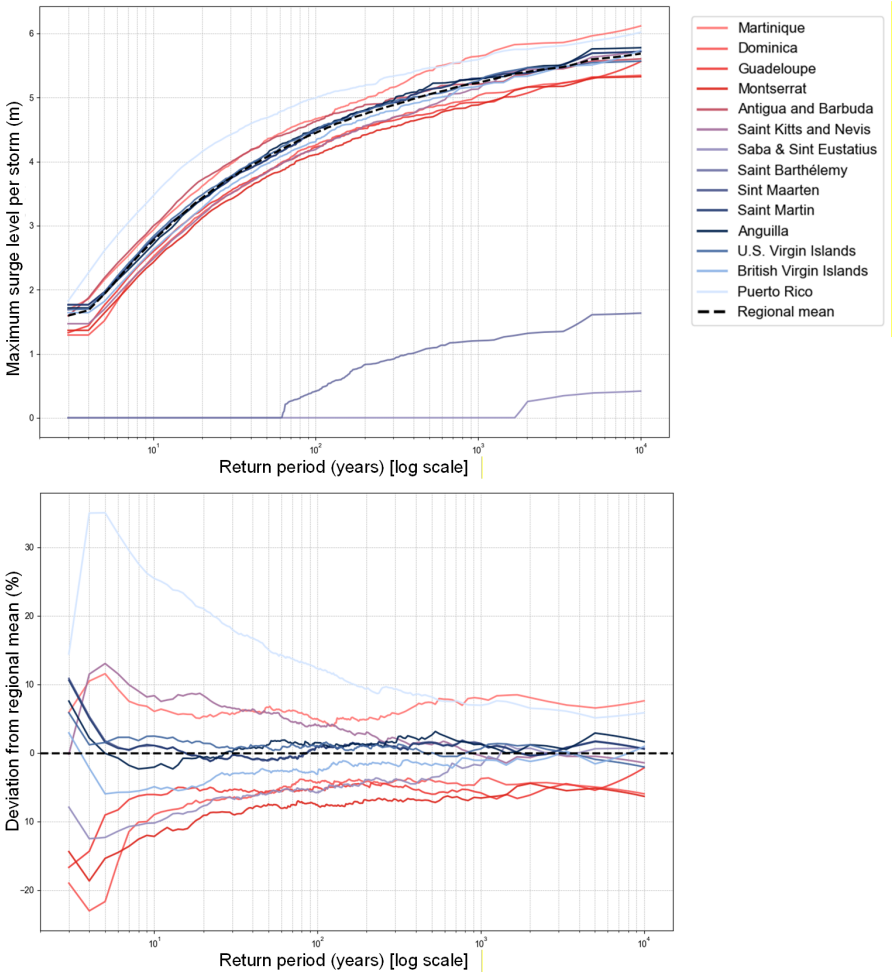

Figure 5.10. Estimated maximum surge level per country, plotted against the corresponding return period. The x-axis, showing the return period in years, is on a log scale. The black dotted line shows the regional mean, taken as a mean over all countries, except for Saint Barthélemy and Saba & Sint Eustatius. The lower figure shows the relative deviation from this region's mean over the range of return periods, in percentage.

In Appendix F the same graph is shown again, for different kinds of colour orderings, based on land size and on the presence of high elevation. The first two Figures F.5a and F.5b, where the deviation is colour coded based on location and size, do not indicate a clear trend in their colour codes, meaning that location and country size are not clear indicators for expected surge levels on land. The third Figure, F.5c, indicates that countries that have lower maximum heights within their boundaries are expected to experience higher surge levels on land.

5.2.3 Spatial reach of a tropical cyclone

For the storm surge results, a clustering is made based on the similarity between the hit rates of the countries. These hit rates are based on a binary dataset of the results of the synthetic TC tracks, where a country is considered 'hit' when, for at least one point, a surge height above 0.2 meters is reached.

The clustering is shown in Figure 5.11. When looking at surge levels, based on the modelled output of this study, four clusters can be defined:

- Dominica and Guadeloupe
- British Virgin Islands, Anguilla, Saint Martin and Sint Maarten
- Puerto Rico and U.S. Virgin Islands
- Antigua and Barbuda, Saint Kitts and Nevis and Montserrat

These clusters seem to be mainly based on location, which indicates that the surge levels are highest close to the eye of the storm (compact impact). That way, one track affects countries that are close together. Saba & Sint Eustatius are not included in the clustering, since at these islands no surge is modelled. Martinique has little overlap with other islands, probably because it is the southernmost island. Saint Barthélemy is not included in any cluster either, which is due to its very small surge in the modelled output.
Even though the modelled surge levels are not considered very accurate, a clustering mainly based on location makes sense, since storm surge is indeed highest right at the centre of the storm system where the central pressure is at its minimum. Other drivers, such as the slope of the bathymetry, also correlate between neighbouring islands.

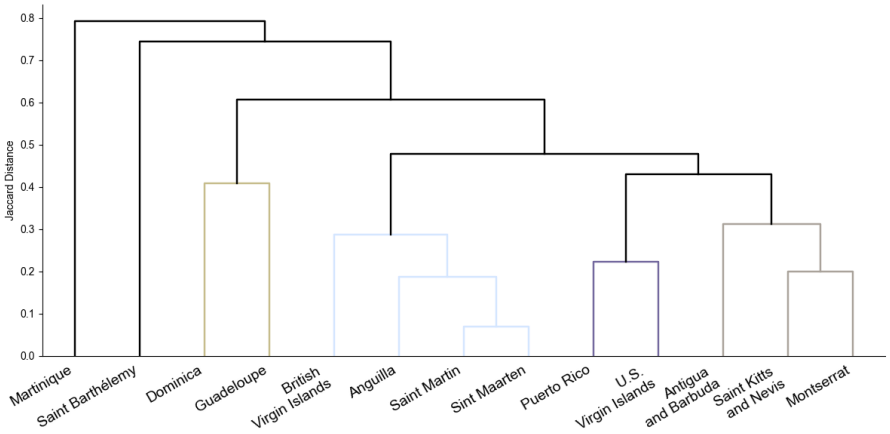

Figure 5.11. Clustered countries based on being affected by the same storms, on their modelled maximum reached surge heights above land. Clustering based on modelled hazard from synthetic tropical cyclones.

5.3 Modelling tropical cyclone-related precipitation

For all historical TC tracks between 1940 and 2024, the precipitation is estimated by means of the TCR model, interpreted by the CLIMADA Python package. Per storm event, the total precipitation over the whole duration is calculated. The output value is the total precipitation in millimetres over the total duration of the storm, at a certain location. When considering the precipitation per country, the mean total precipitation over all points within the country is determined.

5.3.1 Precipitation for historical TC tracks

For all historical tracks, the expected total precipitation amounts are modelled. A pre-selection is done to reduce the total number of tracks that are to be included, based on passing the region of the Leeward Islands. In total, 443 tropical storm tracks were included and computed for a total point grid of 3,669 points (the 2-km grid). A larger number of tracks is included than for the modelling steps of wind speeds and storm surge for historical TC tracks. This is done because rainfall can reach further from the eye than the other hazards. In the pre-selection, a region of tracks passing anywhere between 10 and 25 degrees North and 55 and 85 degrees East is included. Of these 443 tracks, 248 led to modelled outputs of at least 50 mm of precipitation over the duration of an event, for at least one of the points. Only these 248 tracks are considered for further analysis.

The maximum amount of total precipitation in one place is modelled to be 5200 in Saint Kitts and Nevis, for Hurricane Lenny (1999). This is followed by maximum total precipitation amounts of 2311 mm during Hurricane Maria (2017) and 2177 mm during Hurricane Beulah (1967). It is already notable that these extreme rainfall amounts are very high. Literature showed for these three storms the following: On Saint Kitts and Nevis, a NOAA report gives a range of 20-25 inches (up to 635 mm) for Hurricane Lenny (NOAA 1999). On Hurricane Maria (2017), a study by Keellings and Ayala (2019) reports a maximum total precipitation amount of 1029 mm in Puerto Rico, which is accumulated over three days. Hurricane Maria caused the highest precipitation since 1956 in Puerto Rico and can therefore be seen as very extreme in its precipitation. On Hurricane Beulah, the NOAA reports high amounts for Texas,

but only up to 9.76 inches (250 mm) in Puerto Rico (NOAA 1967).

The precipitation values per point are translated to empirical return periods. The return levels that are expected to be exceeded every five years are shown in Figure 5.12. It shows that precipitation levels vary highly over an island, mainly due to elevation differences. The same effect is seen for other return periods. Figures G.1 and G.2 in Appendix G include the maps of precipitation levels for the return periods 1, 2, 5, 10, 50, and 80 years.

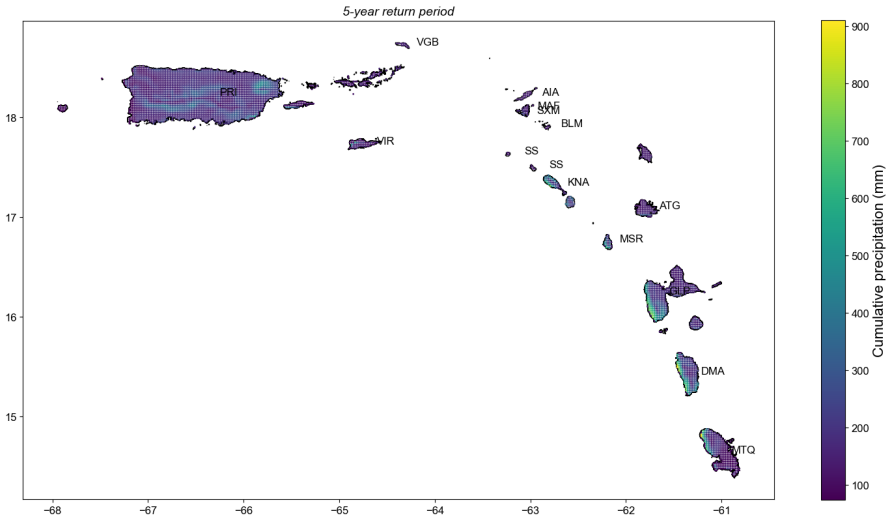

Figure 5.12. The estimated total precipitation amounts per storm for a five-year return period, based on IBTrACS data.

Figure 5.12 shows no trend in modelled precipitation amounts over the range of islands based on their location. It does show a high variability in expected exceedance levels for total precipitation within a country. This is linked to elevation differences within a country. A cloud carrying precipitation that has to rise will cool down and lose precipitation in the process. Especially the countries of Saint Kitts and Nevis, Montserrat, Guadeloupe, Dominica, and Martinique seem to show very high precipitation amounts on their western sides. In total, the expected total precipitation varies between 100 and 900 mm for a return period of 5 years, based on 248 TC tracks in the historical database IBTrACS for the period 1940 to 2024.

5.3.2 Spatial distribution per country

Instead of taking all points together, the results are also separated by country. We have chosen to take the mean for all output values of all points per country. This represents the mean total precipitation over the duration of the storm for a specific country. Additionally, we have chosen to also determine the maximum for all output values of all points per country. This represents the maximum total precipitation over the duration of the storm, at at least one grid point, for a specific country. This second value provides insight into the local extremes per country.
The results per country are summarised in Table 5.3 below. The data represents 248 historical TC tracks, as is stated above.

The number of storms that cause precipitation in a country ranges between 200 and 242. Of the total number of storms included of 248, it can be concluded that the model estimates precipitation for all countries for the vast majority of storms causing any precipitation in the region. However, not always high extreme precipitation is expected in all countries, with mean values ranging between 40 and 100 mm of total precipitation, for the storms with precipitation.

Table 5.3. Summary statistics of estimated total precipitation amounts per storm event, in mm, per country. The first two statistics concern the mean total precipitation over the total land surface per country. The second two statistics concern the maximum total precipitation amounts per country. For the last two, only storms reaching over 50 mm of accumulated precipitation for at least one point in that country are considered.

Country	Maximum of mean	Mean of mean	Maximum of maximum	Mean of maximum	Number of storms with precipitation	Mean of mean for storms with precipitation
Anguilla	757	36.7	948	45.3	221	41.2
Antigua and Barbuda	489	38.9	1120	96.3	235	40.9
Saint Barthélemy	1350	40.2	1360	41.5	200	49.8
Dominica	878	87.7	2180	368	218	99.8
Guadeloupe	700	64.7	2320	321	231	69.5
Saint Kitts and Nevis	1310	84.3	5200	277	240	87.1
Saint Martin	739	41.6	1060	66.7	235	43.9
Montserrat	818	83.2	2240	268	237	87.1
Martinique	445	51.7	2280	322	209	61.3
Puerto Rico	938	55.6	2310	265	234	58.7
Saba & Sint Eustatius	1010	35.7	1130	39.1	201	44.1
Sint Maarten	1300	50.5	1660	75.1	228	54.7
British Virgin Islands	604	39.9	1180	80.1	242	40.8
U.S. Virgin Islands	991	44.8	2390	180	241	46.1

High maximum precipitation amounts are expected in Dominica, Guadeloupe, Saint Kitts and Nevis, Montserrat, Martinique, and Puerto Rico. These are all islands with steep mountains, and are also all large countries in the region.
High mean precipitation amounts are expected for Dominica, Guadeloupe, Saint Kitts and Nevis, and Montserrat. This represents high precipitation amounts over the entire country, not only local extremes. High maximum values of the mean precipitation over a country are given for Saint Barthélemy, Saint Kitts and Nevis, Saba & Sint Eustatius, and Sint Maarten. These are all small countries, which explains the high probability of TC-related precipitation being extreme for the entire country.

For the other two hazards, return period graphs are only given for the output based on 10,000 years of synthetic TC tracks. The return periods are determined empirically, and therefore, the length of the dataset is of high importance to the statistical value of the return period graphs, especially for the higher periods. However, since the hazard of extreme precipitation cannot be modelled for the synthetic TC tracks, return period graphs are determined for the historical TC tracks, in Figure 5.13. An important note here is the low statistical relevance of the expected return levels for higher return periods. The dataset has a length of 85 years, and therefore, the return levels up to 10 / 20 years are considered to be representative.

Figure 5.13 shows how the accumulated precipitation increases for increasing return periods, in a logarithmic way. This means that for higher return periods, the rate of increase slows down. For the range of 1 to 85 years for the return period, precipitation amounts of 0 to 5200 mm are shown. However, this maximum value of 5200 mm seems to be a clear outlier and does not represent the general expected extreme precipitation. When excluding that one outlier, the range goes from 0 to 2200 mm.

For further analysis, only the return periods up to 40 years are included, since the higher values are not considered representative of the general trends. Note that the return period ranges differ between the upper and lower graphs in Figure 5.13. The lower graph shows that the southern countries have resulted in higher maximum precipitation amounts as opposed to the northern countries, except for Puerto Rico, which also scored quite high.

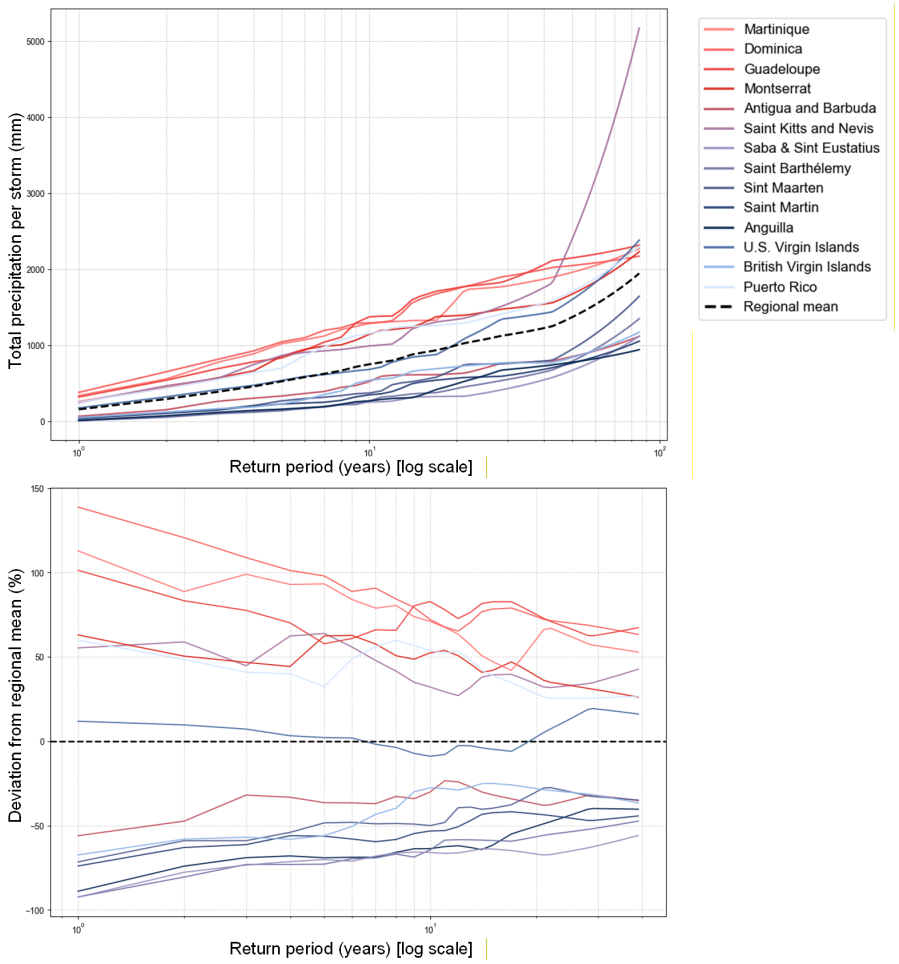

Figure 5.13. Modelled total precipitation, in mm, over the duration of a storm, plotted against the corresponding return period, which is empirically determined. The x-axis, showing the return period in years ranging from 1 to 85 years in the upper figure and from 1 to 40 years in the bottom figure, is on a log scale. The black striped line represents the regional mean, taken as the mean value of all return levels per country. The bottom figure shows the relative deviation from this regional mean, in percentage.

In Appendix G the same relative deviation is included, but with other colour orderings. This is done in order to identify driving factors to explain the spatial distribution between countries. Figure G.3b shows that smaller countries experience lower maximum precipitation amounts than larger countries. Montserrat, however, is one of the smaller countries, reaching higher maximum precipitation amounts, and Antigua and Barbuda shows the opposite.
Figure G.3c shows the clearest distinction, indicating that countries with higher maximum elevation levels within their boundaries are more prone to high maximum precipitation amounts.

Clustering countries

For the total precipitation results, a clustering is made based on the similarity between the hit rates of the countries. These hit rates are based on a binary dataset of the results of the synthetic TC tracks, where a country is considered 'hit' when, for at least one point, a total precipitation of at least 50 mm is reached.

The clustering is shown in Figure 5.14. When looking at precipitation, based on the modelled output of this study, three clear clusters can be defined:

- Martinique, Dominica, Guadeloupe, Saint Kitts and Nevis and Montserrat
- Saba & Sint Eustatius, Anguilla and Saint Barthélemy
- British Virgin Islands, Saint Martin and Sint Maarten

Figure 5.14 shows a significant lower relation within clusters based on their location for the modelled precipitation, compared to the other two hazards. This can indicate various things. Firstly, that other features, such as the presence of high elevation and steep slopes, as is already mentioned in this section, highly affect the occurring precipitation. Secondly, precipitation doesn't necessarily occur close to the storm centre. In that case, you would expect clusters showing how the hit rates of countries per storm align, to comply with the surroundings of the track.

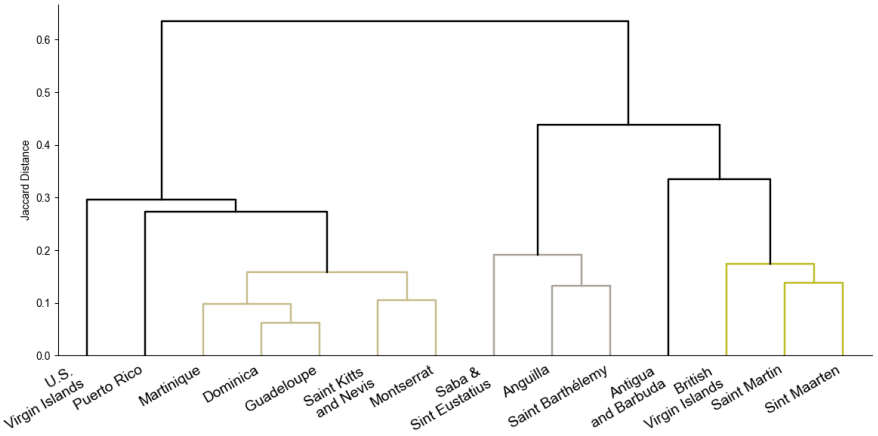

Figure 5.14. Clustered countries based on being affected by the same storms, on their modelled total precipitation. Clustering based on modelled hazard from synthetic tropical cyclones (1000 years).

5.4 Joint-hazard analysis on tropical cyclone-related wind speeds and precipitation

For the historical storms, on a 2-km grid, per point, both the expected rainfall and wind speeds are known. To see whether this correlates with each other, a joint frequency plot is created. Contrary to the previous results, the joint hazard per storm is considered here. Figure 5.15 shows the count per joint hazard for all the points in the grid.

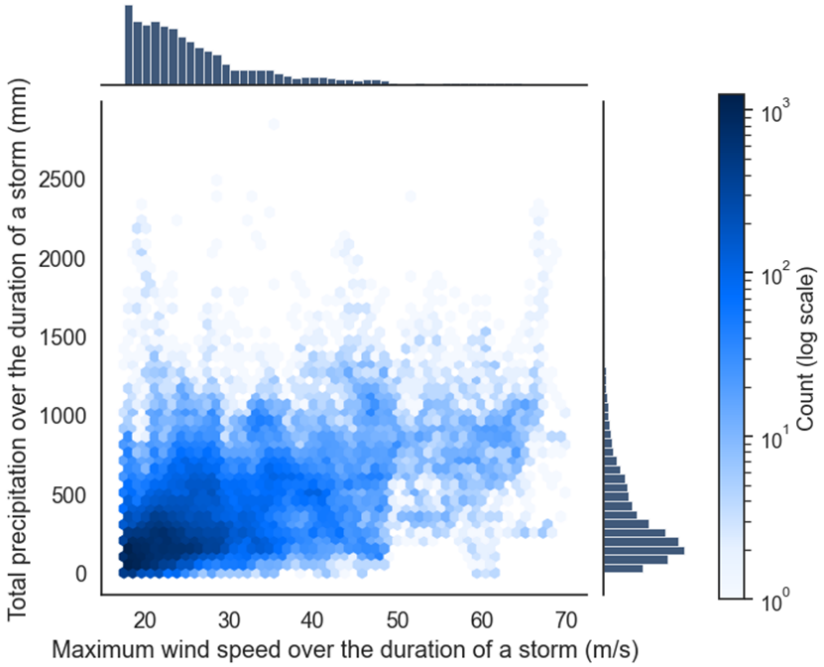

Figure 5.15. Joint frequency plot of maximum 1-minute sustained wind speed at 10 m height and total precipitation amounts per grid point, per storm, for modelled hazards based on IBTrACS TC tracks. The cunt is scaled logarithmically.

It shows that the highest count is given for low maximum wind speeds in combination with low total precipitation amounts. For higher wind speeds, the precipitation is more spread, and the correlation is less significant. The figure shows how the count rate spreads out in both directions, meaning that also for higher precipitation amounts, the wind speeds are more spread out. It is important to note that for the wind speed, all values below 17.5 m/s are left out, and for the total precipitation, no threshold is applied. This explains the difference in distributions, shown on the upper and right axes.

5.5 Comparing tropical cyclone scales for historical storms

To gain insight into the total risk profile for tropical cyclones affecting the Leeward Islands, the results of the three modelled hazards are translated to category classifications, based on the Tropical Cyclone Severity Scale (TCSS). Hereby, a comparison is made to the commonly used classification based on the Saffir-Simpson Hurricane Wind Scale (SSHWS), only including the hazard of high wind speed.

Every storm is ranked per country, using the modelled hazards within that country. This gives one storm fourteen 'scores'. All historical storms passing the region of the Leeward Islands between 1940 and 2024 from the best-track dataset IBTrACS are considered, which are 209 tracks. So, in total, 2926 scores are determined.

Ranking tropical cyclones on hazards per country deviates from normal practice, since usually the ranking is based on the maximum reached hazard over the storm, along the track. Often, a category is given upon landfall and represents the maximum wind speeds in the eye wall.
A tropical cyclone is usually ranked on the Saffir-Simpson Hurricane Wind Scale (SSHWS), designed by Herbert Saffir and Robert Simpson in 1971. The scale of a TC varies over time, along its track, and represents the maximum hazard at that moment. However, at some distance from the eye, a tropical cyclone of scale 5 can be experienced by wind speeds corresponding to scale 2, for example. In this study, a category classification is given for the experienced hazard within the boundaries of a country, even if the tropical cyclone did not make landfall in that country.

Applying thresholds

For all historical tracks, the modelled experienced wind speeds are translated to a scale, using the thresholds of the SSHWS scale (see Table 2.1). The maximum scale value reached within a country is considered the scale value for that country.

In the same way as the SSHWS ranks are established for historical tracks, the TCSS ranks are determined. However, this rank is made up of a combination of all three hazards. Firstly, per hazard, a rank is given to a country, per storm. The modelled outputs that reflect the experienced hazard, over a point grid, per country, are translated to scale values based on the thresholds of the TCSS (see Table 2.2). The modelled output values equal the parameters that are included in the TCSS. Therefore, no interpretation steps are required. Per hazard, the maximum reached value is considered per country. Subsequently, the three scale values are combined into one value. This calculation method is based on how the TCSS is designed, by Bloemendaal, Moel, Mol, et al. (2021), which is followed accurately. The goal of this scale, as opposed to the 'traditional' SSHWS, is to enhance clear risk communication. These values are interpreted based on the given thresholds for categories of severity.

Counting scores per category

Table 5.4 shows the count of the categories that were reached within the countries for all storms. The wind speed-based category of the TCSS is equal to the category of the SSHWS, and is included only once in the results, for clearity. The multi-hazard category is a combination of the three hazard categories per storm and per country, using the rescaling factors and thresholds included in Section 2.1.4.

Table 5.4. Counts of the resulting categories, per hazard, and for the multi-hazard scale. A score is given for 14 countries and 209 storms, thus totalling 2926 outputs in every categorisation.

Category	Count for wind speed	Count for storm surge	Count for accumulated rainfall	Count for multi-hazard category
0	2821	2872	1622	1621
1	54	29	594	593
2	32	13	309	307
3	10	7	154	156
4	9	2	81	78
5	0	3	166	169
6	0	0	0	2

Scores of category 6 are given only for Hurricanes Irma and Maria in 2017, for the countries British Virgin Islands and Puerto Rico, respectively. These two hurricanes have been mentioned several times earlier in this report, in relation to their high impact in the region.
It is seen that the counts for higher classifications are significantly higher for the accumulated rainfall. This indicates that rainfall is very important to include in the scale, but also confirms the presumption that the model outputs for precipitation overestimate the actual hazard. Especially local extremes are expected to be overestimated, which are represented in this classification, where the maximum values are taken. This will be further discussed in Chapter 6.

Comparing the results

The surge categories appear to be lower than the wind speed categories. This might be due to different definitions of storm surge between the data used by Bloemendaal, Moel, Mol, et al. (2021) and the data used in this study. We determine surge levels above land, e.g. inundation depths, while the TCSS is designed based on surge levels compared to the mean sea level as is measured along the coast. These values will be higher than the remained surge on land.

Since one of the constraints used in the design process of the TCSS is that no final (multi-hazard) category can be lower than the highest category per hazard, it does not happen that in the output, the SSHWS scores are higher than the TCSS scores. In 56% of the cases, the score is equal for both the classification methods. Per difference in score, the percentage of occurrence for this dataset is:

- 21% resulted in a difference of 1;
- 11% resulted in a difference of 2;
- 5% resulted in a difference of 3;
- 3% resulted in a difference of 4;
- 4% resulted in a difference of 5.

The recent storms that resulted in a score higher by five categories in at least one country are listed: Dean (2007), Hanna (2008), Earl (2010), Maria (2011), Hilary (2011), Rafael (2011), Irma (2017), Maria (2017), Dorian (2019), Earl (2022), Fiona (2022), Gert (2023) and Philippe (2023). Observations of the experienced hazards of these storms are not studied. Large differences in the scores are found in the countries Guadeloupe, Saint Kitts and Nevis, Martinique, Dominica, Puerto Rico, U.S. Virgin Islands, Montserrat, British Virgin Islands, and Antigua and Barbuda.

Rankings as return periods

Figure 5.16 shows the results of the scaling based on the Tropical Cyclone Severity Scale, per country, as they are translated to return periods (empirically). It is shown how higher categories are given for higher return periods, which is in agreement with the return period graphs per hazard. It also seems to slightly indicate that the southern countries are more at risk for high-category tropical cyclones, as opposed to the northern countries. Especially Martinique, Dominica, Guadeloupe, Montserrat, Saint Kitts and Nevis, and Puerto Rico score high on the multi-hazard classification method for low return periods already.

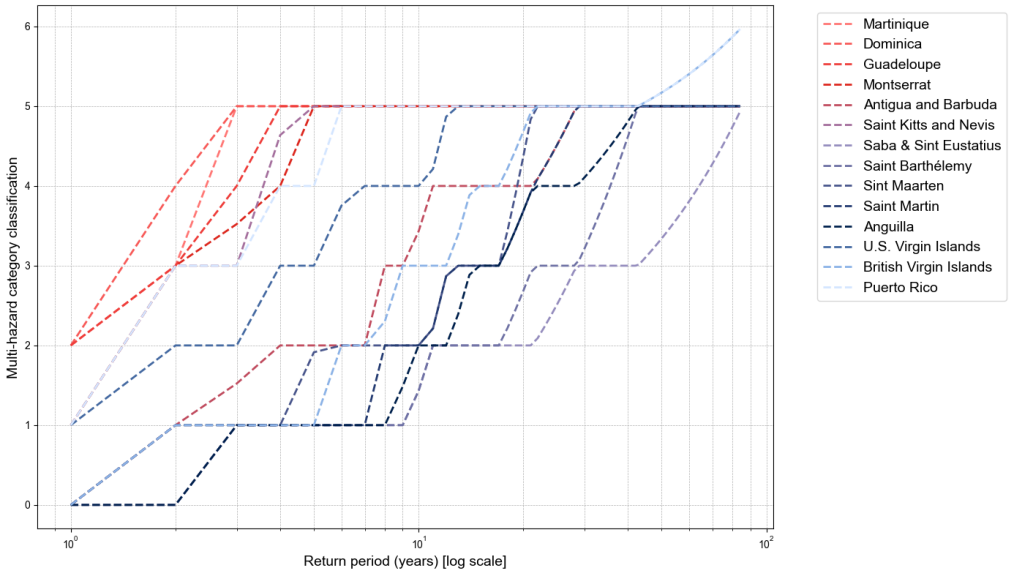

Figure 5.16. The multi-hazard classification, based on the TCSS, per country and per storm, against its empirically determined return periods. In the legend, the colours represent, from top to bottom, southern to northern countries.

The same result is given for the Saffir-Simpson Hurricane Wind Scale-based categories, in Figure 5.17. It shows how the SSHWS results in significantly lower categories for the same storms and the same countries, by only including the hazard of high wind speeds. A category 1 tropical cyclone responds to a return period of 7 years for the British Virgin Islands, where that same category for that same country responds to a return period of 2 years in Figure 5.16. This large difference is partly expected, since total higher scores are expected in the multi-hazard scale, but is also partly attributed to the overestimation of accumulated rainfall amounts in the model.

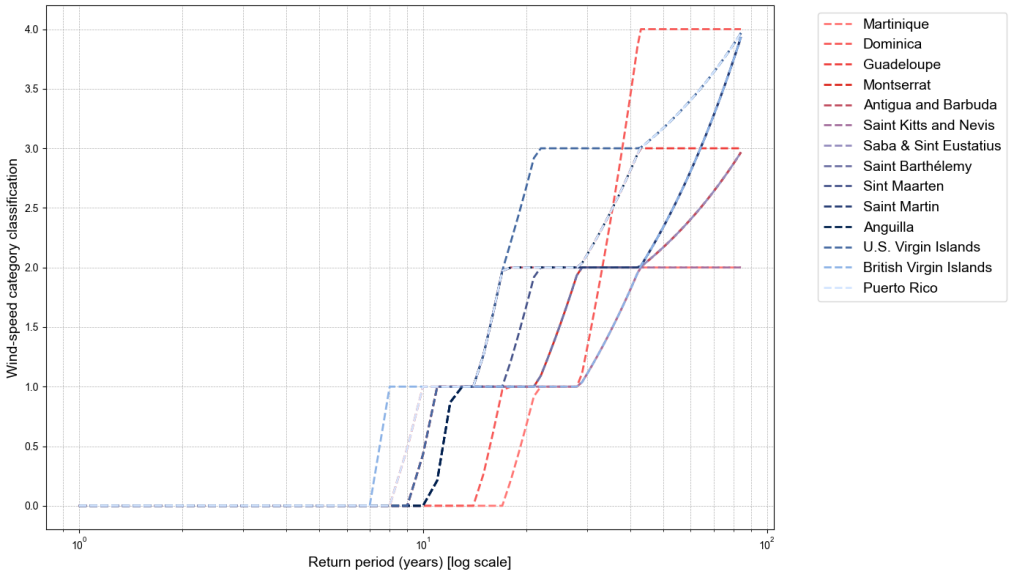

Figure 5.17. The wind speed-based classification, using the SSHWS, per country and per storm, against its empirically determined return periods. In the legend, the colours represent, from top to bottom, southern to northern countries.

6 Discussion

Reflection on the decisions concerning the definition of research questions, methodology choices, and the results is included in this chapter. All considerations have been included in the report as thoroughly and transparently as possible to ensure clear communication of the research conducted and the results found. The Python code used to generate the results presented in this thesis is publicly available at `https://github.com/lisettedevalk/thesis_CLIMADA_TChazards`.

The study aims to contribute to the feasibility study on the development of regional Early Action Protocol(s) for tropical cyclones in the Caribbean, within the context of the Early Warnings For All goals. The research questions set the focus on the different hazards that are related to tropical cyclones, and the goal of the study is to identify spatial variation in the occurrence and severity of three hazards over the study area. The emphasis on including all hazards aligns with the motivation mentioned in Bazo et al. (2021) and by World Meteorological Organization (). By identifying the spatial variation of these hazards, the study contributes to the aspired regional approach in the Caribbean. However, the implications of finding either little spatial variation or high spatial variation are not further described within this study. Further research and discussion with all parties involved in the development would be beneficial. This study should therefore be considered informative, but not prescriptive.

A motivation for a regional protocol could be to group islands that are often hit together, since one trigger could suffice for the whole region. On the other hand, a regional protocol could be fitted for a group of islands that are almost never hit by the same event, so that relief supplies can be shared. The clustering of islands, as is given for experienced wind speeds in Figure 4.3, provides an approach to dive deeper into this motivation. It is concluded that more operational and financial considerations should be included to decide on this step.
At the same time, we would recommend modelling experienced TC-related impact based on the experienced hazards first in order to advise on the EAP development. Before being able to translate the modelled precipitation amounts to impact, the secondary hazards related to extreme precipitation need to be included. Precipitation can lead to high river discharges, flash floods, inundation, and even land and mudslides.

6.1 Discussion of results

For the modelled hazards, the results are discussed. Uncertainties are listed, and the results are compared to literature. Additionally, a comparison is made between the results for the historical and synthetic datasets, investigating possible causes of deviation between the datasets.

6.1.1 Spatial distribution of TC-related experienced wind speeds

The maps showing the expected exceedance levels for a return period of five years, one based on 85 years of historical tracks and one based on 10,000 years of synthetic tracks, do not show similar results. The first, Figure 5.1, ranges from 0 to approximately 24 m/s, and shows the highest values in the north-east. The second, Figure 5.2, ranges from 26.5 to 29.5 m/s approximately, with (slightly) higher expected wind speeds for the south. These second results seem to be more reliable, since high spatial variations are not expected on this relatively small scale for wind speeds. A return value of

+/- 28 m/s of experienced wind speeds caused by hurricanes is also within the range of expectations, corresponding to being just below the threshold of Category 1. However, the unexpected result of the map based on the IBTrACS data remains unexplained, only attributed to the small number of storms in the IBTrACS dataset (57 storms) reaching the threshold of 17.5 m/s.

Comparing results to literature

Bloemendaal et al, who designed and generated the STORM dataset, estimated return periods for maximum experienced wind speeds for many small islands worldwide as well. In order to verify the results, the wind speeds for some fixed return periods are compared. An important difference between the two methodologies, is that Bloemendaal determined the return periods of the experienced maximum wind speeds for the capital of the islands, including a 100-km buffer surrounding the capital (Bloemendaal, Moel, Muis, et al. 2020), while we have determined the return periods of experienced maximum wind speeds for a point grid covering the land surface of an island, and taking the mean value per island. The results of Bloemendaal et al are included in Table E.1 in Appendix E. They have determined the wind speeds as the 10-meter 10-minute sustained maximum. We have determined 10-meter 1-minute sustained maximum wind speeds. In order to account for this, our values are divided by a conversion factor of 0.88 (Bloemendaal, Moel, Muis, et al. 2020).
Table 6.1 shows the mean values of our calculations for both 1-minute and 10-minute sustained wind speeds. The results are nearly identical, indicating that the methodology is performing as intended.

Table 6.1. Mean over the entire region for the determined wind speeds for four different return periods. Every point in the total point grid has equal weight.

	1-in-10 years	**1-in-20 years**	**1-in-50 years**	**1-in-100 years**
1-minute sustained	36.77	43.05	49.17	52.82
10-minute sustained	41.78	48.92	55.88	60.02
10-minute sustained (Bloemendaal)	41.52	50.08	56.23	59.89

A study by Hemmati et al. (2025) has determined expected wind speeds using synthetic tropical cyclone tracks generated by the Columbia tropical cyclone HAZard model (CHAZ) and employing the Holland (1980) model. They found, among other statistics, the following:

- In Puerto Rico, a category 5 storm has a return period of 500 years, and a category 1 storm has a return period of 2.5 years.
- In Guadeloupe, a category 5 storm has a return period of 700 years, and a category 1 storm has a return period of 1 year.
- A 100-year event has an exceedence value of 58 m/s in Cuba, Puerto Rico and Guadeloupe.

When comparing these results to our results, we see that the CHAZ tracks lead to higher expected wind speeds (we find a category 1 storm approximately correlating to a return period of 7 years) compared to STORM tracks. A 100-year event is associated with wind speeds of 54 m/s (see Figure E.4), which is quite close to the result of the CHAZ data.

6.1.2 Spatial distribution of TC-related experienced storm surge

The storm surge is modelled and expressed as surge levels over land for the fourteen countries within the study area. This is done because this is the common output within the CLIMADA Python package, used for the modelling steps, since surge levels on land are easily translated to impact on land. However, the results for this output value is not considered to be very accurate due to the coarse resolution (0.5 by 0.5 km) of the digital elevation model and the lack of inclusion of barriers and other water-retaining structures. Small, low-lying areas can cause flooding in the hinterland. But also the other way around, narrow elevations can prevent flooding.
Additionally, surge is not commonly expressed as surge levels on land, but usually as surge levels in regard to the mean sea level that a storm has caused near the coast. This is considered a more objective measure when considering the spatial distribution of the hazard of storm surge. More accurate,

hydrodynamic models with higher-resolution data need to be applied when interested in the expected surge levels on land, for these small islands with steep and irregular coastlines.
In conclusion, the results for the TC-related experienced storm surge do indicate areas prone to coastal flooding, but do not provide accurate insights into the exposure to high storm surge per island.

6.1.3 Spatial distribution of TC-related experienced precipitation

The return period graphs show some higher deviation for smaller return periods. This is attributed to the threshold used for sampling of TC tracks leading to extreme values. Relatively few tracks resulting in low values are left in the dataset. Additionally, within the precipitation modelling, firstly, the wind speeds are modelled, where all wind speeds below 17.5 m/s are set to 0.0 m/s, which is in fact a double threshold. The larger deviation between countries for precipitation amounts corresponding to low return periods is attributed to the modelling steps and is not considered representative of the real-world distribution.

Overestimating peak precipitation

The model is evaluated by Feldmann et al. (2019) and is considered to capture extreme-event precipitation quite well, mainly along coastal regions. However, noted areas for refinement include: a tendency to overestimate rainfall in the inner core (eyewall region), a slight underestimation in the outer regions, and limited capability in accurately simulating rainfall maxima in complex mountainous regions where orographic effects are dominant but simply parametrised. This is stated by Lu et al. (2018) as well. Since the geographical scope of this study includes steep mountainous areas and highly variable friction coefficients, sensitivity analyses are recommended for the use of the TCR model in this region. The studies of Lu et al. (2018) and Feldmann et al. (2019) both use a resolution of 0.25 by 0.25 degrees, which is coarser than the resolution of the digital elevation model used in this study (of 0.045 degrees). The default option of CLIMADA of 0.1 degrees (ETH Zürich 2025) is coarser as well.
However, even though local peak precipitation is likely overestimated, the results are still considered to represent the spatial distribution of precipitation over the countries sufficiently.

6.1.4 Comparing historical to synthetic data

When comparing the return period maps of both wind and storm surge, the following is concluded:

- The variation in experienced hazards is significantly larger over the study area for the results based on the historical data.
- The spatial trend differs between the results obtained from the historical data and those obtained from the synthetic data.
- The estimated experienced wind speeds corresponding to a return period of five years are higher based on the synthetic data than those obtained from the historical data.

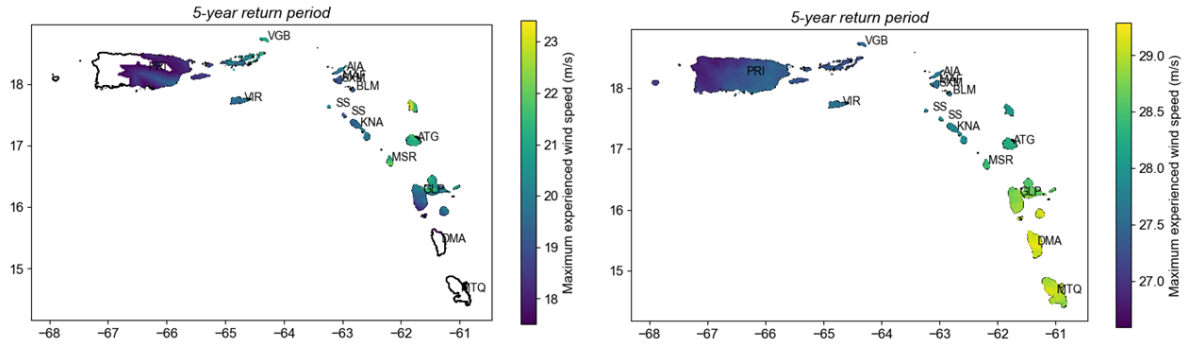

(a) Return values of maximum wind speeds (m/s) for a 5-year return period. Wind speeds are 1-minute sustained at 10 meters height. Left: historical data. Right: synthetic data.

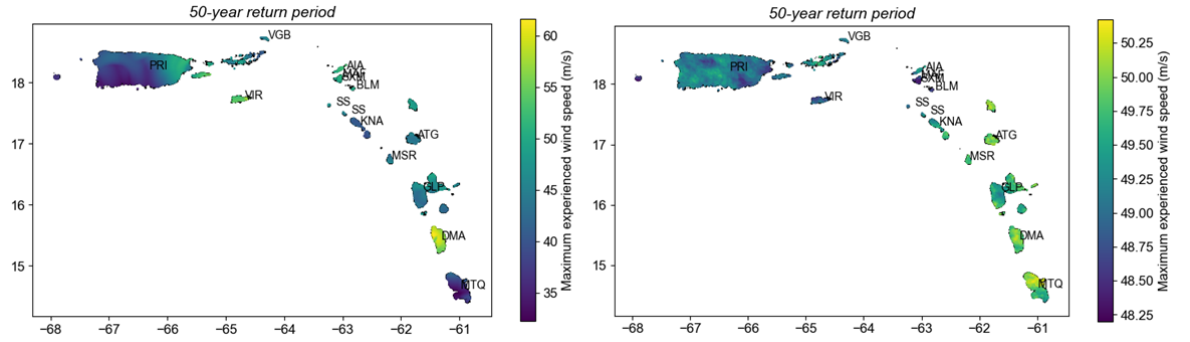

(b) Return values of maximum wind speeds (m/s) for a 50-year return period. Wind speeds are 1-minute sustained at 10 meters height. Left: historical data. Right: synthetic data.

Figure 6.1. Maps of return values of maximum wind speeds (m/s) for different return periods (5 and 50 years). The wind speeds are determined as 1-minute sustained winds at 10 meters height. Each subfigure compares historical (left) and synthetic (right) data.

Figure 6.1 shows maps of the return values corresponding to both five and ten years for the hazard of wind speed, for the two datasets next to each other, which confirms the statements made above. The datasets are further analysed in order to investigate the found differences.

The return maps based on the synthetic data are based on a total of 10,000 years of tropical cyclone tracks, whereas the maps based on the historical data are based on a total of 85 years. The methodology used to determine experienced wind speeds within the study area is equal for both datasets. In determining the return period maps, the difference in variation is attributed to the length of the datasets. The return values are determined empirically, meaning that, for example, for a dataset of 200 years, the maximum value corresponds to the expected return period of 200 years, the second-highest value corresponds to the expected return period of 100 years, the third-highest to 50 years, etcetera. All return periods in between are interpolated. When applying this logic to the two data lengths at issue, the values corresponding to a return period of five years are based on a number of values of five and twelve, respectively, for the historical and synthetic data. The return maps show the return periods per centroid separately, meaning that the maps don't show five and twelve storms, but can represent way more. Logically, the return periods are more robust for the smaller periods than for the longer periods, and when using similar data, they should be more aligned for smaller periods as well.

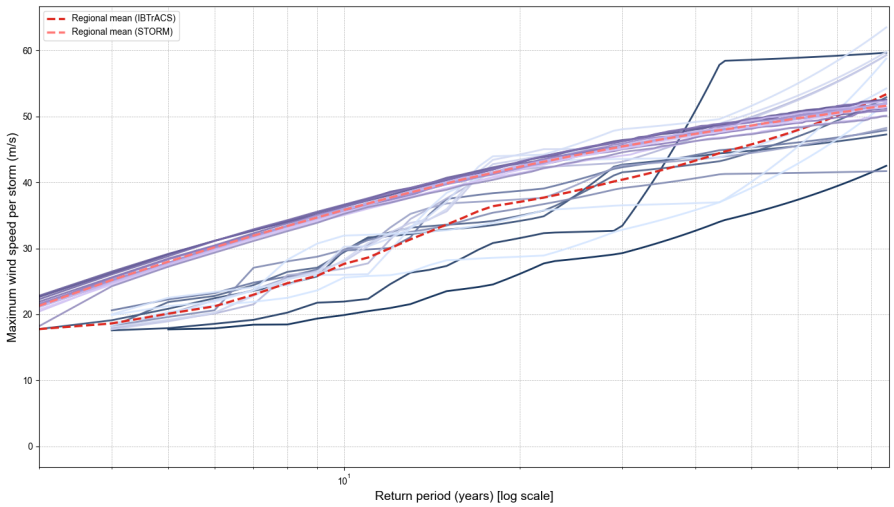

Figure 6.2. Return period graphs for the hazard of high wind speeds, showing the mean maximum reached 1-minute sustained wind speeds at 10 m height per country. The purple lines represent the fourteen countries when using the synthetic data as input. The blue lines represent the fourteen countries when using the historical data as input. Return values corresponding to return periods of 3 to 85 years are shown, since the results for the historical data only result in this range.

The mean values over all points are taken for both datasets over the return periods from 0 to 85 years and shown in Figure 6.2. This shows that the results based on synthetic data result in higher expected wind speeds compared to the results based on historical TC tracks. For higher return periods (30 to 85 years), the difference seems smaller; however, the range of the countries enlarges for the historical graphs. Overall, the results based on STORM show more uniform return period graphs. What drives this difference in expected wind speeds is further examined. Since the modelled wind speeds are incorporated in the results for the other two hazards, wind speeds are considered most important to look into.

Comparing the raw data

Since the applied methodologies do not differ between the two datasets, any difference should be caused by differences between the datasets themselves. The synthetic data generated by the STORM algorithm is validated against the historical IBTrACS data by Bloemendaal, Haigh, et al. (2020) as a performance assessment of the STORM algorithm. They have compared genesis events (avg/year), genesis pressure, average pressure along track, minimum pressure along track, maximum wind speed along track, total landfall counts, landfall pressure, and radius to maximum winds. For the North Atlantic basin, they have concluded that the data generated by STORM aligns with the IBTrACS data for all of these features. Only the number of landfall counts is smaller for STORM (6.0 compared to 8.2), and the radius to maximum winds is smaller (50.3 km compared to 69.7 km). For the landfall counts, both datasets show a relatively large standard deviation, indicating that there is a substantial year-to-year difference (Bloemendaal, Haigh, et al. 2020). The average landfall counts of the two datasets do fall within one standard deviation of each other. The difference in the radius to maximum winds (Rmax) is attributed by Bloemendaal et al. to the sampling process used in the STORM model to calculate Rmax, which is further explained in their article. However, lower Rmax values should lead to lower expected experienced wind speeds when working with the Holland model to determine these. This contradicts our findings and is therefore quite certainly not the cause.

Since this validation by Bloemendaal, Haigh, et al. (2020) is only done on a global scale, a similar comparison is made here for the data used in this study. The IBTrACS data is preprocessed to only contain the period 1940 to 2024. All tracks not crossing the area of interest, defined as anywhere between 55 and 85 degrees East and 10 and 25 degrees North, are excluded. All values below 17.5 m/s are excluded from both datasets, since this is standardised for the STORM data. Five variables are included in the comparison, of which the coordinates tell something about the tracks, and the other three tell something about the size and severity of the storms.

Table 6.2. Summary statistics for selected IBTrACS variables (North Atlantic, ≥1940).

Variable	Mean	Min	Max	Std	Mean of Max per Year
Latitude (°N)	25.64	7.80	72.50	10.79	—
Longitude (°E)	-65.53	-132.30	30.00	17.06	—
Maximum Wind Speed ($m\,s^{-1}$)	33.27	18.01	84.88	13.28	62.29
Minimum Pressure (hPa)	982.69	882.00	1016.00	21.93	—
Radius of Maximum Wind (km)	20.09	2.70	134.99	15.42	39.47

Table 6.3. Summary statistics for selected STORM dataset variables.

Variable	Mean	Min	Max	Std	Mean of Max per Year
Latitude (°N)	21.83	5.10	59.30	9.30	—
Longitude (°E)	-60.37	-101.80	-1.10	14.88	—
Maximum Wind Speed ($m\,s^{-1}$)	37.03	17.50	76.70	12.76	58.97
Minimum Pressure (hPa)	968.89	896.80	1005.90	21.37	—
Radius of Maximum Wind (km)	45.62	9.26	282.62	20.06	100.26

From these statistics, we conclude that the maximum wind speeds along the tracks (m/s) are slightly lower for the historical data, but approximately equal. The minimum pressure along the tracks (hPa) is approximately one standard deviation lower for the STORM data (meaning more severe storms). The radius of the maximum winds (km) is significantly higher for the STORM data, contrary to what was found for the whole North Atlantic basin. These statistics indicate that the synthetic data include more severe storms than the historical data for our area of interest, which aligns with the results of the wind speed modelling. This indicates that the STORM data and/or the IBTrACS data differ in the region of the Leeward Islands compared to the whole basin.

Trends in historical data

The STORM algorithm is applied to historical data ranging from 1980 to 2017, which is considered to represent the current climate (Bloemendaal, Haigh, et al. 2020). However, we use a larger range of historical data, from 1940 to 2024. Hypothetically, this difference could cause the found deviation in severity. The time series are compared in terms of frequency and intensity, shown in Figure 6.3 and Figure 6.4.

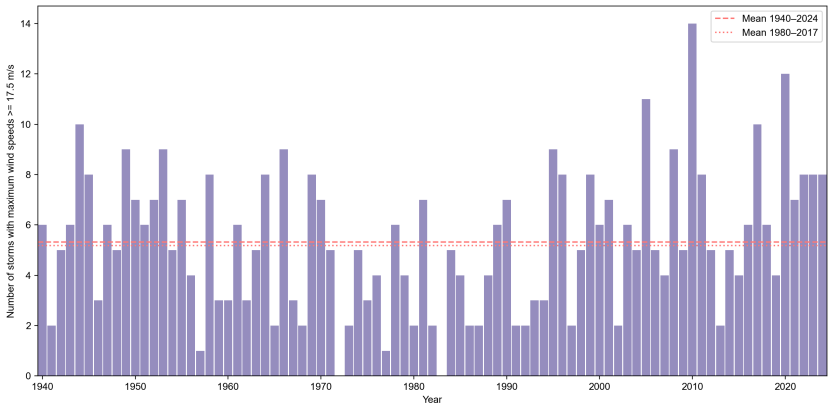

Figure 6.3. A count of the number of storms, with at least one point within the area of interest with a maximum wind speed over 17.5 m/s, per year. Means are determined for the time ranges 1940 to 2024 (the complete time series as shown) and 1980 to 2017.

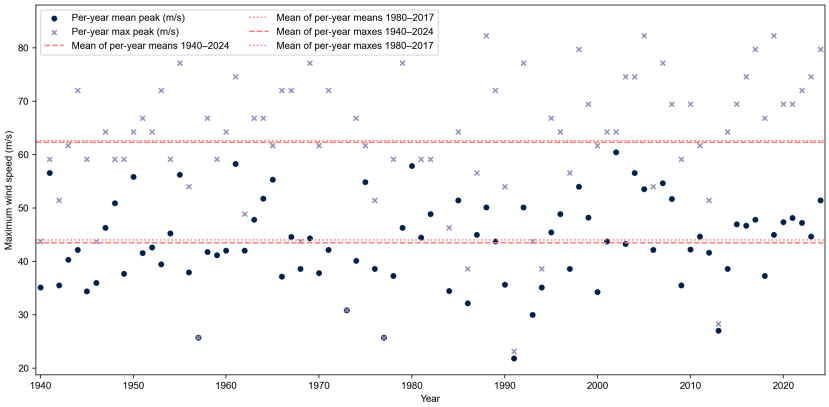

Figure 6.4. The yearly mean and maximum of the maximum wind speed of a storm, of all tracks within the area of interest. For both variables, means are determined for the time ranges 1940 to 2024 and 1980 to 2017.

Comparing these two time ranges, it is concluded that no higher frequency and/or intensity is experienced between 1980 and 2017 compared to 1940 to 2024. Some trend over time is visible, showing a higher frequency and higher maximum wind speeds in the storms later than 1990, approximately; however, not between the two time ranges that are of importance in this study. Therefore, the mismatch between the historical data used to generate the synthetic data and the historical data used in this study does not explain the difference in modelled wind speeds.

Conclusions

To conclude, we see that for our region of interest, the synthetic data generated by the STORM algorithm includes, on average, tracks with lower minimum pressures along the track, and larger radii of maximum wind speed, compared to the historical data of IBTrACS; resulting in higher expected wind speeds in the surroundings using the Holland model (Holland 2008).
Since we determine return periods empirically, the number of data points in the results has a large influence on the resulting return values. The synthetic data, therefore, provides high statistical value with 10,000 years of data, and the return period graphs show a uniform and clear result, where the smaller historical dataset resulted in higher spatial variance and a more scattered pattern over time. The results based on the STORM data, available for the hazards of wind speeds and storm surge, are considered of higher value than the results based on the IBTrACS data. However, before making design decisions based on these results, it is recommended to further investigate the local deviation on the STORM dataset around the Caribbean.

6.2 Discussion of the methodology

The uncertainty of the output of a model depends on the uncertainty of the input. The main input in this study is track data, including location, minimum atmospheric pressure, and maximum wind speeds around the eye wall. These tracks are considered a given in this study; the starting point, since this study is interested in the distribution of hazards given the tropical cyclone tracks that are likely to occur. However, when modelling hazard outputs for real-time forecasting, the uncertainty of a track is of very high importance.
The tracks are given at either a 6-hourly interval for the historical tracks or at a 3-hourly interval for the synthetic tracks. To prevent missing out on experienced hazards in the countries, the tracks are interpolated to 0.5-hourly intervals. However, rapid changes in the track can be missed within the interpolation step. When comparing to observational data or applications in real-time forecasting, attention should be paid to this, especially around landfall.

Interpretation of the results is highly affected by the way the results are presented. The distribution of return periods over the countries is presented in return period graphs, per hazard, showing the relative deviation from the regional mean. The regional mean is defined as the mean of all return levels per country; hence, all countries have equal weight. Another possibility would have been to take the mean for all return levels of all points in the region; hence, all countries would not have equal weights, but all

points in the grid would have equal weights. This would have resulted in different distributions shown in the graphs. The choice of assigning an equal weight was made to illustrate the variance between national protocols as opposed to regional protocols.
CLIMADA is a relatively new tool in risk estimation for natural hazards; hence, no exemplary studies estimating TC-related hazards using CLIMADA were found, except for the examples given by CLIMADA itself. This study has tested the capability of CLIMADA to model TC-related hazards. However, CLIMADA is not designed to use only one aspect of the total package, and therefore, it could be argued that the next steps in their total package still should be executed: incorporating exposure and vulnerability to estimate impact.

Another choice influencing the interpretation of the results is the definition of the countries themselves. An island, or island group, is considered a country in this study when it has its own ISO code and the government differs from the other islands within the region. An example of how this methodology decision influences the results is given by Antigua and Barbuda. Antigua is a larger island with volcanic mountains and steep coastal slopes. Barbuda is much flatter overall, since it is not a volcanic island and merely has some hills, and the coast is provided with gentle slopes into the sea.

As is common for extreme value analyses, a threshold is used for each hazard to filter only the extreme values, also making the data more manageable. However, the thresholds have been set quite arbitrarily. It is recommended to base the thresholds on certain impact-based thresholds or on a single return period applied to all hazards.
Lastly, the parameter selection for each hazard has implications for how the return periods are interpreted. Per hazard, the parameter is chosen such that it is closest towards the translation to impact. When interpreting the result, attention should be paid to the consequences of the parameter selection.

6.3 Recommendations

For storm surge modelling, the CLIMADA Python package offers two approaches to modelling surge height: the bathtub model based on Xu (2010), and a numerical model, GeoClaw, of the CLAWPACK. Practical considerations led to the use of the bathtub model, since the second option, the GeoClaw model, can only be run on Linux and Mac OS devices, which were not available to me. However, if not for these practical reasons, I hypothesise that some of the barriers and uncertainties we experienced in the surge modelling would have been overcome. A study by Hemmati et al. (2025) has employed the Geoclaw model and compared their results to observations of four locations (within our study area as well) for two historical events and showed that Geoclaw is able to capture storm surge along the shore quite well.

Overall, it is concluded that CLIMADA functions well for hazard modelling on land, and is both useful for historical and synthetic tropical cyclone events. However, its main advantage likely comes when incorporating impact and (financial) damage in the assessments, thereby making use of the full potential of the tool.
When only considering the modelling of hazards themselves, I would not recommend using CLIMADA, but applying the models per hazard yourselves. CLIMADA forms a bit of a black box when processing the tropical cyclone tracks, leading to a higher required investigation of the package to clearly understand what happens. Additionally, some alternative output parameters per hazard could be useful when interested in the typical frequency and severity of TC-related hazards. For example, CLIMADA is designed such that only the maximum reached levels are included, for example, the maximum reached wind speed or the maximum reached surge height, over the duration of a storm. This excludes the temporal component of the hazards between locations and over the duration of a storm.
Especially, the hazards of wind speed and storm surge are easily implemented by yourself, since elaborate documentation is available on the models used in these steps. Interpreting and adjusting methods is easier in a complete and accessible Python code. Modelling the hazard of rainfall is the most complex, and therefore, the advantage of using the pre-coded CLIMADA tool is the largest. However, alternative Python tools interpreting the Tropical Cyclone Rainfall model are available, such as pyTCR (Le et al. 2025). It is recommended to make use of these alternatives when modelling the hazard of precipitation, especially for studies excluding impact assessments and including secondary hazards of precipitation

such as landslides.

Thirdly, I would recommend working with synthetic tracks that are created from climate models. For these synthetic tracks, the additional required climate parameters that are used as input parameters in the precipitation modelling are available. By enabling the possibility of modelling precipitation for a large set of synthetic tracks, you can create precipitation results of higher statistical significance than are available now (only for 85 years of historical data). An example of such a dataset is the open-source Columbia tropical cyclone HAZard model (CHAZ) (Lee et al. 2018).

When operationalising a trigger model for a regional Early Action Protocol, timing and duration of hazards, also compared to other islands within the protocol, will be of importance. In this study, the temporal element is not included at all, since for the three hazards, only one output value per storm is used, such as the maximum reached wind speed over the duration of the storm. When modelling the hazards 'by yourself', so not using the CLIMADA Python package, it would be easier to extract a time series per hazard. This would give very large amounts of data, which would require a large computational capacity, and a temporal analysis could be executed.

Lastly, Bloemendaal et al. have developed similar large tropical cyclone datasets for different climate scenarios of the future. For these scenarios, the results could be compared to the current results to see what the impact of climate change would be concerning the hazards of tropical cyclones for the Leeward Islands. Since the methodology does not need to change to implement these synthetic datasets, it would be a feasible approach.

7

Conclusions

All research questions are answered for the defined study area: the islands in the east of the Caribbean, from Martinique up to Puerto Rico. These are referred to as the Leeward Islands.

1. What are the spatial distributions and return periods of maximum wind speeds, from historical and synthetic tropical cyclone tracks?".

The Holland model (version of 2008) is a common and suitable way to determine experienced wind speeds at certain locations, based on their distance to the eye of a tropical cyclone and the pressure and wind speeds of that tropical cyclone over its track. The implementation of the Holland model within the CLIMADA Python package functions well and is adaptable to both IBTrACS tracks as well as the synthetic STORM tracks. Over the past 85 years, a total of 57 storms have affected the Leeward Islands, with experienced maximum wind speeds over 17.5 meters per second. The synthetic tracks are also used to model experienced maximum wind speeds over the islands, and are translated to return periods. For a return period of five years, a common threshold in anticipatory action, a maximum wind speed of approximately 28 m/s is expected. The expected wind speeds vary little over the area; however, local variations caused by elevation on land, or by buildings, for example, are not included in the model. The mean values per land, for maximum reached wind speeds during a storm, are used to visualise return values for longer periods, up to 1,000 years. A total deviation over this range of 8 to 10% is given, between mean values per country and the regional mean. For the smaller return periods, the southern islands seem to experience higher maximum wind speeds, but for higher return periods, no clear driver for the variation is found. The total variation is considered little, and therefore it is concluded that the spatial distribution of maximum wind speeds is approximately equal.

The modelled maximum wind speeds based on 10,000 years of synthetic TC tracks are translated to a count of hit-rates. When reaching a maximum wind speed of at least 25 m/s within a country, that country is counted as affected by that storm. This resulted in 19% of the storms affecting only one country within the study area, and approximately 52% of the storms affecting over five countries of the Leeward Islands. The category that a storm has reached, in proximity of the Leeward Islands, is included in the bar chart, Figure 5.5. The ratio of higher categories is higher for the storms affecting multiple countries.

2. What are the spatial distributions and return periods of storm surge heights, from historical and synthetic tropical cyclone tracks?".

A so-called bathtub model is used to model surge levels over land for the Leeward Islands, caused by tropical cyclones. The surge levels are based on a linear relation between wind speed and surge heights. Bathymetry of the ocean and elevation levels of the land are used as input for the model as well.
Of all historical tracks, 52 storms resulted in surge levels over 0.2 m at at least one point of the grid. Figure 5.7, based on historical tracks, shows that mainly the coastal areas of Puerto Rico, the British and U.S. Virgin Islands, Anguilla, Saint Martin and Sint Maarten, and Antigua are prone to high surge levels on land, up to 1.7 m. A similar map based on synthetic data, shows the same areas prone to

surge, with some more of the coast of Puerto Rico, and Dominica and Martinique as addition. For a return period of five years surge levels op to 2.0 m is shown, which is slightly higher than the result for historical events.
The return periods of the synthetic tracks, translated to the maximum surge level per country per storm, are given in Figure 5.10. Puerto Rico and Martinique show the highest probability of reaching high maximum surge levels, while the countries Saint Barthélemy and Saba & Sint Eustatius reach significantly lower surge on land, showing return values of 0 meters up to return periods of 50 or even 1,000 years. When excluding these last two countries, the relative deviation as opposed to the regional mean, for maximum surge levels on land per country, is about 30% over a range of return periods up to 100 years, and about 20% for higher return periods. This is considered quite a large range, and one of the main drivers seems to be elevation levels on land, see Figure F.5c.
However, the maximum surge levels on land are not considered the right parameter to answer the research question properly. A better take on the spatial distribution could be given by comparing the surge levels a storm has reached above sea level near the coastlines. This parameter is less dependent on high-resolution elevation maps of the coastal area.

3. What are the spatial distributions and return periods of extreme precipitation, from historical and synthetic tropical cyclone tracks?".

The precipitation related to tropical cyclones is modelled by a parametric model. The input of the model was TC tracks, elevation maps of the land, and some climate parameters (temperature and wind speeds). Due to the need for the last required input, precipitation is only determined for historical tracks. In total, 248 storms have led to extreme precipitation, defined as more than 50 mm over the duration of the storm, in the last 85 years.
Figure 5.12 shows the spatial distribution of accumulated precipitation amounts, in mm, for a return period of 5 years, empirically based on the historical tracks. No clear trend between the countries is shown. High variation within a country is shown, however. This variation is mainly attributed to elevation differences. Some areas in Puerto Rico, Saint Kitts and Nevis, Montserrat, Guadeloupe, Dominica and Martinique show high local extreme precipitation amounts. In total, the map shows a range of 100 to 900 mm for accumulated rainfall.
In order to compare return values between countries, the maximum accumulated precipitation within a country is considered. High local extremes can lead to high impact. Figure 5.13 shows that the return level varies between 0 and 400 mm for a return period of 1 year, and varies between 300 and 2100 mm for a return period of 40 years. Overall, the southern countries seem more prone to high maximum accumulated precipitation in their country. Figure G.3 shows the relative deviation of each country from the regional, which varies between 240% and 150% over the range of return periods (from 1 to 40 years). The clearest driver is the presence of high elevation differences in a country, leading to higher precipitation extremes.

4. How do historical tropical cyclones rankings vary between the multi-hazard tropical cyclone scale TCSS and the wind speed-oriented scale SSHWS, for the Leeward Islands?

Classifications for two tropical cyclone scales are determined for historical tropical cyclones affecting the Leeward Islands. All 209 tracks that pass the region are included. Per country, classifications are determined based on the modelled experienced hazards within that country, considering only the maximum reached hazard levels over the duration of a storm. It is not common to express the classification of a tropical cyclone per country; usually, only one category is given for a track, varying over time during the track, and often expressing the severity of the event during landfall.

Between the wind-based scale of Saffir-Simpson (referred to as SSHWS) and the multi-hazard scale (referred to as TCSS), higher scores are reached for the same storms in the second scale. This is expected, since the multi-hazard scale applies the same thresholds for the hazard of wind as the SSHWS, and applies the principle that no total score can be lower than the minimum out of the three hazards.
The two events scoring the highest in the multi-hazard scale, which offers a Category 6 for tropical cyclones leading to severe impact for all three hazards, are Hurricane Irma and Hurricane Maria (2017), for the countries British Virgin Islands and Puerto Rico, respectively. In reports on these two events for

these two countries, both are classified as Category 5 for the traditional scale.

The classifications for surge levels have resulted in lower categories than for experienced wind speeds. This is attributed to the way the surge levels are modelled, since only surge levels on land are extracted, where the elevation is extracted from the modelled surge. It would be better suited within the scale to use the surge levels as they are expected along the coast, relative to the mean sea level.
The classifications for precipitation amounts have resulted in significantly higher categories than for experienced wind speeds. This is attributed to the sensitivity of the model to drag coefficients and topography, where an overestimation of orographic enhancement is expected for the steep slopes of the mountainous islands.

The return periods for the classifications in the TCSS return higher scores for lower return periods for the souther countries of the study area; Martinique, Dominica, Guadeloupe, Montserrat and Saint Kitts and Nevis. Additionally, Puerto Rico scored high return values.
The return periods for the classifications in the SSHWS return significantly lower return values, and if a general trend needs to be indicated, this would rather be opposite than in the other scale, classifying the northern countries at higher risk for high-category hurricanes. This is attributed to the fact that the southern countries experience higher TC-related precipitation, which is not included in this scale.

The TCSS is considered to provide important extra information in terms of risk communication by providing a classification per hazard. A country can target its early actions better, and all authorities and inhabitants are more aware of the expected event.

References

Anticipation Hub (2023). *A short overview of anticipatory action*. Fact sheet. url: https://www.anticipation-hub.org/download/file-3384.

Bazo, Juan et al. (2021). *WMO Guidelines on Multi-Hazard Impact-based Forecast and Warning Services - Part II: Putting Multi-Hazard IBFWS into Practice*. Tech. rep. World Meteorological Organization. url: library.wmo.int/records/item/57739-wmo-guidelines-on-multi-hazard-impact-based-forecast-and-warning-services?offset=1.

Bell, Gerald D. and Muthuvel Chelliah (2005). *Leading Tropical Modes Associated with Interannual and Multidecadal Fluctuations in North Atlantic Hurricane Activity*. Tech. rep. NOAA/NWS/NCEP Climate Prediction Centre.

Bloemendaal, Nadia, I. D. Haigh, et al. (Feb. 2020). *Generation of a global synthetic tropical cyclone hazard dataset using STORM*. Tech. rep. url: https://www.nature.com/articles/s41597-020-0381-2.

Bloemendaal, Nadia, Hans de Moel, Jantsje Mol, et al. (2021). "Adequately reflecting the severity of tropical cyclones using the new Tropical Cyclone Severity Scale". In: *Environmental Research Letters, Volume 16, Number 1*.

Bloemendaal, Nadia, Hans de Moel, Sanne Muis, et al. (2020). *Estimation of global tropical cyclone wind speed probabilities using the STORM dataset*. Tech. rep. VU Amsterdam, Deltares, University of Southampton, National Oceanography Centre.

Bloemendaal, Nadia, Sanne Muis, et al. (2018). *Global modeling of tropical cyclone storm surges using high-resolution forecasts*. Tech. rep. VU Amsterdam, Deltares, KNMI, TU Delft. doi: https://doi.org/10.1007/s00382-018-4430-x.

Caribbean Community, A Community for All (2025). *Who we are*. url: https://caricom.org/our-community/who-we-are/ (visited on 05/23/2025).

Caribbean Disaster Emergency Management Agency (2025). *About CDEMA*. url: cdema.org (visited on 05/23/2025).

Caribbean Institute for Meteorology & Hydrology (2025). *About CIMH*. url: https://www.cimh.edu.bb/ (visited on 07/29/2025).

Cerveny, Randall S. and Lynn E. Newman (2000). *Climatological relationships between tropical cyclones and rainfall*. Tech. rep. Arizona State University. url: https://journals.ametsoc.org/view/journals/mwre/128/9/1520-0493_2000_128_3329_crbtca_2.0.co_2.xml.

Chen, Rui, Weimin Zhang, and Xiang Wang (2020). *Machine learning in tropical cyclone forecast modeling: a review*. Tech. rep. National University of Defense Technology, China.

Claassen, J.N. (2021). *Parametric Precipitation Model for Tropical Cyclone Radial Rainfall Profiles - Reducing the biases in the Bader model for the North Atlantic*. MSc thesis. Delft University of Technology.

CLIMADA contributors, ETH Zurich (2025). *Hazard: Tropical cyclone surge from linear wind-surge relationship and a bathtub model*. url: https://climada-petals.readthedocs.io/en/stable/tutorial/climada_hazard_TCSurgeBathtub.html (visited on 08/14/2025).

Climate Prediction Centre (2025). *NOAA 2025 Atlantic Hurricane Season Outlook*. url: https://www.cpc.ncep.noaa.gov/products/outlooks/hurricane.shtml (visited on 10/04/2025).

Copernicus (2025). *ERA5 hourly data on single levels from 1940 to present*. url: https://cds.climate.copernicus.eu/datasets/reanalysis-era5-single-levels?tab=overview (visited on 10/04/2025).

Critical Ecosystem Partnership Fund (2020). *Caribbean Islands Biodiversity Hotspot: Ecosystem Profile Summary*. https://www.cepf.net/sites/default/files/cepf-caribbean-islands-ecosystem-profile-summary-2020-english.pdf. Accessed: 2025-05-23.

Das, Swagatalaxmi (2024). *Multi-hazard interaction assessment, case study: tropical cyclone Maria*. Tech. rep. University of Twente, Faculty of Geo-Information Science and Earth Observation.

Deltares (2025). *Global modelling of tides and storm surges*. url: https://www.deltares.nl/en/expertise/projects/global-modelling-of-tides-and-storm-surges (visited on 11/17/2025).

Emanuel, Kerry (2017). “Assessing the prsent and future probability of Hurricane Harvey’s rainfall”. In: *PNAS*.

ETH Zürich (2025). *Hazard: Tropical cyclone rain from R-CLIPER or TCR model*. url: https://climada-petals.readthedocs.io/en/latest/tutorial/climada_hazard_TCRain.html (visited on 08/21/2025).

— (n.d.). *Welcome to CLIMADA*. url: https://climada.ethz.ch/.

European Centre for Medium-Range Weather Forecasts (2025). *Forecasts*. Accessed: 2025-05-12. url: https://www.ecmwf.int/en/forecasts.

Feldmann, Monika et al. (2019). “Estimation of Atlantic Tropical Cyclone Rainfall Frequency in the United Nations”. In: *American Meteorological Society*. url: https://doi.org/10.1175/JAMC-D-19-0011.1.

Forooshani, M. Kooshki et al. (Feb. 2024). *Towards a global impact-based forecasting model for tropical cylcones*. Tech. rep. Netherlands Red Cross 510, pp. 309–329. doi: 10.5194/nhess-24-309-2024. url: https://nhess.copernicus.org/articles/24/309/2024/.

Fu, Zheng-Hang et al. (2025). “Shifting hotspot of tropical cyclone clusters in a warming climate”. In: *nature climate change*.

GADM (n.d.). *Database of Global Administrative Areas*. url: https://gadm.org/about.html.

geoBoundaries (n.d.). *An open database of political administrative boundaries*. url: https://www.geoboundaries.org/.

Georgiou, Peter Nicholas (1985). “Design wind speeds in tropical cyclone-prone regions”. PhD thesis. University of Western Ontario.

Harper, B. and Greg J. Holland (1999). “An updated parametric model of the tropical cyclone”. In: *Proc. 23rd Conf. Hurricanes and Tropical Meteorology*.

Harris, D. Lee (1963). “Characteristics of the Hurricane Storm Surge”. In: *U.S. Department of Commerce, Weather Bureau, Technical Paper No. 48*.

Harrison, S. et al. (2025). “The influence of exposure and vulnerability on designing impact-based warning thresholds: Results of a New Zealand risk modelling experiment”. *EMS Annual Meeting 2025, Ljubljana, Slovenia, 7–12 Sep 2025*, EMS2025–333. doi: 10.5194/ems2025-333. url: https://doi.org/10.5194/ems2025-333.

Hemmati, Mona et al. (2025). “Assessment of Caribbean Coastal Hazard Posed by Tropical Cyclones”. In: *American Meteorological Society*.

Holland, Greg J. (1980). “An analytic model of the wind and pressure profiles in hurricanes”. In: *Montlhy Weather Review*.

— (2008). “A revised hurricane pressure-wind model”. In: *Monthly Weather Review*.

Homberg, Marc van de et al. (2025). “Chapter 4 Impact-based forecasting for anticipatory action”. In: *unpublished*.

IFRC (2019a). *Mozambique/Africa: To coordinate early actions for preparation and response to cyclones in Mozambique*. Tech. rep. International Federation of Red Cross and Red Crescent Societies.

— (2019b). *Philippines: Typhoon - Early Action Protocol summary*. Tech. rep. International Federation of Red Cross and Red Crescent Societies.

— (2021). *Bangladesh: Cyclone Early Action Protocol summary*. Tech. rep. International Federation of Red Cross and Red Crescent Societies.

— (2025). *Early warning, early action*. url: https://www.ifrc.org/our-work/disasters-climate-and-crises/climate-smart-disaster-risk-reduction/early-warning-early (visited on 05/28/2025).

IFRC Climate Centre OECS, AFD Groupe (2022). *Regional forecast-based financing for hurricanes in the Eastern Caribbean: A feasibility study*. Tech. rep.

International Organization for Standardization (n.d.). *ISO 3166 country codes*. url: https://www.iso.org/iso-3166-country-codes.html.

IPCC (2021). *Sixth assessment report*. Tech. rep. Intergovernmental Panel on Climate Change, WMO, UN environment programme.

Jelesnianski, Chester P., Jye Chen, and Wilson A. Shaffer (1992). *SLOSH: Sea, Lake, and Overland Surges from Hurricanes*. Tech. rep. Office of Systems Development, National Weather Service, NOAA.

Jelesnianski, Chester P., Jye Chen, Wilson A. Shaffer, and Amikam J. Gilad (1984). *SLOSH - A Hurricane Storm Surge Forecast Model*. Tech. rep. Office of Systems Development, National Weather Service, NOAA.

Keellings, David and José J. Hernández Ayala (2019). "Extreme Rainfall Associated With Hurricane Maria Over Puerto Rico and Its Connections to Climate Variability and Change". In: *AGU Advancing Earth and Space Sciences*.

Knapp, Kenneth R. et al. (2010). "The International Best Track Archive for Climate Stewardship (IBTrACS): Unifying Tropical Cyclone Best Track Data". In: *Bulletin of the American Meteorological Society* 91.3, pp. 363–376. doi: 10.1175/2009BAMS2755.1. url: https://doi.org/10.1175/2009BAMS2755.1.

KNMI Kennis- & Datacentrum (2025). *Uitleg over Tropische cyclonen*. url: https://www.knmi.nl/kennis-en-datacentrum/uitleg/tropische-cyclonen (visited on 05/23/2025).

Le, Phong et al. (2025). "pyTCR: A tropical cyclone rainfall model for Python". In: *The Journal of Open Source Software*.

Lee, Chia-Ying et al. (2018). "An Environmentally Forced Tropical Cyclone Hazard Model". In: *JAMES - Journal of Advanced Modeling Earth Systems*.

Lombaers, C. J. J. (2025). "Using Synthetic Data to Support Decision-Making in Pre-Positioning for Caribbean Hurricane Season Preparedness". MA thesis. Delft University of Technology.

Lu, Ping et al. (2018). "Assessing Hurricane Rainfall Mechanisms Using a Physics-Based Model: Hurricane Isabel (2003) and Irene (2011)". In: *American Meteorological Society*.

Ministry of Saint Vincent and the Grenadines (2025). *Regional Organisations*. url: https://foreign.gov.vc/foreign/index.php/regional-organisations (visited on 05/23/2025).

Ministry of Trinidad and Tobago (2025). *International Organizations in Trinidad and Tobago*. url: https://foreign.gov.tt/missions-consuls/foreign-representatives-accredited-tt/international-organizations-trinidad-and-tobago/ (visited on 05/23/2025).

Moraes, Osvaldo Luiz Leal de (2024). *An impact-based forecast system developed for hydrometeorological hazards*. Tech. rep. National Center for Monitoring and Early Warning of Natural Disasters. doi: https://doi.org/10.1016/j.ijdrr.2023.103803.

Muis, Sanne et al. (2016). *A global reanalysis of storm surges and extreme sea levels*. Tech. rep. VU Amsterdam, Deltares, EEMCS.

Nabukulu, Catherine, Victor. G. Jetten, and Janneke Ettema (2024). "Implications of Tropical Cyclone Rainfall Spatial–Temporal Variability on Flood Hazard Assessments in the Caribbean Lesser Antilles". In: *GeoHazards*.

NASA Global Precipitation Measurement (n.d.). *IMERG: Integrated Multi-satellitE Retrievals for GPM*. url: gpm.nasa.gov/data/imerg.

National Hurricane Center (2021). *Tropical Cyclone Report - Hurricane Irma*. Tech. rep. NOAA.

National Oceanic and Atmospheric Administration (Mar. 2025a). *About our agency*. Accessed: 2025-05-12. url: https://www.noaa.gov/about-our-agency.

— (2025b). *International Best Track Archive for Climate Stewardship (IBTrACS)*. url: https://www.ncei.noaa.gov/products/international-best-track-archive (visited on 05/09/2025).

NOAA (1967). *Hurricane Beulah - September 8-24, 1967*. Tech. rep. National Oceanic and Atmospheric Administration, National Weather Service. url: https://www.wpc.ncep.noaa.gov/tropical/rain/beulah1967.html.

— (1999). *Hurricane Lenny - November 14-21, 1999*. Tech. rep. National Oceanic and Atmospheric Administration, National Weather Service. url: https://www.wpc.ncep.noaa.gov/tropical/rain/lenny1999.html.

NOAA Hurricane Research Division (2025). *Hurricane Database*. url: www.aoml.noaa.gov/hrd/hurdat/Data_Storm.html (visited on 06/06/2025).

NOAA's National Weather Service (2025). *Precipitation Frequency Data Server (PFDS)*. url: https://hdsc.nws.noaa.gov/pfds/pfds_map_pr.html (visited on 11/19/2025).

NRC 510 and FRC PIRAC (2025). "Small project agreement - Regional EAP Caribbean". Internal document on project agreements, not yet finalized, february 2025.

PARATUS-EU (2025). *Promoting disaster preparedness and resilience by co-developing stakeholder support tools for managing the systemic risk of compounding disasters*. url: paratus-project.org (visited on 04/18/2025).

Phadke, Amal C. et al. (2002). *Modeling of tropical cyclone winds and waves for emergency management*. Tech. rep. Department of Ocean and Resources Engineering, University of Hawaii at Manoa, Hurricane Research Division, NOAA National Weather Service. url: https://doi.org/10.1016/S0029-8018(02)00033-1.

Pielke, Roger A. and Roger A. Pielke (1997). *Hurricanes - their Nature and Impacts on Society*. WILEY.

Pilkington, Stephanie F. and Hussam N. Mahmoud (2016). *Using artificial neural networks to forecast economic impact of multi-hazard hurricane-based events*. Tech. rep. Colorado State University, Civil and Environmental Engineering Department.

Research on the Epidemiology of Disasters, Centre for (2025). *EM-DAT THe International Disaster Database*. url: emdat.be (visited on 05/09/2025).

Science Education, UCAR Center for (2025). *What causes storm surge?* url: https://scied.ucar.edu/learning-zone/storms/what-causes-storm-surge (visited on 05/20/2025).

Sedhain, Sahara (2022). "Evaluating the explainability and performance of an elementary versus a statistical impact-based forecasting model - A case study of tropical cyclone early action in the Philippines". MA thesis. University of Twente.

Sedhain, Sahara et al. (2025). "Evaluating Impact-based Forecasting Models for Tropical Cyclone Anticipatory Action". In: *International Journal of Disaster Risk Reduction* 105782.

Shultz, James M. et al. (2019). *Risks, health consequences and response challeges for small-island-based populations: Observations from the 2017 Atlantic hurricane season*. Tech. rep. url: https://www.cambridge.org/core/product/identifier/S1935789318000289/type/journal_article.

Sikking, Wessel (2023). *Future climate change impacts for a small island nation*. Tech. rep. Ministry of Public Housing, Spatial Planning, Environment and Infrastructure (VROMI).

The Netherlands Red Cross 510 (2025). *Improving humanitarian action with data and digital*. url: 510.global (visited on 08/15/2025).

Tuleya, Robert, Mark DeMaria, and Robert Kuligowski (2007). "Evaluation of GFDL and Simple Statistical Model Rainfall Forecasts for U.S. Landfalling Tropical Storms". In: *American Meteorological Society*.

UN OCHA (2025). *Anticipatory Action*. url: www.unocha.org/anticipatory-action (visited on 06/02/2025).

UNDRR (2025a). *Early Warnings for All*. url: https://www.undrr.org/implementing-sendai-framework/sendai-framework-action/early-warnings-for-all (visited on 05/28/2025).

— (2025b). *UNDRR Focus areas: disaster risk reduction in action - Small Island Developing States*. url: www.undrr.org/implementing-sendai-framework/sendai-framework-action/small-island-developing-states (visited on 06/02/2025).

UNDRR DesInventar (n.d.). *Sendai Framework for Disaster Risk Reduction*. url: https://www.desinventar.net/index.html.

Wallace, John M. and Peter V. Hobbs (2006). *Atmospheric Science - An introductory survey*. Volume 92 in the International Geophysics Series.

Weibull, W. (1939). "A Statistical Theory of the Strength of Materials". In: *Generalstabens litografiska anstalts förlag*.

Willoughby, H. and M. Rahn (2004). "Parametric representation of the primary hurricane vortex. Part 1: Observations and evaluation of the Holland (1980) model". In: *American Meteorological Society*.

World Bank Group (2025). *A 360 degree look at Dominica post Hurricane Maria*. url: www.worldbank.org/en/news/feature/2017/11/28/a-360-degree-look-at-dominica-post-hurricane-maria (visited on 06/06/2025).

World Meteorological Organization (2025a). *risking Risks*. url: wmo.int/about-us/world-meteorological-day/wmd-2022/rising-risks (visited on 06/02/2025).

— (2025b). *Tropical cyclone*. url: https://wmo.int/topics/tropical-cyclone (visited on 05/24/2025).

Worldatlas (2025). *Caribbean geography*. url: https://www.worldatlas.com/webimage/countrys/namerica/caribb/caribland.htm (visited on 05/23/2025).

Xu, Liming (2010). "A simple coastline storm surge model based on pre-run SLOSH outputs". In: *29th Conference on Hurricanes and Tropical Meteorology*.

Yan, DanChen and Zhang (2022). "Research progress on tropical cyclone parametric wind field models and their application". In: *Regional Studies in Marine Science*.

Zhu, Laiyin, Steven Quiring, and Kerry Emanuel (2013). "Estimating tropical cyclone precipitation risk in Texas". In: *Advanced Earth and Space Sciences*.

A

Intergovernmental organisations in the Caribbean

There are multiple intergovernmental organisations within the Caribbean, encouraging collaboration between islands. Almost all of the islands have a colonial history. Nowadays, most of the islands are governmentally independent. In 1973, after the independence of Barbados, Jamaica, Guyana and Trinidad & Tobago from the United Kingdom, a political and economic union was formed called the Caribbean Community (CARICOM). This union now consists of fifteen member states and five associate members. CARICOM focuses on four pillars: economic integration, foreign policy coordination, human and social development, and security (Caribbean Community, A Community for All 2025).

Other intergovernmental organisations include:

- the Caribbean Natural Resources Institute (CANARI),
- the Association of Caribbean States (ACS),
- the Organisation of Caribbean States (OECS),
- the Community of Latin American and Caribbean States (CELAC),
- the Development Bank of Latin America and the Caribbean (CAF),
- the Caribbean Development Bank (CDB),
- the Caribbean Food Corporation (CFC),
- the Caribbean Agricultural Research & Development Institute (CARDI),

and more, as is found in various sources (Critical Ecosystem Partnership Fund 2020, Ministry of Saint Vincent and the Grenadines 2025, Ministry of Trinidad and Tobago 2025, IFRC Climate Centre 2022). Three key actors are further illustrated below.

CDEMA

The Caribbean Disaster Emergency Management Agency (CDEMA) is an intergovernmental agency for disaster management within CARICOM. The agency was established in 1991 under the name of CDERA, and is responsible for the coordination of emergency response and relief efforts for its twenty participating states, largely overlapping with the member states of the Caribbean community (Caribbean Disaster Emergency Management Agency 2025).
CDEMA is considered one of the main disaster response stakeholders for the region, along with the IFRC, the UNDRR and the World Food Programme (WFP). A feasibility study on forecast-based financing of hurricanes builds upon the existing Regional Response Mechanism (RRM) of CDEMA, showing the role of this stakeholder (IFRC Climate Centre 2022). However, with CDEMA's scope limited to the participating states, collaboration with other parties is needed when considering disaster risk management in the whole Caribbean region. CDEMA currently uses their own platform, CRIS, for hazard and impact forecasting. On a regional level, CDEMA faces challenges with data availability, since this differs strongly between countries.

CCRIF

The Caribbean Catastrophe Risk Insurance Facility (CCRIF) was formed in 2007 as the first multi-country risk pool in the world, as an initiative of the World Bank. It was designed as a regional catastrophe fund for Caribbean governments to limit the financial impact of natural hazard events by quickly providing financial liquidity when a policy is triggered. There are six insurance policies: on earthquakes, tropical cyclones, excess rainfall, the fisheries sector, and the electric and water utilities. The CCRIF uses a Real-Time Forecast System, which provides weather forecasts at 1-km resolution for local wind speed and storm surge inundation, but not for precipitation. It also predicts estimations of the impact on the region, categorised in four different intensity levels (IFRC Climate Centre 2022).

CIMH

The Caribbean Institute for Meteorology & Hydrology (CIMH) is a training and research institute, formed by the amalgamation of the Caribbean Meteorological Institute (CMI) and the Caribbean Operational Hydrological Institute (COHI). The mission of CIMH is to assist in improving and developing meteorological and hydrological services of the member states, as well as providing awareness of the benefits of meteorology and hydrology for the economic well-being. Products of CIMH are, among others, a Caribbean Drought and Precipitation Monitoring Network (CDPMN) and numerical weather predictions. The CIMH also provides monthly weather summaries (Caribbean Institute for Meteorology & Hydrology 2025).

B

Defining a geographical scope

B.1 Historical data analysis on impact and frequency of TC's

Historical data is analysed for all Caribbean islands, excluding the mainland, which is also geographically seen also part of the Caribbean. In the analysis, the islands are split up into four regions, to define the most impacted region. The regions are defined as is also mentioned in Paragraph 2.2, namely the Greater Antilles, the Lucayan Archipelago, the Leeward Islands, the Windward Islands, and the Leeward Antilles. The countries are defined as 'per ISO code'. The ISO codes are defined by the International Organization for Standardization (ISO) and base their codes on information of the United Nations (International Organization for Standardization n.d.).

B.1.1 Historical impact of TC's in the Caribbean

For all Caribbean islands, the collected and registered impact of historical hurricanes is considered. The EM-DAT database gives both human and economic impact in the following parameters:

- Human impact: total deaths, no. injured, no. affected, no. homeless, total affected (sum).
- Economic impact (all in '000 US$): reconstruction costs, insured damage, total damage. All parameters are also adjusted for inflation as separate parameters.

For this study, the parameters total deaths, no. affected and total damage (adjusted) are selected.

The database covers many types of disasters, firstly split up into the groups natural and technological disasters. The natural disasters consist of the following subgroups: geophysical, hydrological, meteorological, climatological, biological and extra-terrestrial. For each disaster subgroup, disaster types are defined. Of all categories, I have chosen to include two 'collections' in the analysis:

- All hydrological and meteorological disasters. The hydrological disaster types are flood, landslide, and wave action. The meteorological disaster types are storm, extreme temperature, and fog. *Number of events in the database: 527*
- Only tropical cyclones. This is a subtype of the disaster type storm. *Number of events in the database: 342 (out of the 359 events in the group of meteorological disasters)*

The list below describes the results that will be created in order to provide insight in the experienced and registered impact of hurricanes in the past for the Caribbean islands.

1. Sum of the absolute impact per parameter per country;
2. Sum of the absolute impact per parameter divided by the total, per country, for both disaster collections;
3. Sum of the absolute impact per parameter divided by the total, per region, for both disaster collections;
4. Sum of the relative impact per parameter, for the period 2000-present, per country;
5. Sum and mean of the relative impact per parameter divided by the total, for the period 2000-present, per country, for both disaster collections;

6. Sum and mean of the relative impact per parameter divided by the total, for the period 2000-present, per region, for both disaster collections.

The relative impact is defined as the number of deaths and the number of affected people per country, divided by the total population of the country, and as the total damage (adjusted) per country divided by the total GDP of the country. Socio-economic information on the Caribbean islands is included in C. The relative impact is only determined for events later than 2000, since the demographic information would otherwise not be representative.
Figure B.1 and B.2 show the sums of the relative impact parameters per country and region. The values are divided by the total in order to relate the countries to each other and to show the three parameters in one plot. When considering human impact, the Windward Islands account for the highest relative impact, as is collected in the EM-DAT database. The Leeward Islands score highest on the total damage relative to national GDP's, and also score high on the number of affected people. It should be noted that the Leeward Antilles are not included in the bar charts, since no events for these countries exist in the database.
Countries that have high (relative) impact scores, both for 'all disasters' and for 'tropical cyclones only', are: Anguilla, Bahamas, Cuba, Dominica, Grenada, Haiti, Saint Lucia, Saint Martin, Sint Maarten, Saint Vincent and the Grenadines, British Virgin Islands.

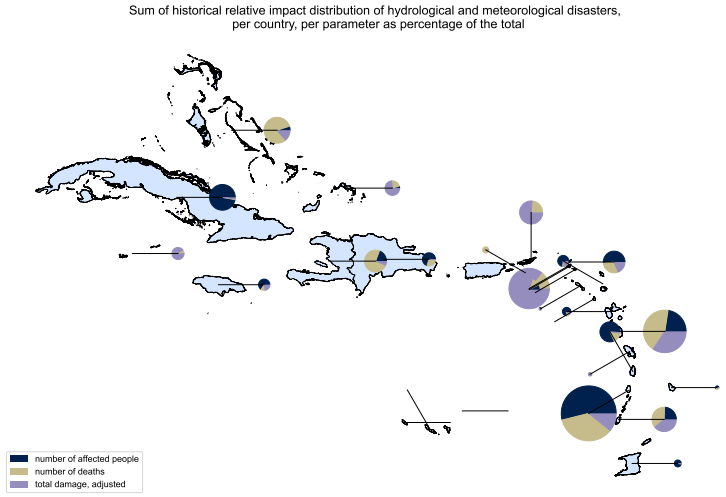

Figure B.1. Impact parameters relative to population numbers per country, and national Gross Domestic Product, summed for events in the EM-DAT database of the period after 2000

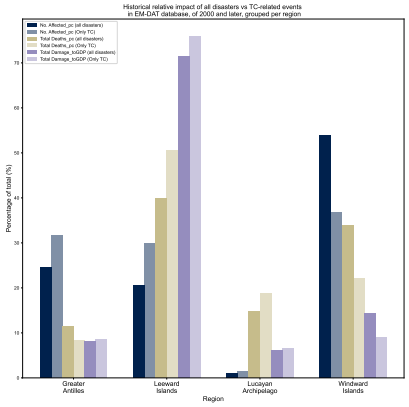

Figure B.2. Same data, but grouped per region

Figure B.3 and B.4 show the means of the relative impact parameters. These values indicate the impact per event. Overall, the same countries stand out in the impact database. Overall, the same countries tend to stand out in the impact database. When looking at the grouped regions, the Leeward Islands show the highest impact rates. This matches findings from the literature which highlight that Small Island Developing States, many of which are in the Leeward and Windward Islands, are highly exposed to natural hazards and particularly vulnerable due to their limited economic resources.

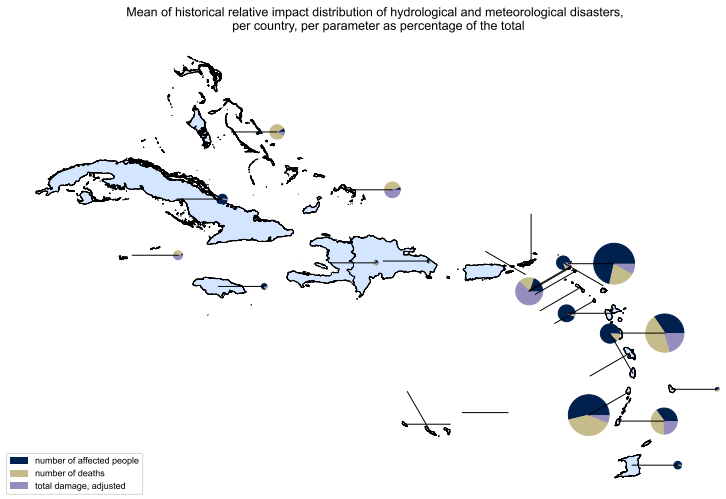

Figure B.3. Impact parameters relative to population numbers per country, and national Gross Domestic Product, as a mean of the events in the EM-DAT database of the period after 2000

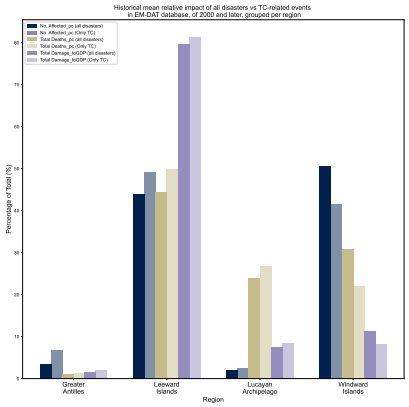

Figure B.4. Same data, but grouped per region

It is important to note that EM-DAT is not considered to give a complete and unbiased picture of natural hazards worldwide. For example, EM-DAT only includes disasters of >100 people affected. Hence, smaller but still impactful disasters are not considered. Moreover, it is known that Caribbean countries have limited disaster reporting infrastructure, which can lead to a lack of or wrong numbers in global databases. However, the EM-DAT database will be used in this study to define broad patterns in the historical impact of tropical cyclones in the Caribbean.

Historical impact data:

- EM-DAT is an international disaster database, created in 1988 as a joint initiative between the Centre for Research on the Epidemiology of Disasters (CRED) and the World Health Organization (WHO). EM-DAT contains data on the occurrence and impacts of over 26,000 mass disasters worldwide from 1900 to the present day. The database is compiled from various sources, including UN agencies, non-governmental organizations, reinsurance companies, research institutes, and press agencies. The CRED, now part of the Institue of Health and Society attached to the University of Louvain (UCLouvain), distributes the data in open access for non-commercial use. The EM-DAT database and project are primarily sponsored by the United States Agency for International Development (USAID). EM-DAT includes the following disaster types: earthquake, flood, drought, extreme temperature, epidemic, wildfire, storm, and industrial accident (chemical spills) (Research on the Epidemiology of Disasters 2025).
- DesInventar is a global disaster database that compiles local-level data on disaster impacts, focusing on small- and medium-scale events. It includes information on hazard type, location, and impacts such as deaths and damages, supporting risk analysis and disaster management efforts. DesInventar Sendai is specific software that stakeholders can download in order to contribute impact data. The same software also gives access to the database (UNDRR DesInventar n.d.). The database covers events from 1994 to the present. The DesInventar data is currently not considered, but might be included in the research at a later stage.

B.1.2 Spatial distribution of historical TC tracks in the Caribbean

The historical TC tracks are analysed based on the IBTrACS database. The database combines multiple data sources and therefore contains a very high number of parameters (163). The information of the sources is combined and averaged. The database covers the period 1851-2024. The number of storms per year, and the mean maximum wind speed of the storms per year, is given in Figure B.5. It can be seen that the number of storms increases, which is probably due to increase in measurements and data storage. A storm consists of both data points and lines. Each data point has the following parameters given:

- Day and time,
- Location (lon, lat in degrees),
- Maximum sustained wind speed for 1 minute,
- Minimum pressure,

- SSHWS category,
- and for storms after 2004 also size and radius for 34, 50 amd 60kt max wind speeds.

The data is downloaded from the IBTrACS website for the entire period available and only for the North Atlantic basin. By counting the number of unique SID (storm id), the number of storms is determined, which is 2304 for the total dataset. The data is preprocessed in three steps. Firstly, the empty columns are deleted to get a more manageable dataset, and all empty fields are replaced by NaN. Secondly, only the storms that contain at least one data point with a maximum sustained wind speed of 25 m/s are included. This threshold was chosen based on the assumption that hurricanes generating wind speeds of 25 m/s or lower are unlikely to cause impact. The threshold value of 25 m/s follows the example of (Forooshani et al. 2024). Thirdly, to reduce the database size, only the storms of which at least one data point crosses the Caribbean region are included. The Caribbean region is defined as anything between 9 and 28 degrees North and between -87 and -57 degrees West. Now, still 758 storms are included in the dataset.
The number of storms per country is defined by counting the number of storms of which at least one data point lies within the boundaries of a country. The boundaries are collected from GADM, a spatial database that provides detailed maps of administrative boundaries worldwide (GADM n.d.). Since tropical cyclones are very large systems, with diameters of 200-500 km, the country will also experience the storm even when the eye of the storm missed the actual country boundaries. Therefore, each country has an additional buffer of 100 km for this analysis. Similar to the analysis of impact data, is the number of storms also grouped per region. The relative number of landfalls is determined by dividing by the total area of a country (including the buffer).
The count of the number of storms is split for the Saffir-Simpson scale category that is experienced within the country.

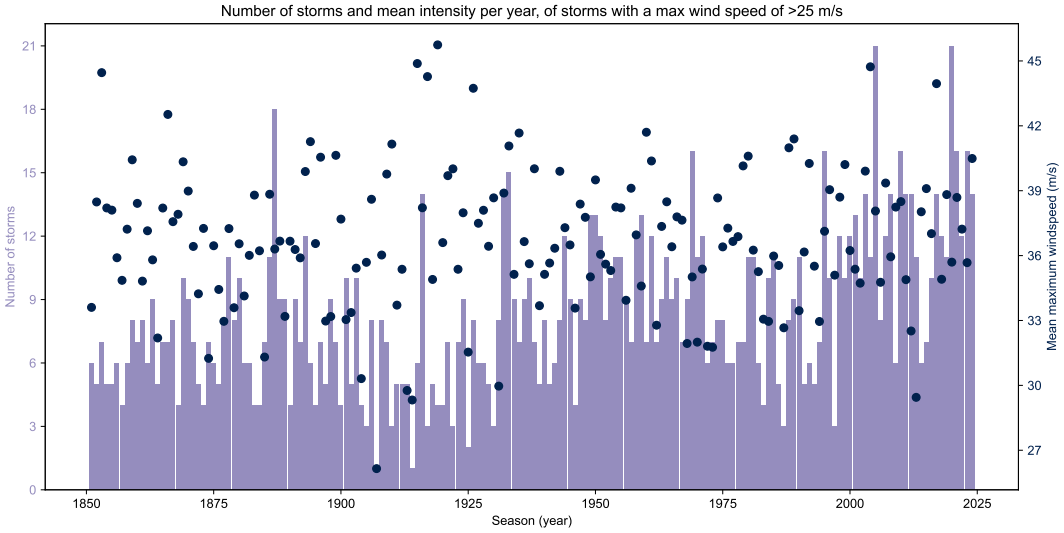

Figure B.5. General information on the number of storms and their intensity in the IBTrACS database of the North Atlantic basin

Figure B.6 gives a bar chart of the number of storms that have crossed each country over the period 1854-2024, according to the IBTrACS database. The Bahamas and Cuba have experienced the most hurricanes, over 150 events. Over a period of 170 years, this is +/- 0.88 hurricanes per year. Aruba, Curaçao, and Trinidad and Tobago have experienced the fewest hurricanes, around 10 events. Figure B.7 shows the sum of the number of storms per region. The regions are defined similarly as for the impact data analysis and can be found in C. The Greater Antilles and Leeward Islands experience the most hurricanes. When looking at the tracks of the historical tropical cyclones, this seems to be due to a clear pattern in the path of a tropical storm. The southern part of the Caribbean, where the Leeward Antilles and the Windward Islands are located, is generally missed by the TC tracks.

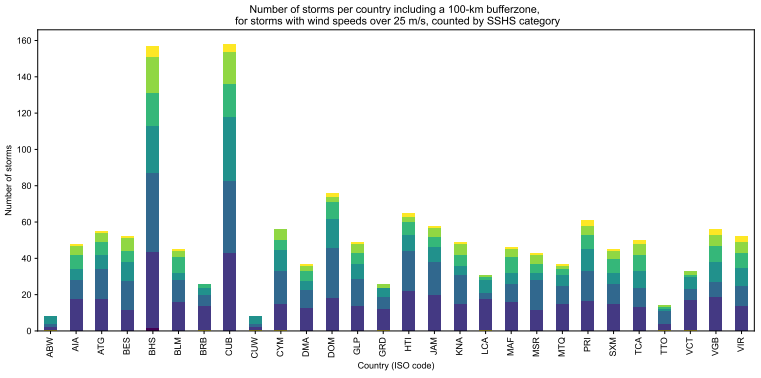

Figure B.6. Bar chart of the number of storms that have passed each Caribbean country within a 100 km buffer, categorised by intensity. The country name for the ISO code can be found in the table in C.

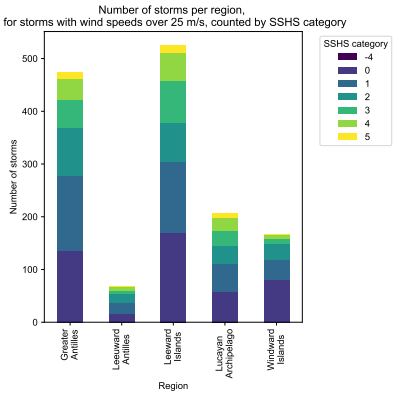

Figure B.7. Bar chart of the number of storms that have passed the countries of a region within a 100 km buffer, categorised by intensity.

Larger countries experience more hurricanes. To eliminate this effect, the number of storms over the years is divided by the area of the country, including the buffer of 100 km around the borders that was included in the count. This gives the number of storms per 100 km2, which is shown in Figure B.8 and B.9. The differences per country have decreased. The relatively most hit countries are Saint Barthélemy, Saint Kitts and Nevis, Saint Martin, Sint Maarten, Montserrat and the British Virgin Islands. The least hit countries have remained the same. The change in result is very clear when grouping by region. The Leeward Islands, all quite small, are hit very often relative to their areas. This must be due to their geographical location.

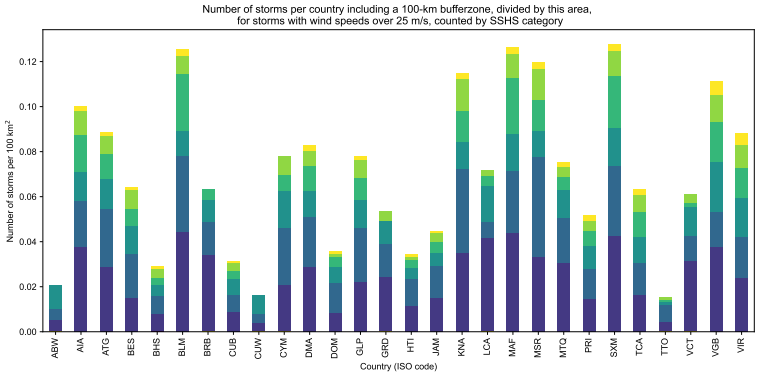

Figure B.8. Bar chart of the number of storms that have passed each Caribbean country within a 100 km buffer, divided by this area, categorised for intensity. The country name for the ISO code can be found in the table in C.

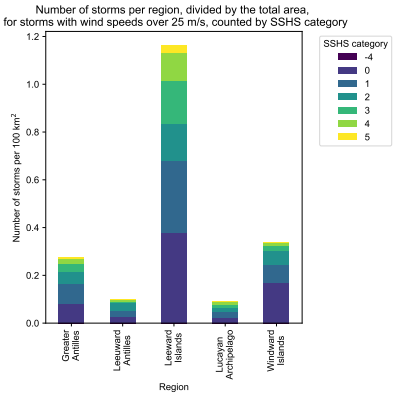

Figure B.9. Bar chart of the number of storms that have passed the countries of a region within a 100 km buffer, divided by the sum of these areas, categorised for intensity.

The results match with the tracks (of the IBTrACS database) when drawn on a map of the Caribbean. The tracks seem to move from east to west, and when arriving at the continent, the storms move upwards. See Figure B.10.

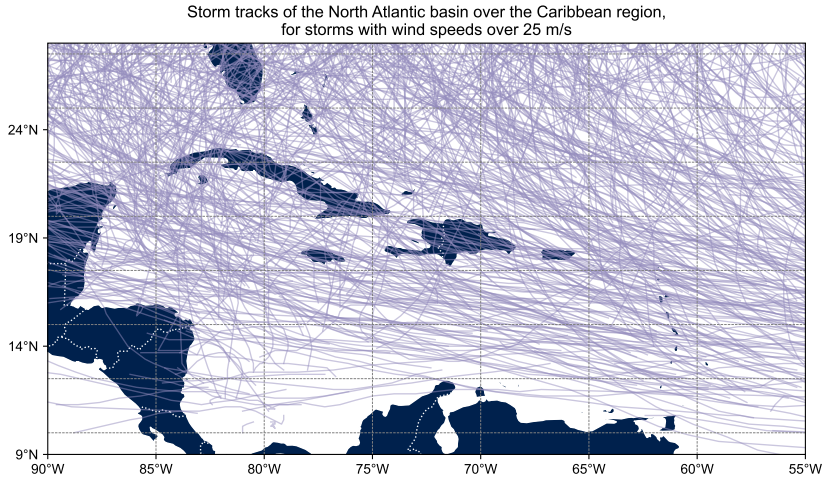

Figure B.10. TC tracks of IBTrACS data, for the Caribbean region, for the period 1854-2024

B.2 Clustering of countries based on exposure to hurricanes

Selecting a region for a common trigger model and Early Action Protocol can be based on many different aspects. Deciding on the selection procedure should be achieved in collaboration with local partners and the key stakeholders. For example, you could differ in focusing on the early action execution when grouping a region. Are there relationships between disaster management institutes of different islands? Are there well-functioning and robust transport methods for relief goods between islands? Is there a common agreement on the financing of early action between islands? Etc. On the other hand, you could focus on the exposure to the hazard. Are different islands likely to be affected by the same storm and could therefore benefit from a common trigger model? Are different islands very unlikely to be affected by the same storm and could therefore share the same relief materials? Are islands alike in their vulnerability and therefore suited for combined financing and early action procedures? Etc.

In this section, a purely data-driven approach to selecting a region is illustrated, answering the question of the spatial distribution of tropical cyclones within the Caribbean region and the likelihood of being affected by the same storm.

B.2.1 Methodology

The islands are clustered based on their exposure to tropical cyclones, where islands that are often hit by the same hurricane are clustered together.

The synthetic hurricane tracks of the STORM dataset are used as input for this spatial analysis. A subset of 1000 years of hurricane tracks is considered. This data size is considered large enough for the purpose, and limiting the data size results in limited computational effort. To further limit the size of the dataset, only the tracks that overlap with the Caribbean region are used.
A 4-km point grid is created for all Caribbean islands: Anguilla, Antigua and Barbuda, Aruba, Bahamas, Barbados, Bonaire, British Virgin Islands, Cayman Islands, Cuba, Curaçao, Dominica, Dominican Republic, Grenada, Guadeloupe, Haiti, Jamaica, Montserrat, Martinique, Puerto Rico, Saba and Sint Eustasius, Saint Barthélemy, Saint Kitts and Nevis, Saint Lucia, Saint Martin, Saint Vincent and the Grenadines, Sint Maarten, Trinidad and Tobago, Turks and Caicos Islands, and the U.S. Virgin Islands.

Based on the Holland 2008 model and utilising the CLIMADA package, similar to section 4.3, the maximum estimated experienced wind speed per storm is determined for each point in the grid. We are interested in the rate of being affected by a certain storm, per island. Therefore, we only consider the maximum experienced wind speed per country (so the maximum of all points in the grid per country). An island is considered to be 'hit' when a wind speed of 17.5 m/s or higher is estimated due to that storm. This wind speed does not necessarily lead to an impact on the island, but is chosen since it is the lower limit of what is considered a tropical storm in the Saffir Simpson scale, see 2.1.

Now we have a table showing the storm, the country, and whether it was hit: yes or no. So for every storm-country pair, a binary indicator is assigned, resulting in a binary exposure matrix.
Subsequently, the similarity between the hit-rate of islands is determined using the Jaccard distance, a measure designed for binary data.

$$d_J(A,B) = 1 - \frac{|A \cap B|}{|A \cup B|} \tag{B.1}$$

Where $|A \cap B|$ is the number of storms that affected both country A and country B, and $|A \cup B|$ is the number of storms that affected either one. The lower the $d_J(A,B)$, the higher the overlap of being hit. The Jaccard distance should always be between 0 and 1.
When the Jaccard distance is known for every possible pair of the islands, a hierarchical clustering is applied. Countries are clustered iteratively based on the average pairwise distance between all countries in that cluster. The result is shown in Figure B.11. A number of clusters was predefined to six, to which all islands were assigned, visualised by using colours in the figure. The clusters are as follows:

- Leeward Antilles: Aruba, Bonaire, Curaçao
- Windward Islands excluding Martinique: Trinidad and Tobago, Barbados, Saint Lucia, Grenada, Saint Vincent and the Grenadines
- Leeward Island including Puerto Rico and Martinique: Guadeloupe, Dominica, Martinique, Anguilla, Saint Barthélemy, Saint Martin, Sint Maarten, Antigua and Barbuda, Montserrat, Saint Kitts and Nevis, Saba and Sint Eustasius, Puerto Rico, British Virgin Islands, U.S. Virgin Islands
- Lucayan Archipelago: Bahamas, Turks and Caicos Islands
- Greater Antilles: Dominican Republic, Haiti, Cuba, Cayman Islands, Jamaica

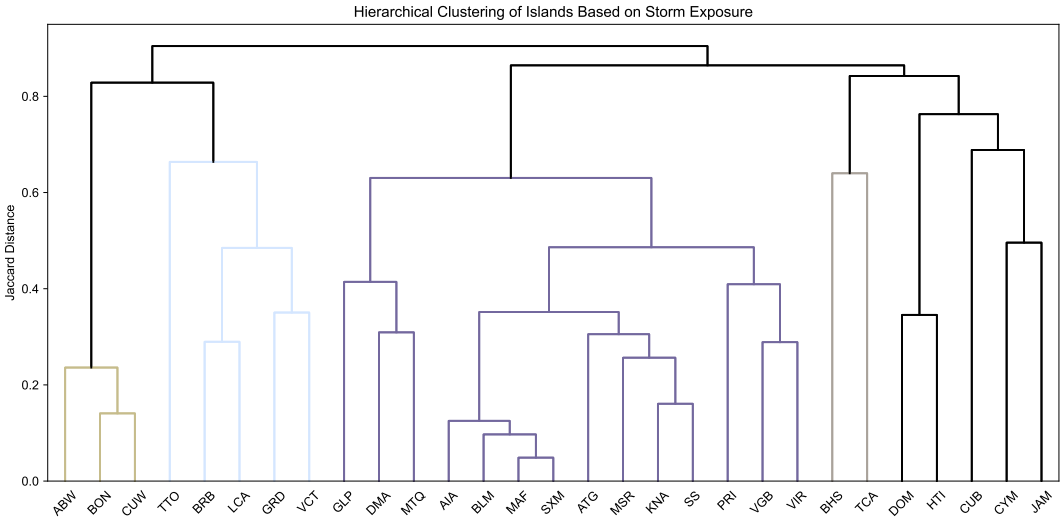

Figure B.11. Clustering of countries based on estimated experienced wind speeds per synthetic TC track for a total dataset of 1000 years, showing the average Jaccard distance within a cluster per country on the y-axis.

Within the largest cluster (the Leeward Islands), four subclusters could be identified: the lower three countries GLP, DMA, MTQ; the middle countries ATG, MSR, KNA, SS and above that AIA, BLM, MAF, SXM; the upper countries PRI, VGB, VIR.

C

Demographic information per country

Table C.1. Socio-economic indicators of Caribbean and surrounding islands. The total GDP per country is given in millions US dollar, the GDP per capita in thousands US dollar, and the total population is given in thousands of persons. The surface area is in km^2 and the population density in people per km^2. The information is mainly retrieved from the World Bank, and represents the year 2023. When not available, information is retrieved from the UN or Wikipedia.

Country	ISO	Total GDP	GDP per capita	Pop.	Surface area	Pop. density	Region
Anguilla	AIA	454	29	16	91	173	Leeward Islands
Antigua and Barbuda	ATG	2,033	22	93	440	212	Leeward Islands
Aruba	ABW	3,649	34	107	180	596	Leeward Antilles
Bahamas	BHS	14,339	36	399	13,880	29	Lucayan Archipelago
Barbados	BRB	6,721	24	282	430	657	Windward Islands
Bonaire, Sint Eustasius, Saba	BES	800	25	32	322	99	Leeward Antilles
British Virgin Islands	VGB	1,506	39	39	150	260	Leeward Islands
Cayman Islands	CYM	7,137	98	73	264	277	Greater Antilles
Cuba	CUB	20,1984	18	11,020	109,880	100	Greater Antilles
Curaçao	CUW	3,281	22	148	444	333	Leeward Antilles
Dominica	DMA	651	10	67	750	89	Leeward Islands
Dominican Republic	DOM	121,448	11	11,331	146,839	77	Greater Antilles
Grenada	GRD	1,317	11	117	340	344	Windward Islands
Guadeloupe	GLP	9,904	26	379	1,628	233	Leeward Islands
Haiti	HTI	19,853	2	11,637	27,750	419	Greater Antilles
Jamaica	JAM	19,424	7	2,839	10,990	258	Greater Antilles
Montserrat	MSR	94	18	5	103	50	Leeward Islands
Martinique	MTQ	8,439	24	350	1,129	310	Windward Islands
Puerto Rico	PRI	117,902	37	3,206	8,870	361	Greater Antilles
Saint Barthélemy	BLM	515	52	10	22	453	Leeward Islands
Saint Kitts and Nevis	KNA	1,056	23	47	260	180	Leeward Islands
Saint Lucia	LCA	2,430	14	179	620	289	Windward Islands
Saint Martin	MAF	596	22	28	50	550	Leeward Islands
Saint Vincent and the Grenadines	VCT	107	11	10	390	26	Windward Islands
Sint Maarten	SXM	1,628	38	43	34	1,257	Leeward Islands
Trinidad and Tobago	TTO	27,372	20	1,368	5,130	267	Windward Islands
Turks and Caicos Islands	TCA	1,402	30	46	950	49	Lucayan Archipelago
Virgin Islands, U.S.	VIR	4,650	44	105	350	300	Leeward Islands

D

Hurricane Irma, 2017

D.1 General information

Hurricane Irma struck the northern Caribbean and Florida between September 5–11, 2017. The storm reached category 5 intensity east of Barbuda on September 5 and maintained this strength for an exceptional 60 hours. A list of moments of impact is included below (National Hurricane Center 2021).

- Barbuda, St. Martin, and Virgin Gorda (6 September): Irma made multiple landfalls as a category 5 hurricane with winds of 155 kt.
- Puerto Rico and Hispaniola: The eye passed just north of these islands, keeping the strongest winds offshore.
- Bahamas (8 September): Landfall on Little Inagua as a category 4 hurricane (135 kt), followed by brief reintensification to category 5.
- Cuba (9 September): Landfall near Cayo Romano at category 5 intensity (145 kt), then weakening along the Cuban Keys to category 2.
- Florida (10 September): Final landfall at Marco Island as a category 3 hurricane (100 kt), weakening rapidly over land.
- 11 September: Downgraded to a tropical storm near Gainesville, Florida.

The best track of Irma's path is included in Figure D.1.

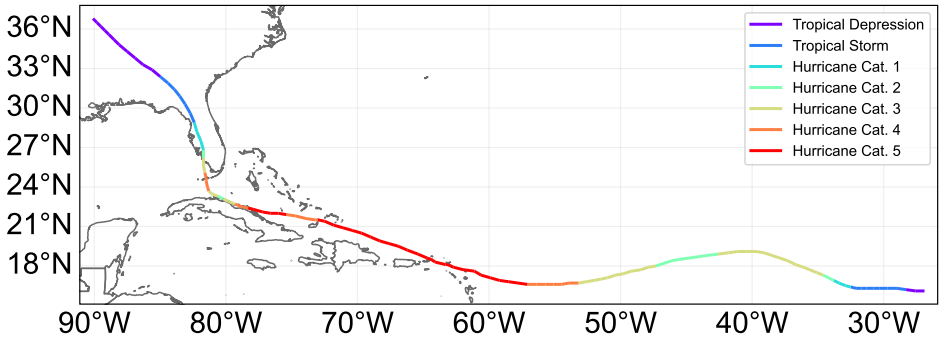

Figure D.1. The track of TC Irma as it is extracted from IBTrACS. The data is interpolated from a 6-hourly to a 0.5-hourly interval.

The several landfalls and the large size of the storm have led to a large impact over a large area. The hurricane is recorded as the second-costliest Caribbean hurricane, after Maria. On Wikipedia, the impact is collected per country, and a summary is given below. This impact will be compared to the results of the modelling methods for the same hurricane, within this chapter. All parameters that could be verified are bold.

Antigua and Barbuda
The peak of the intensity of Hurricane Irma was measured just east of Barbuda, the smaller of the two islands. A weather station observed **a wind gust of 260 km/h** on the island. A day before landfall, all inhabitants were evacuated to Antigua, and the impact of the storm was unclear for several hours after the storm had passed. Irma damaged or destroyed 95% of all structures on Barbuda, including its hospital, schools, hotels, the island's sole airport and large parts of the infrastructure. A total of three deaths were reported on the island. Antigua was affected much less, remaining just outside Irma's strongest windfield. Some flooding took place in low-lying areas. In total, the damage for the country was estimated between 120 and 250 million US dollars, equivalent to approximately 9% of the country's GDP at that time.

Saint Martin / Sint Maarten
On the island of Saint Martin and Sint Maarten, the storm caused a total blackout and severe damage to several structures and roads. On the French part, about 95% of the buildings were damaged, and about 60% were totally uninhabitable. Total losses are estimated at 4.17 billion US dollars. There were four deaths and another 50 were injured. On the Dutch part, about 70% of the buildings were severely damaged. There were four deaths and 23 injuries. The total loss is estimated at 2.98 billion US dollars.

Saint Barthélemy
Widespread destruction and disastrous flooding have been recorded on the island of Saint Barthélemy. At the coast, severe damage occurred due to **storm surge**. A reanalysis stated that an **unofficial wind gust of 320 km/h** was recorded on the island. In the capital, roads were flooded, and at the fire station inundation up to 2.0 meters was observed. The total loss is estimated at 480 million US dollars.

Anguilla
On Anguilla, **high wind speeds** led to severe damage on land, and in several bays and harbours, a rough sea caused heavy damage. One death was recorded on the island, and the total economic damage is estimated at 190 million US dollars.

British Virgin Islands
On the island of Tortola, numerous buildings and roads were destroyed. Four deaths were recorded. Along Cane Garden Bay, **storm surge** caused severe damage. Also, on the other islands, buildings were damaged and/or destroyed.

U.S. Virgin Islands
On Saint Thomas, at least **300 mm of rainfall** led to high impact. On this island, three deaths were recorded. On all islands together, a total loss of 1.1 billion US dollars was estimated.

Puerto Rico
Although the hurricane did not make landfall in Puerto Rico, significant damage was recorded. Along the northern coast, a tide gauge observed **waves up to 0.46 meters**. A **peak sustained wind speed of 89 km/h** and a wind gust of 119 km/h was measured at a weather station along San Juan Bay. Portions of Puerto Rico received heavy rainfall, with **a peak total of 331 mm of rain** in Bayamón, causing widespread flash flooding and at least six landslides. The country lost approximately 1 billion US dollars, and a total of six deaths were recorded.

D.2 Modelling wind fields for Hurricane Irma, 2017
Figure D.2 shows the estimated intensity of wind around the track for Irma.

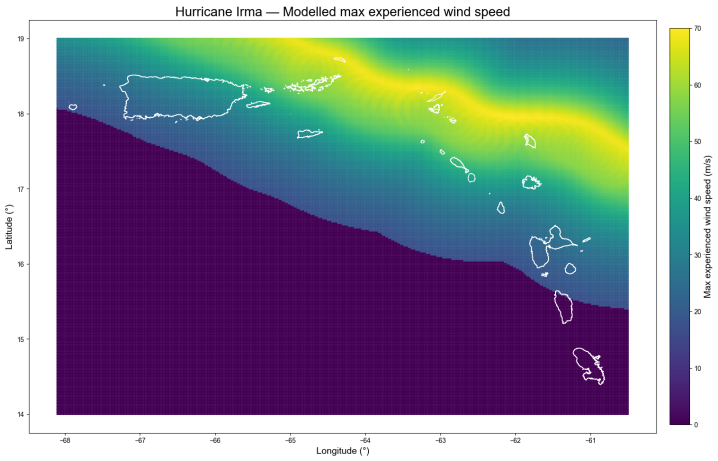

Figure D.2. The wind field in m/s for the area around the Leeward Islands for TC Irma.

Since we are mainly interested in the estimated experienced wind speeds on land, the wind fields are extracted for a point grid on a 2-km scale, for the specified region. See Figure D.3.

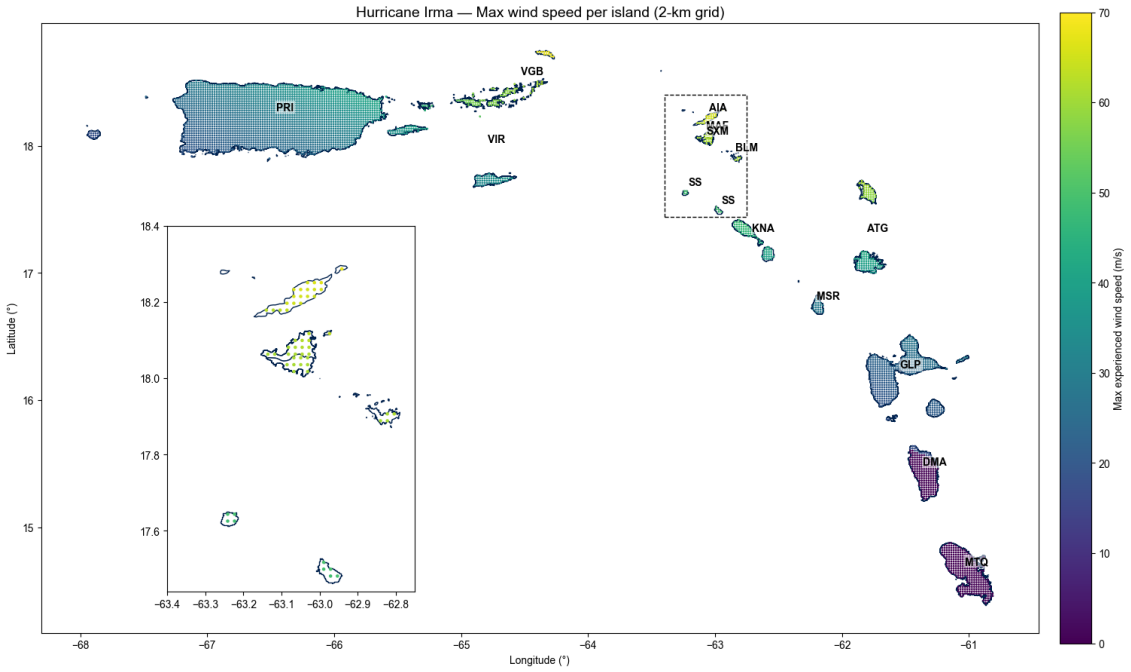

Figure D.3. The wind fields as calculated for hurricane Irma (2017) for the Leeward Islands. The colour scale is shown on the side, showing the maximum wind speed that was reached per point in the grid over the duration of the entire storm.

It can be seen that Anguilla, Barbuda, Saint Martin and Sint Maarten, Saint Barthélemy and the British Virgin Islands have experienced the highest wind speeds of the Leeward Islands during hurricane Irma in 2017. This aligns with literature on this storm, and is also to be expected when looking at the track in Figure D.1. These calculations, which could be validated, confirm that the methodology is working properly. The wind field modelling gives plausible experienced wind speeds for the selected points.

D.3 Modelling storm surge for Hurricane Irma, 2017

For the same TC track, the storm surge is hindcasted using CLIMADA's TCSurgeBathtub. The methodology is explained in Chapter 4. For a grid with points spaced every 0.5 km, the surge height was modelled. A finer resolution was not possible because the surge height calculation depends on the digital elevation model used as input, which has a resolution of approximately 0.5 x 0.5 kilometres.

Figure D.4 shows the estimated surge heights. It is important to notice that the surge height is given in meters, which represents the storm water level minus the ground elevation at that point. By assuming equal surge height per grid cell, of $0.5 * 0.5 = 0.25$ km^2, the flooded area per country is determined. The relative flooded area is determined as the total flooded area divided by the length of the coastline. An area is considered flooded when a surge height of more than 0.2 meters is estimated. Additionally, the total volume of the inundation is calculated.

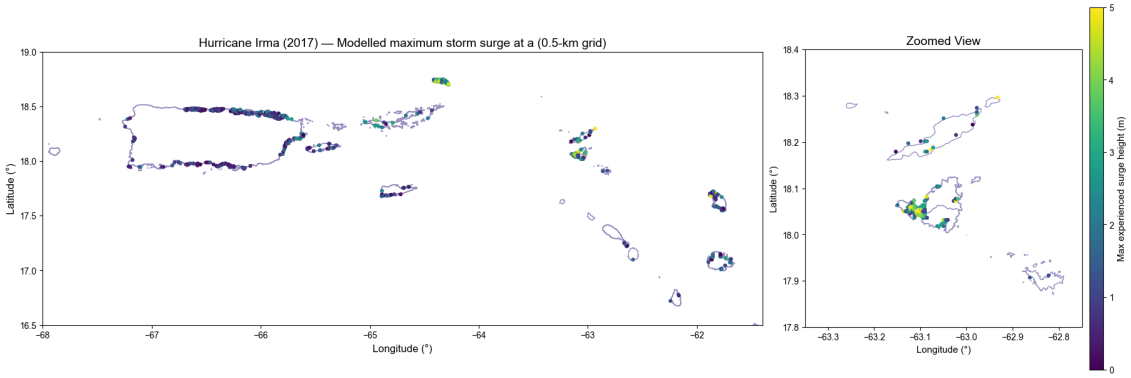

Figure D.4. Modelled maximum storm surge for the entire duration of Hurricane Irma, Sep 2017, in the northern half of the defined scope. The southern half showed no storm surge. For clarity, an extra zoomed view is made for Anguilla, Saint Martin, Sint Maarten and Saint Barthélemy.

The storm surge caused by Hurricane Irma for the scope of the Leeward Islands, including Puerto Rico and Martinique, is given in Table D.1.

Table D.1. Results of the modelled surge over land over the entire duration of Hurricane Irma, per country.

Country	Max surge over whole country (m)	Flooded area (%)
Anguilla	5.95	2.33
Antigua and Barbuda	5.01	2.94
Saint Barthélemy	1.29	0.56
Dominica	0.0	0.0
Guadeloupe	1.33	0.11
Saint Kitts and Nevis	3.22	0.31
Saint Martin	5.17	10.54
Montserrat	1.66	0.49
Martinique	0.0	0.0
Puerto Rico	3.27	1.40
Saba & Sint Eustatius	0.0	0.0
Sint Maarten	5.18	12.17
British Virgin Islands	5.83	6.70
U.S. Virgin Islands	3.94	0.90

D.4 Modelling precipitation for Hurricane Irma, 2017

The precipitation, caused by Hurricane Irma, is modelled for a 2-km grid over all the islands. The methodology is outlined in Section 4.5.

Figure D.5 presents the total precipitation (mm) at each point. Higher precipitation amounts are observed near the storm track (see Figure D.1). In addition, elevation appears to have a notable influence on the spatial distribution of precipitation.

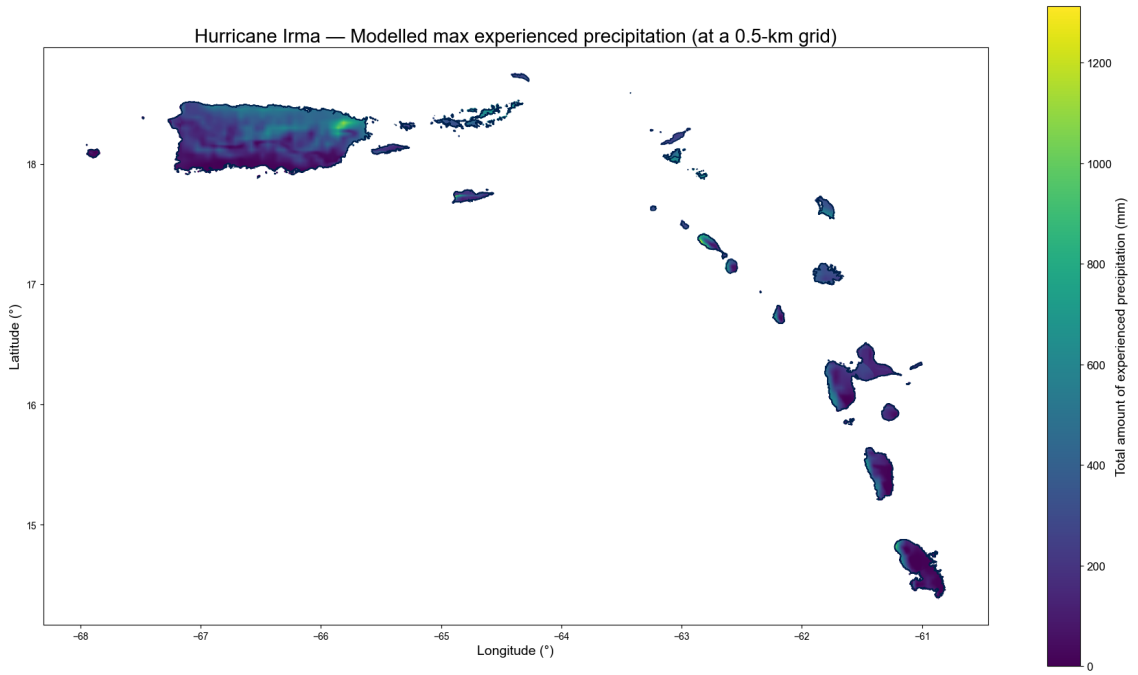

Figure D.5. The precipitation fields as calculated for hurricane Irma (2017) for the Leeward Islands. The colour scale is shown on the side, showing the total precipitation amounts over the duration of the storm that is modelled per point in the grid.

As can be seen in the Figure above, the precipitation varies spatially over an island. Table D.2 includes the mean amounts per country and the maximum amounts per country.

Table D.2. Results of the modelled total precipitation over land over the entire duration of Hurricane Irma, per country.

Country	Mean precipitation (mm)	Max precipitation (mm)
Anguilla	252	261
Antigua and Barbuda	355	609
Saint Barthélemy	647	679
Dominica	104	195
Guadeloupe	159	280
Saint Kitts and Nevis	279	380
Saint Martin	474	547
Montserrat	201	243
Martinique	44	195
Puerto Rico	240	676
Saba & Sint Eustatius	304	330
Sint Maarten	569	602
British Virgin Islands	535	699
U.S. Virgin Islands	280	497

The mean total precipitation over the duration of the storm ranges from 44 mm in Martinique (the most southern island) to 647 mm in Saint Barthélemy, in the modelled outputs. The maximum precipitation amount per country ranges from 195 mm in both Dominica and Martinique to 699 mm in the British Virgin Islands.

E

Modelling wind fields

E.1 Wind speeds for historical TC tracks

Figure E.1 shows the estimated maximum experienced wind speed over the total duration of a storm, per defined return period. The figure shows subplots for the different defined return periods, each with its own scale. The range of the scale shows the range of wind speeds that are expected per return period in the Leeward Islands. Overall, it is concluded that the range of expected maximum wind speeds is small per return period. A spatial trend is not concluded from these figures. The maps for the higher return periods only represent a handful of events and thus cannot be used for any conclusions about the expected spatial distributions.

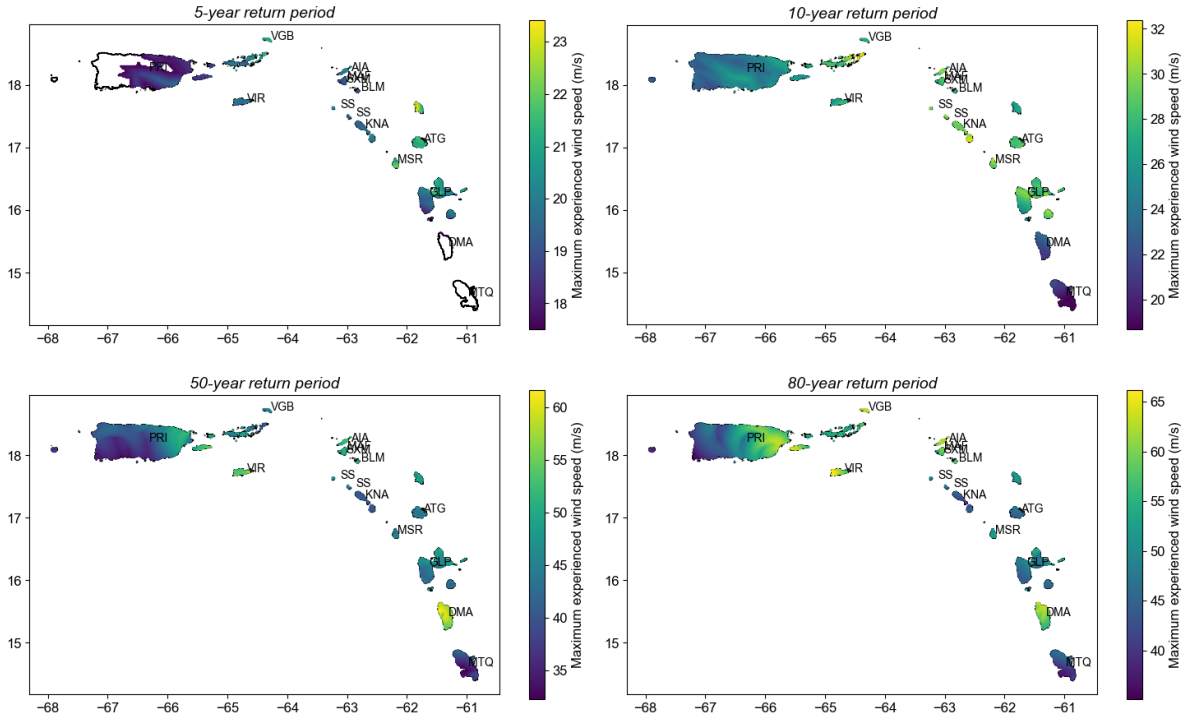

Figure E.1. The estimated maximum wind speed for different return periods for the defined region, based on IBTrACS TC tracks. Per plot, a scale is given for the wind speed, in m/s.

Figure E.2 shows the estimated maximum experienced wind speed over the total duration of a storm, per defined return period. The values are the same as the previous Figure; however, now one fixed scale is used. This better visualises the increasing expected wind speeds for increasing return periods. The total range, for return periods of 1 to 80 years, is approximately 0 to 65 meters per second.

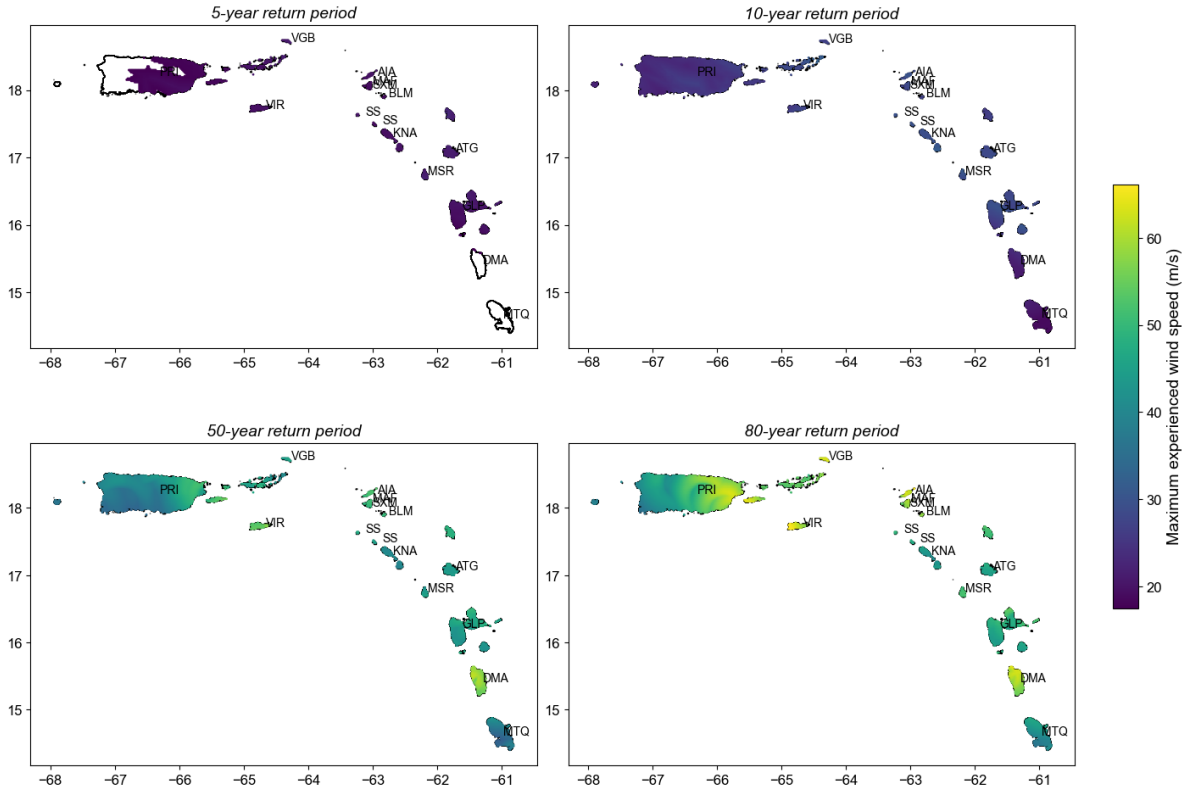

Figure E.2. The estimated maximum wind speed for different return periods for the defined region, based on IBTrACS TC tracks. Per plot, a scale is given for the wind speed, in m/s.

E.2 Wind speeds for synthetic TC tracks

Figure E.3 shows the estimated maximum experienced wind speed over the total duration of a storm, per defined return period. The figure shows subplots for the different defined return periods, each with its own scale. The range of the scale shows the range of wind speeds that are expected per return period in the Leeward Islands. The maps seem to indicate that, in general, higher wind speeds are expected in the south, but not as clearly for each return period. Overall, it is concluded that the range of expected maximum wind speeds is small per return period.

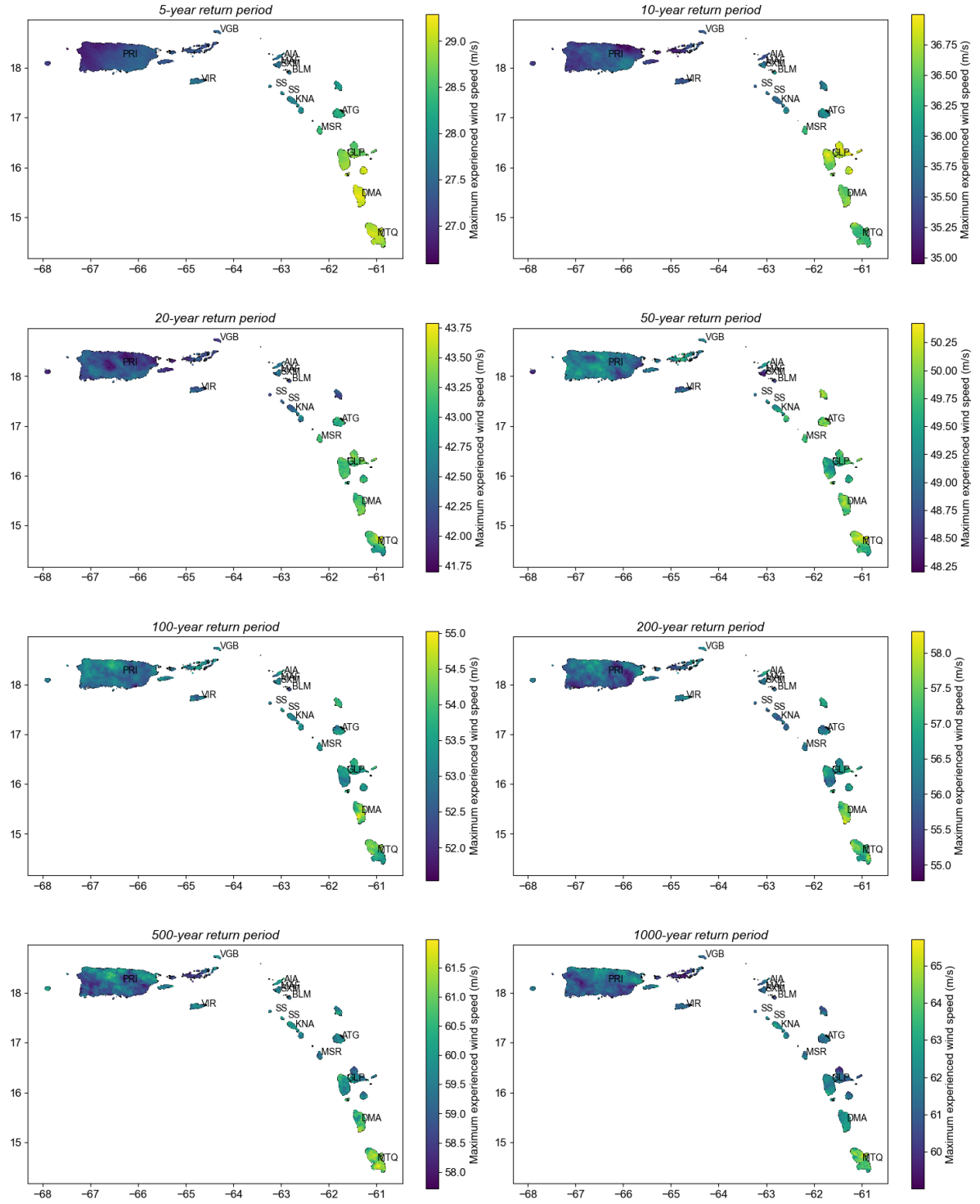

Figure E.3. The estimated maximum wind speed for different return periods for the defined region. Per plot, a scale is given for the wind speed, in m/s.

Figure E.4 includes the same result; however, the scale is fixed for each scale. The range shows the increase in expected wind speeds for increasing return periods.

E.2.1 Relative deviation to regional mean with different drivers

The two figures below show the deviation from the regional mean for the modelled wind speeds expressed in their empirical return period. In Figure E.5 the countries are scaled from south to north.

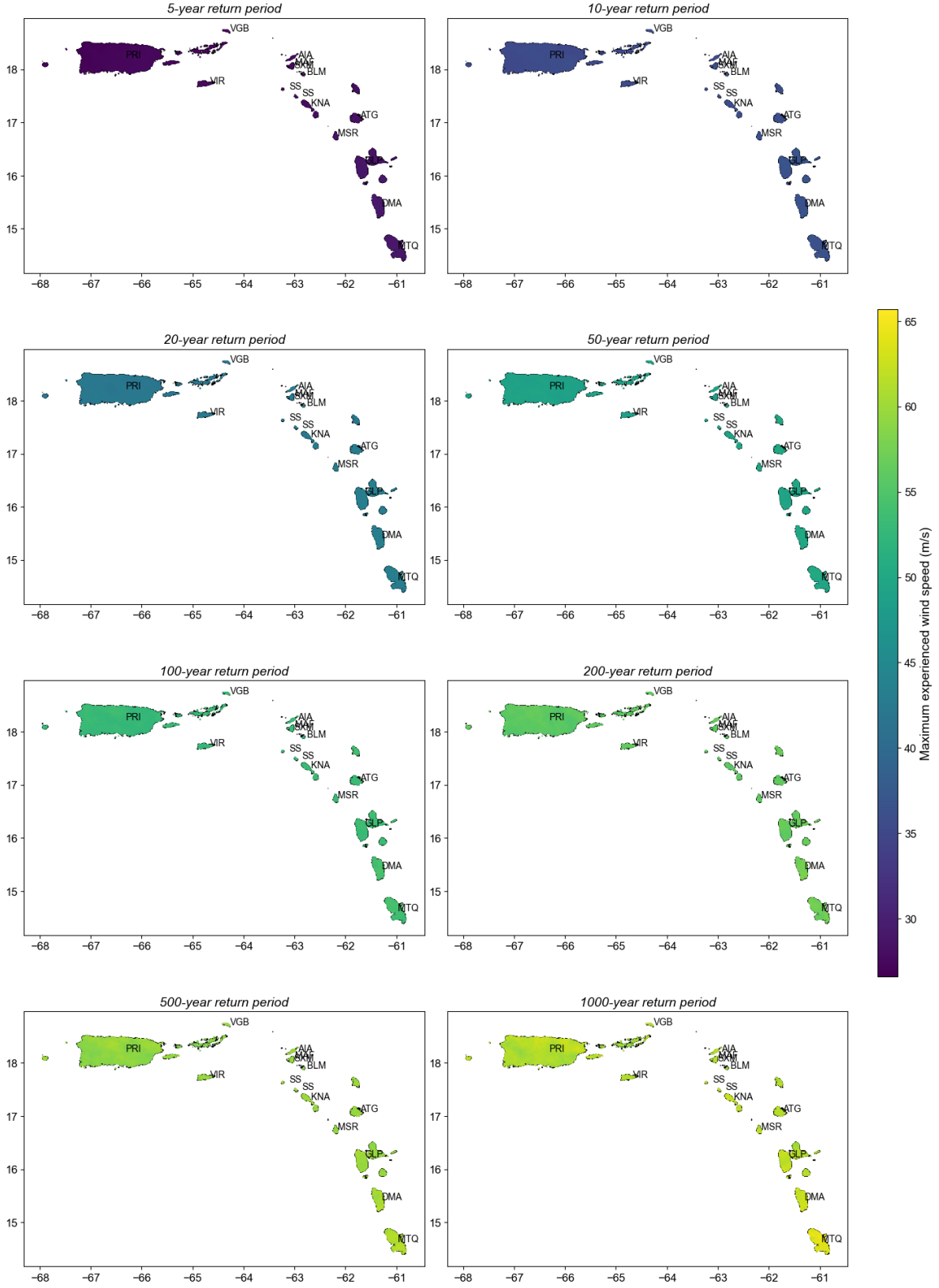

Figure E.4. The estimated maximum wind speed for different return periods for the defined region, based on STORM TC tracks. Per plot, a scale is given for the wind speed, in m/s.

Figure E.6 shows the same relative deviation from the regional mean, but now the countries are ordered by size instead of by location. The areas are included in Table C.1 in Appendix C.

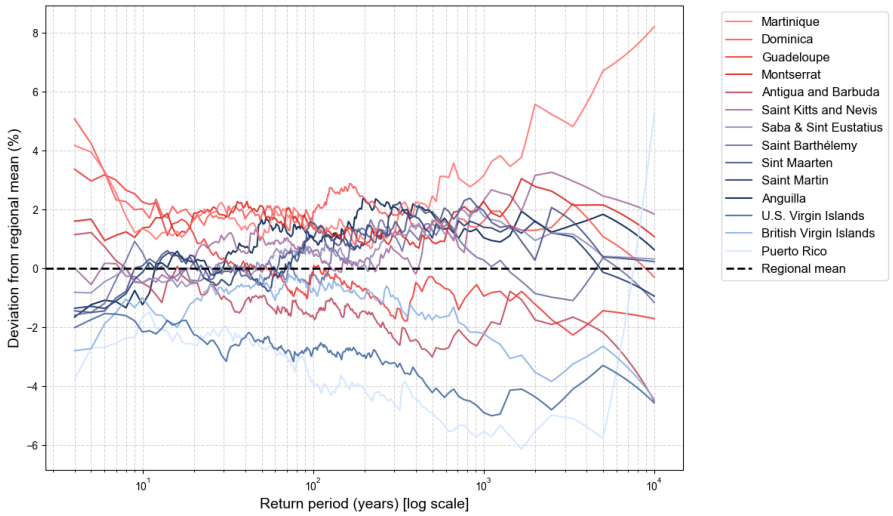

Figure E.5. Estimated maximum 1-minute sustained wind speeds at 10 m as a mean over all points, per country, as their relative deviation from the regional mean, in percentage. The countries are coloured based on location.

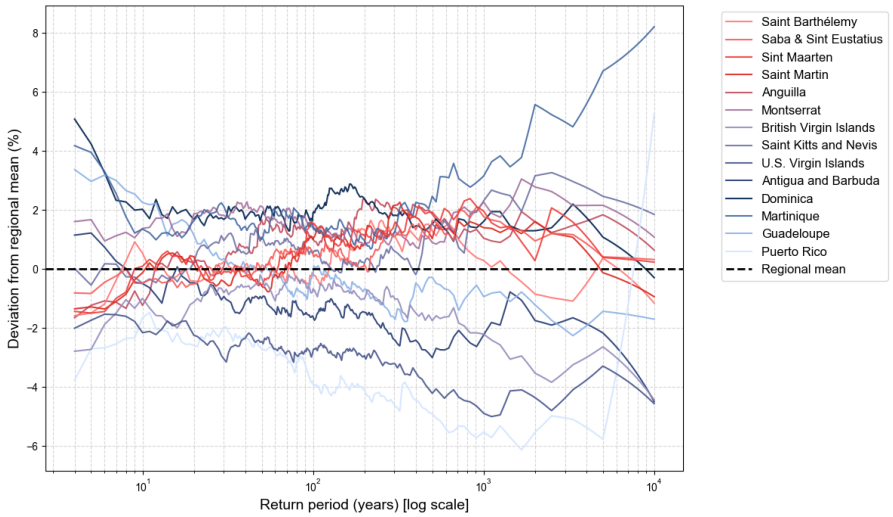

Figure E.6. Estimated maximum 1-minute sustained wind speeds at 10 m as a mean over all points, per country, as their relative deviation from the regional mean, in percentage. The countries are coloured based on size. The colour scale, going from red to purple to blue, is based on the total area of a country, from small to large.

The result shows no proof that area size affects expected maximum wind speeds, as mean values per country. Tropical cyclones weaken when reaching land, since the moisture, and therefore latent heat supply, is cut off. However, since the islands are very small, significant effects of the landfall are not expected.

E.3 Results Bloemendaal et al.

Table E.1. Wind speed in meters per second, occurring within 100 km of the capital city of the respective island, for 4 defined return periods. Probabilistic wind speeds are calculated empirically using the STORM dataset of 10,000 years of synthetic hurricane tracks for the North Atlantic basin. Wind speeds are defined as the maximum estimated wind speeds per storm for that location, at 10 meters high and sustained for 10 minutes (Bloemendaal, Moel, Muis, et al. 2020).

Island	1-in-10 years	1-in-20 years	1-in-50 years	1-in-100 years
Anguilla	41.57	50.52	56.78	60.32
Antigua and Barbuda	42.08	50.06	56.13	59.55
British Virgin Islands	40.98	50.21	56.30	60.18
Dominica	42.44	50.12	56.40	60.65
Guadeloupe	41.71	49.52	55.92	59.72
Martinique	42.18	49.93	56.45	60.51
Montserrat	41.38	49.53	55.69	59.41
Puerto Rico	40.74	50.01	56.64	60.37
Saint Kitts and Nevis	41.44	49.80	55.55	59.40
Sint Maarten	41.58	50.40	56.40	59.95
U.S. Virgin Islands	40.87	50.32	56.40	59.96
Saint Martin	41.67	50.45	56.68	60.19
Sint Eustatius	41.26	49.97	55.80	59.47
Saba	41.28	49.88	55.99	59.58

F

Modelling storm surge

F.1 Storm surge for historical TC tracks

Figure F.1 shows the estimated maximum experienced surge level over the total duration of a storm, per defined return period. The figure shows subplots for the different defined return periods, each with its own scale. The range of the scale shows the range of surge levels that are expected per return period in the Leeward Islands.

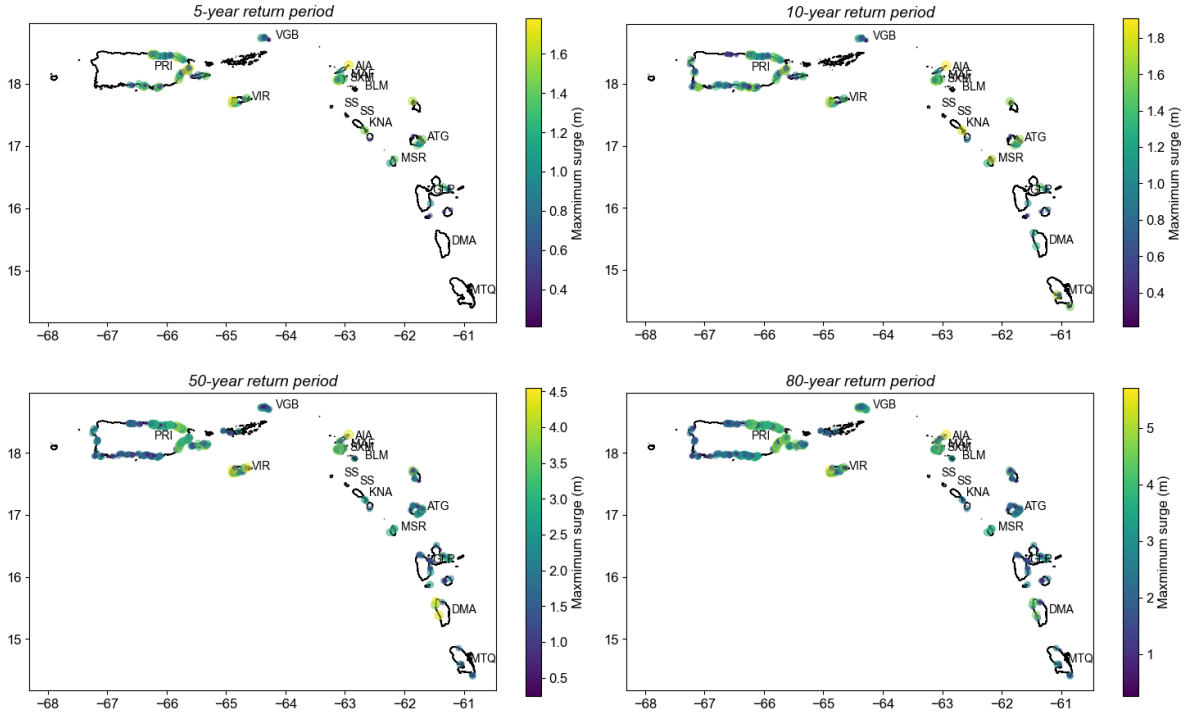

Figure F.1. The estimated maximum surge levels for different return periods for the defined region, based on IBTrACS TC tracks. Per plot, a scale is given for the surge level, in meters.

Figure F.2 shows the estimated maximum surge level over the total duration of a storm, per defined return period. The values are the same as the previous Figure; however, now one fixed scale is used. This better visualises the increasing expected surge levels for increasing return periods. The total range, for return periods of 1 to 80 years, is approximately 0 to 5.5 meters.

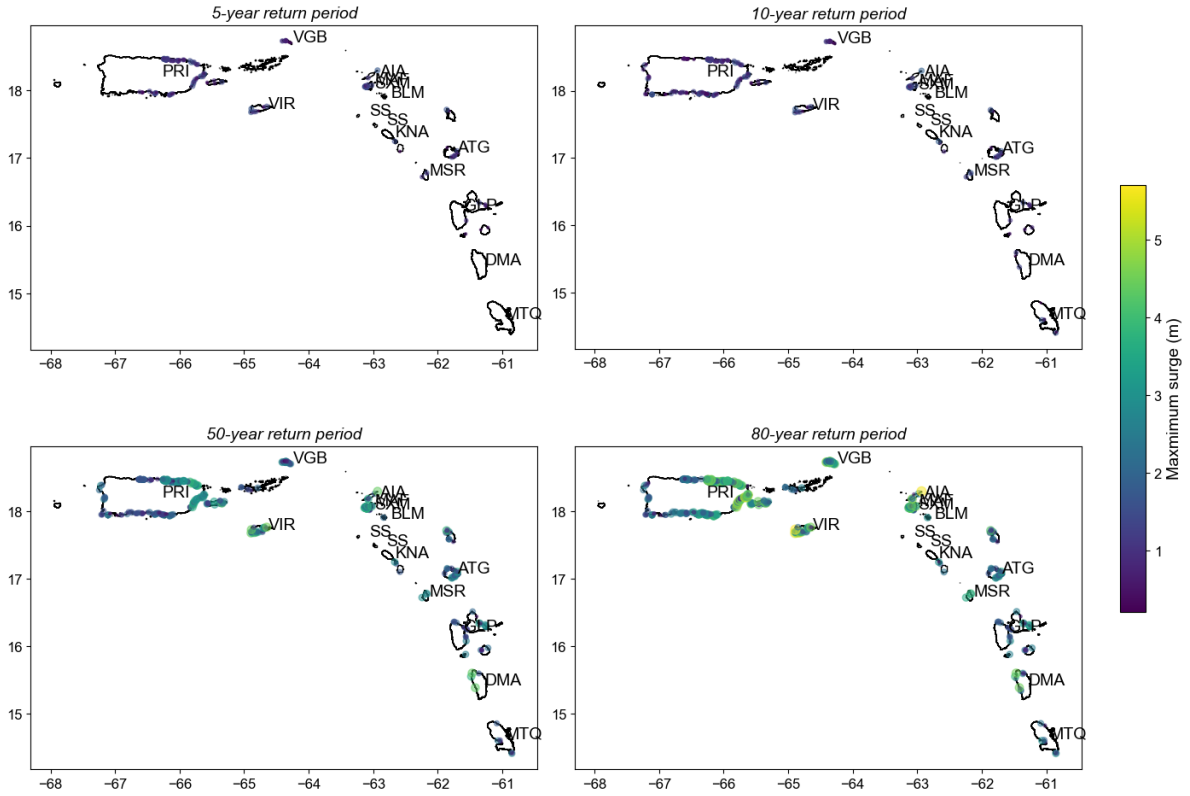

Figure F.2. The estimated maximum surge levels for different return periods for the defined region, based on IBTrACS TC tracks. Per plot, a scale is given for the surge level, in meters.

F.2 Storm surge for synthetic TC tracks

Figure F.3 shows the estimated maximum experienced surge level over the total duration of a storm, per defined return period. The figure shows subplots for the different defined return periods, each with its own scale. The range of the scale shows the range of surge levels that are expected per return period in the Leeward Islands.

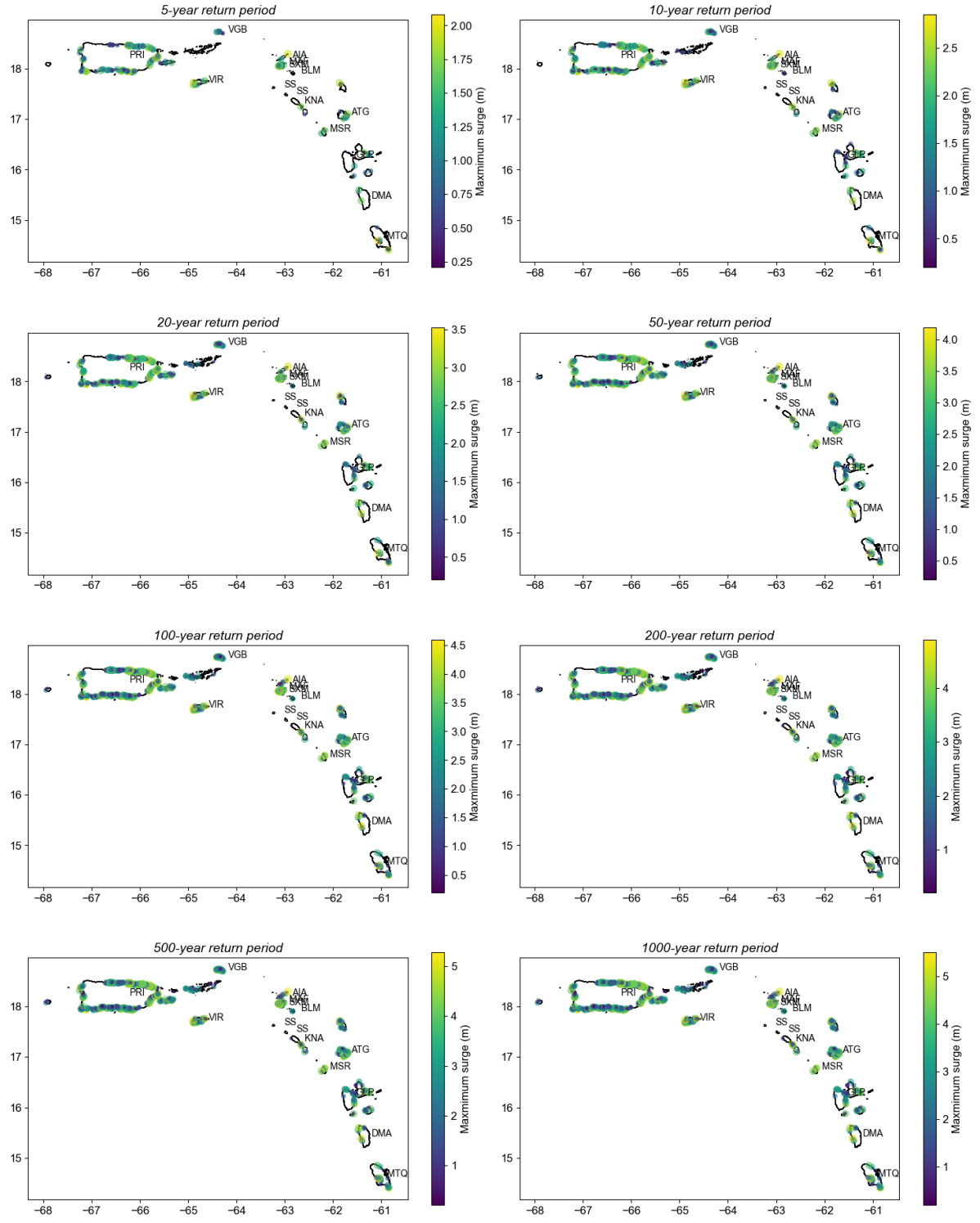

Figure F.3. The estimated maximum surge level for different return periods for the defined region. Per plot, a scale is given for the surge level, in meters.

Figure F.4 includes the same result; however, the scale is fixed for each scale. The range shows the increase in expected surge levels for increasing return periods, although this increase seems to decrease for the high return periods.

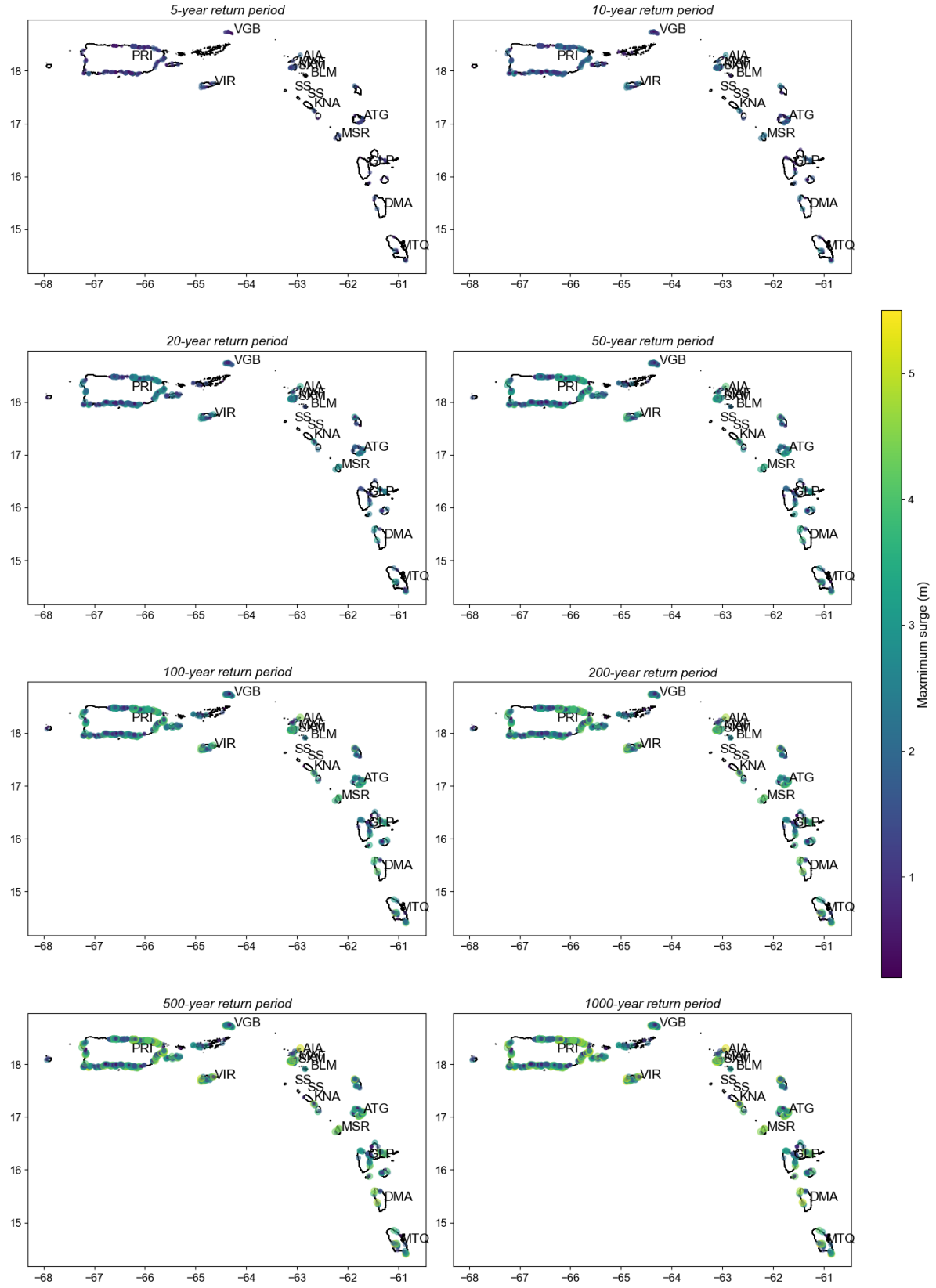

Figure F.4. The estimated maximum surge level for different return periods for the defined region, based on STORM TC tracks. Per plot, a scale is given for the surge level, in meters.

F.2.1 Relative deviation to regional mean with different drivers

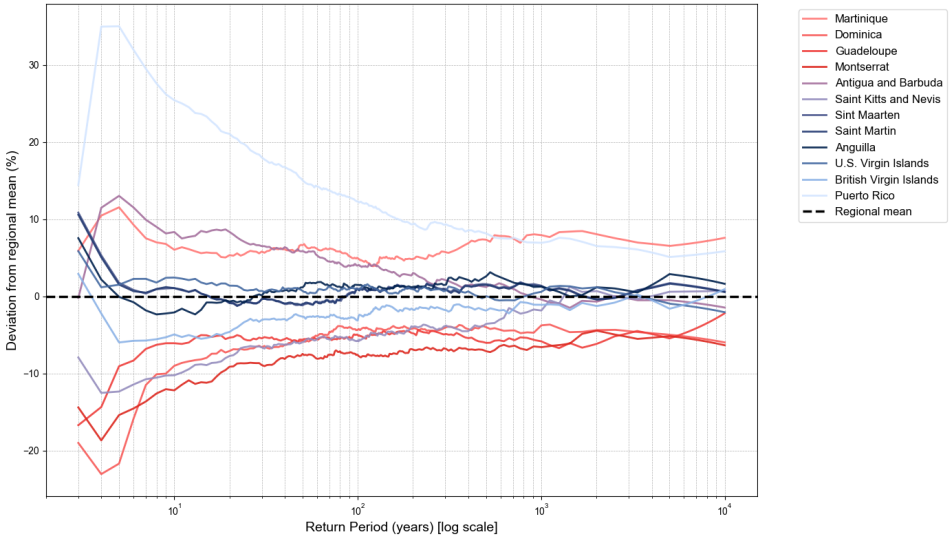

(a) The countries are coloured based on location. In the legend, the colours represent, from top to bottom, southern to northern countries.

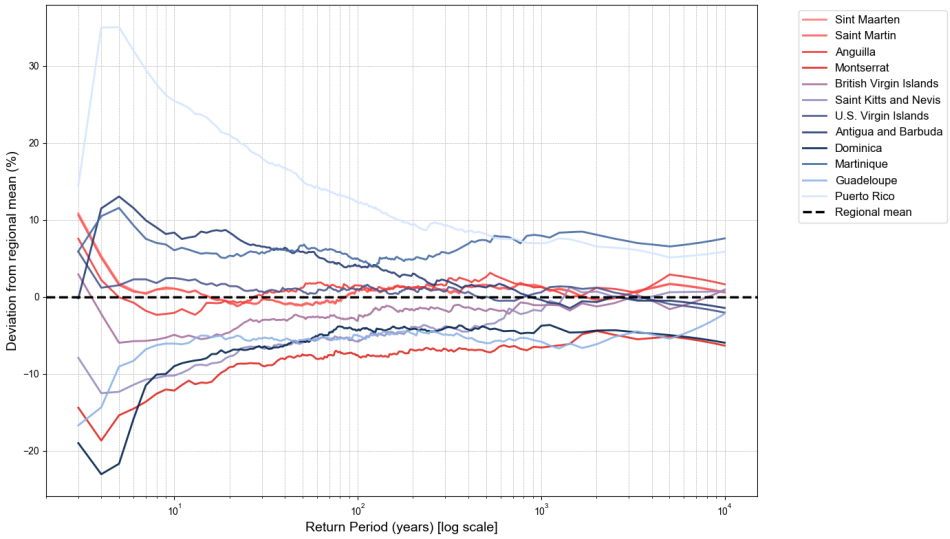

(b) The countries are coloured based on area size. In the legend, the colours represent, from top to bottom, larger countries.

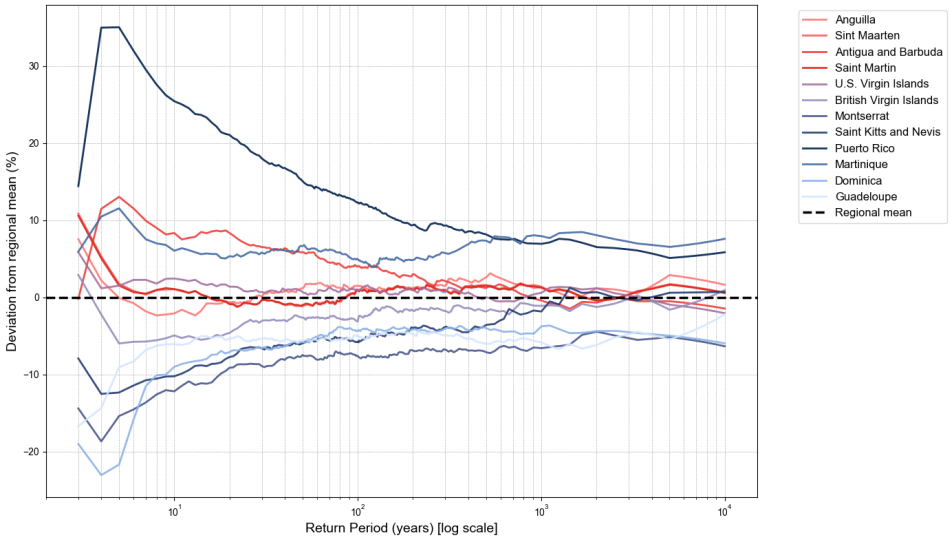

(c) The countries are coloured based on maximum elevation. In the legend, the colours represent, from top to bottom, lower to higher maximum elevation per country.

Figure F.5. Estimated maximum surge levels, per country, as their relative deviation from the regional mean, in percentage.

G

Modelling precipitation

G.1 Precipitation for historical TC tracks

Figure G.1 shows the estimated total precipitation amounts over the total duration of a storm, per defined return period. The figure shows subplots for the different defined return periods, each with its own scale. The range of the scale shows the range of total precipitation amounts expected per return period in the Leeward Islands.

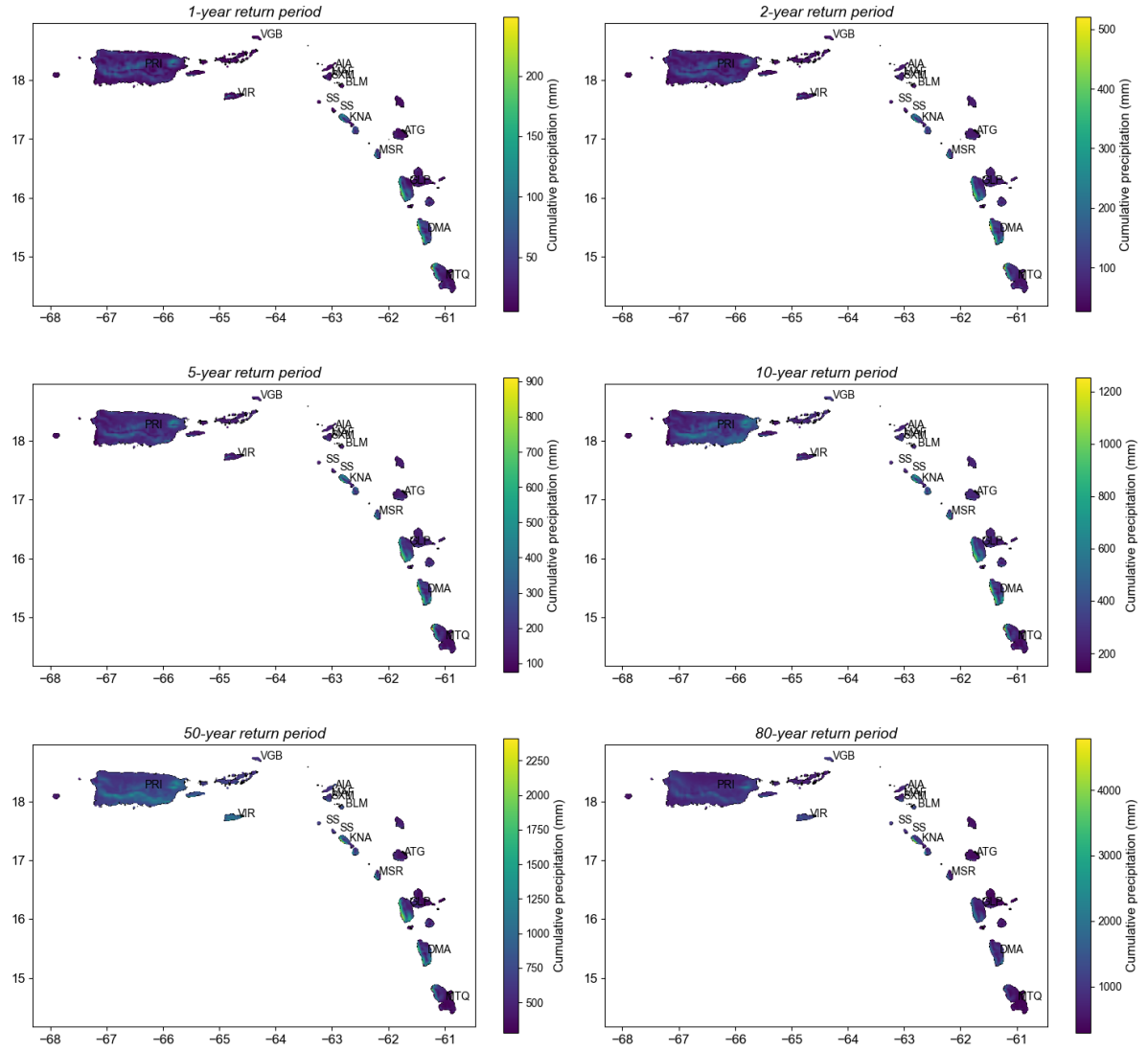

Figure G.1. The estimated total precipitation amounts (in mm) for different return periods for the defined region, based on IBTrACS TC tracks. Per storm, the maximum modelled output per country is taken. Every map is shown with its own scale.

Figure G.2 shows the estimated total precipitation amounts over the total duration of a storm, per defined return period. The values are the same as the previous Figure; however, now one fixed scale is used. This better visualises the increasing expected surge levels for increasing return periods. The total range, for return periods of 1 to 80 years, is approximately 0 to 4500 mm of precipitation in one place over the duration of a storm.

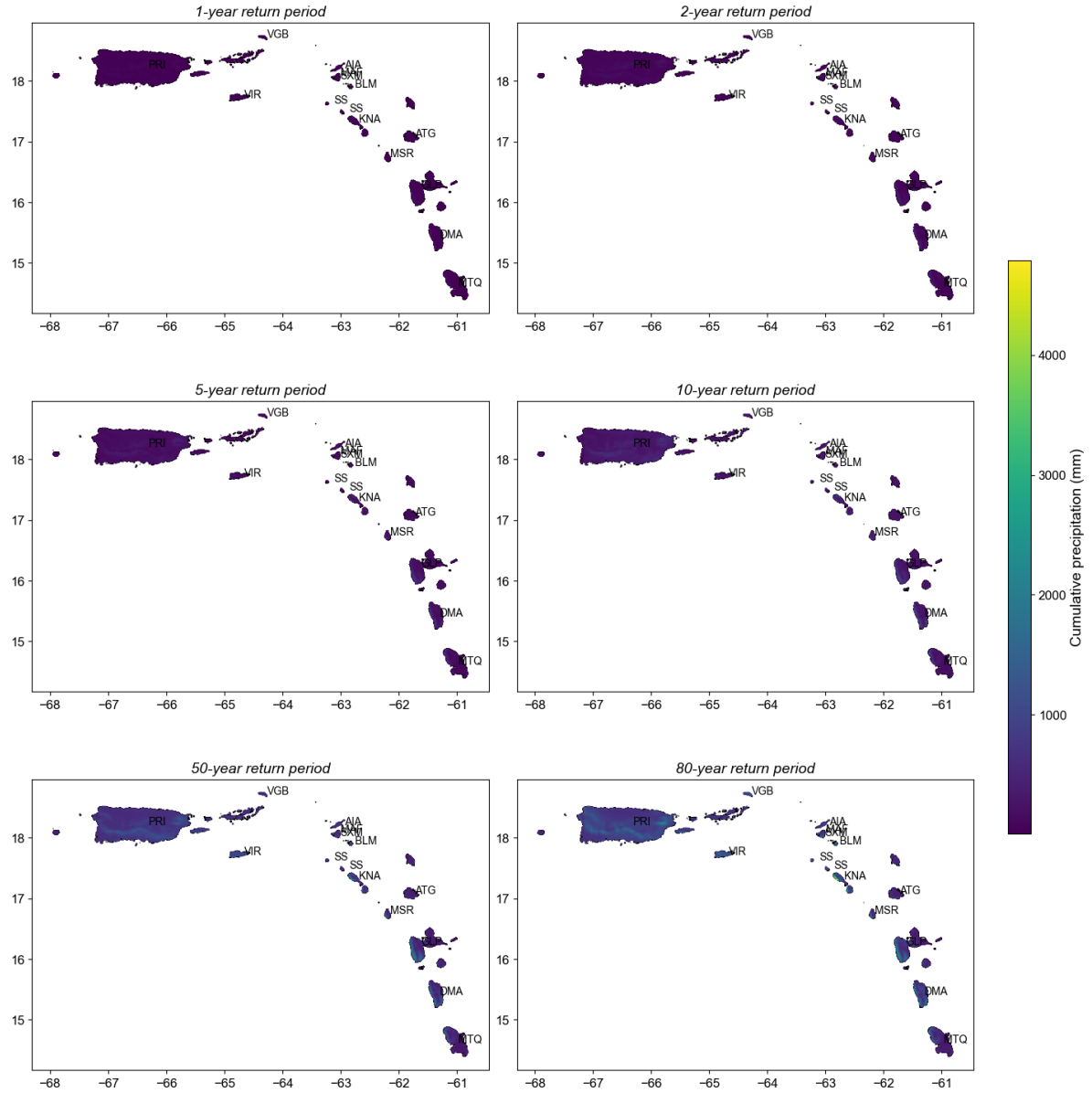

Figure G.2. The estimated total precipitation amounts (in mm) for different return periods for the defined region, based on IBTrACS TC tracks. Per storm, the maximum modelled output per country is taken. One scale is used for all maps together.

G.1.1 Relative deviation to regional mean with different drivers

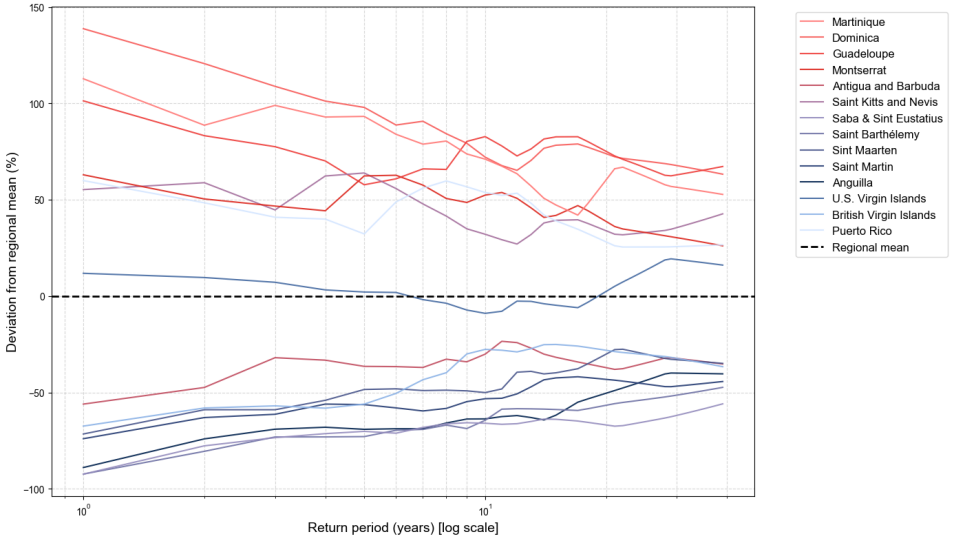

(a) The countries are coloured based on location. In the legend, the colours represent, from top to bottom, southern to northern countries.

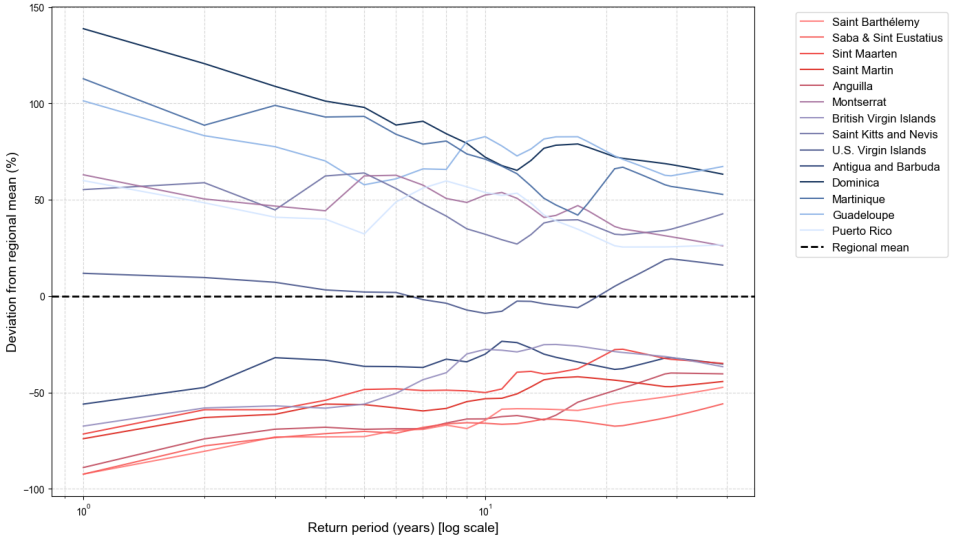

(b) The countries are coloured based on area size. In the legend, the colours represent, from top to bottom, small to larger countries.

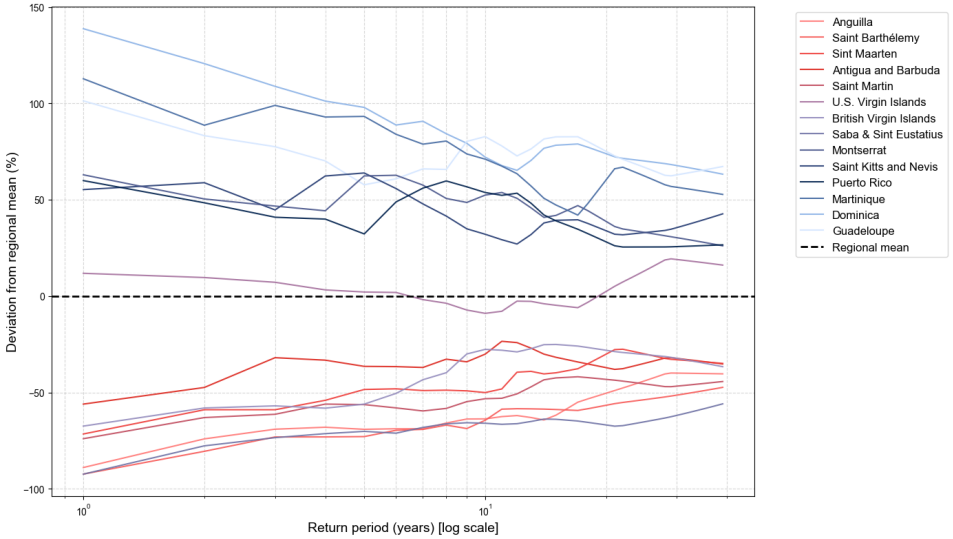

(c) The countries are coloured based on maximum elevation. In the legend, the colours represent, from top to bottom, lower to higher maximum elevation per country.

Figure G.3. Estimated accumulated precipitation (mm) over the duration of the storm, per country, as their relative deviation from the regional mean, in percentage.